C00–1569–85

FLUCTUATION BROADENING OF THE RESISTIVE TRANSITION TO THE SUPERCONDUCTING STATE OF $Nb_{.88}Ti_{.12}N$ THIN FILMS

F. M. Schaer

Solid State and Low Temperature Physics Group

SCHOOL OF PHYSICS AND ASTRONOMY

UNIVERSITY OF MINNESOTA
MINNEAPOLIS, MINNESOTA

WORK SUPPORTED IN PART BY THE U. S. ATOMIC ENERGY COMMISSION

DISCLAIMER

FLUCTUATION BROADENING OF THE RESISTIVE TRANSITION TO THE SUPERCONDUCTING STATE OF $Nb_{.88}Ti_{.12}N$ THIN FILMS

A THESIS

SUBMITTED TO THE FACULTY OF THE GRADUATE SCHOOL

OF THE UNIVERSITY OF MINNESOTA

By

FREDERICK MICHAEL SCHAER

IN PARTIAL FULFILLMENT OF THE REQUIREMENTS

FOR THE DEGREE OF

DOCTOR OF PHILOSOPHY

DECEMBER 1971

ABSTRACT

FLUCTUATION BROADENING OF THE RESISTIVE TRANSITION TO THE SUPERCONDUCTING STATE OF $Nb_{.88}Ti_{.12}N$ THIN FILMS

Measurements of resistance of short mean free path $Nb_{.88}Ti_{.12}N$ thin films are reported. Evidence for fluctuation conductivity is found at temperatures at least twice the 11 K transition temperature. In the upper part of the transition, there is qualitative agreement with the fluctuation conductivity (σ') calculation by Aslamasov and Larkin (AL).

Resolution was one part in 10^5 for both the resistance (R) and temperature (T) measurements. Stray magnetic and RF fields were shielded from the samples. The electrostatic fields to which the samples were exposed during resistance measurements were at most 2 mV/cm. Some measurements made in perpendicular magnetic fields (H) are also reported.

For this material $\frac{dR}{dT}$ was negative above 20 K and $\frac{dR}{dH}$ was negative above 60 K. The normal resistivity was 1.4×10^{-3} ohm cm. Sample thickness (d) was 1500Å, about 40 times the zero temperature coherence length ($\xi(0)$). $\xi(0)$ was determined from $H_{c_2}(T)$.

With a linear extrapolation of the normal resistance (R_n) from high temperatures and no other free parameters, the temperature dependence of σ' agrees with AL from $R/R_n = 0.8$ to 1.0. The data is also consistent with a change in temperature dependence predicted by AL for $\frac{d}{\xi(T)} = 1$. There is no overall quantitative agreement; $\xi(0)$ must be

replaced by $2\Sigma(0)$ in the AL expressions to bring the theory to within 100% of the data. The assumed $R_n(T)$ is supported, though not conclusively, by high temperature and high magnetic field measurements.

Below $R/R_n = 0.8$, σ' follows $((T/T_c^*) - 1)^{-5/2}$ for more than a decade of sample resistance. T_c^* is about ½ K below the mean field T_c. This two-fold nature of the transition is distinct in fields up to 2 kOe. At 10 kOe the transition is referred unambiguously to a single $T_c(H)$ ($\sigma' \sim ((\frac{T}{T_c(H)})-1)$ for almost three decades in R).

ACKNOWLEDGEMENTS

The author is indebted to Professor Allen M. Goldman for suggesting this research and for constant guidance and support.

The assistance of Jon Zbasnik in data taking, of Paul Steinback in computer programming, and of Bob Riess in the drawing of figures is gratefully acknowledged. The author would also like to express gratitude for the hospitality extended him by the Ames Laboratory of the U.S. Atomic Energy Commission at Iowa State University where the high magnetic field measurements were made.

Thanks are also due Steve Kral, Pete Kreisman, and other fellow graduate students, and to Professor Michael Moldover, for encouragement and friendship without which the physics would often have been little fun. A special debt of gratitude is owed Bev Schaer, who typed and typed and was patient.

Support for this research was provided by the Metallurgy Division of the Atomic Energy Commission through Contract AT(11-1) 1569 and by the National Science Foundation through a four year tenure of a research traineeship.

CONTENTS

CONTENTS (continued)

LIST OF FIGURES

LIST OF TABLES

CHAPTER ONE: INTRODUCTION AND THEORY

Historical Background

The present interest in fluctuation effects in thin film superconductors can be understood best by considering the historical environment in which it grew. There have been three areas of activity, not distinct, which have contributed to this environment. The oldest is concerned with the use and misuse of mean field theoretical techniques in the description of phase changes. A second can be described as a long standing argument over the improbability (or possibility) of crystalline or momentum space long range order in one and two dimensions. The third area of interest had its origin in work on critical phenomena, in particular those exhibited by superfluid He^4. An interest in the flow properties of superfluid He^4 was an outgrowth of this work. This in turn led to interest in decay of persistent currents, in both superfluids and superconductors.

The decay of persistent currents has been treated by many theoreticians as a one dimensional* problem. As such, this body of work is not of direct interest to us in the discussion of the thin film results to follow below. So

---

* A sample with two of its dimensions smaller than the temperature dependent coherence length $\xi(T)$ is one dimensional (1D). A thin film (two dimensional or 2D sample) has its thickness smaller than $\xi(T)$.

we will dispense with this background first, with only a few words, and refer the reader to recent literature for details.

The theoretical point of view taken in work on persistent current decay has been that transitions are broadened by resistance creating fluctuations. This is in contrast to the theoretical work on thin films and bulk materials,* where emphasis is on fluctuations that enhance the conductivity.

The first theoretical work on decay of persistent currents was due to Langer and Fisher(1) (1967) who worked out the problem for superfluid He^4. Shortly thereafter, encouraged by comments by Little(2) (1967), experimental and similar theoretical efforts found their way into the field of superconductivity. Experimental work was done by Parks and Groff(3) (1967), Hunt and Mercereau(4) (1967), Groff et al.(5) (1967) and by Webb and Warburton(6) (1968). This was accompanied by beginnings of a theoretical picture worked out by Langer and Ambegaokar(7) (1967).

In the following years, progress was confined to the theoretical front. A recent theoretical paper(8) and a survey(9) can serve as a summary and review of work in this area.

---

* Bulk or three dimensional (3D) samples are those for which all dimensions exceed $\xi(T)$.

It is generally believed that long range order is impossible in one and two dimensional systems.[10] There has, however, been no consensus on what this means in terms of observable quantities such as the conductivity. Interest in one dimensional superconductors began with Little's[11] (1964) conjecture that superconducting effects might be observable in certain long chain organic molecules. The conjecture did not go unchallenged.[12] The arguments over this matter were an important factor in maintaining interest in one dimensional systems. Two dimensional behavior has recently been commented on in an article by Mikeska and Schmidt.[60] These authors show that the absence of long range order does not prevent a transition into state with zero resistivity.

From the historical point of view, interest in fluctuation phenomena can probably best be regarded as part of interest in phase transitions in general. Phase transitions have interested physicists since the first days of thermodynamics and statistical mechanics. It has been this interest that has lured some of the best minds and most active contributors to this and related fields. It is the work on second order phase transitions, and the theoretical apparatus that has evolved to handle these phenomena, that will concern us here.

In 1937, Landau[13] introduced a general theory of second order phase transitions. This was a phenomenological model in which the free energy of a system could be written as a sum of powers and gradients of an "order parameter".* The name "mean field theory" has attached itself to this model because of similarities it bears to a much older one[14] for magnetic materials.

It has turned out that the expansion of a free energy in terms of an order parameter indicated above is probably not valid for most of the phase transitions for which it was intended. Indeed, the superconducting phase transition may be the only one for which such an expansion can be made.

It was in 1950 that Landau and Ginzburg[15] introduced this mean field technique to the problem of superconductivity. Pippard[16] (1950), and later Ginzburg[17] (1960), made estimates of the region of validity, in temperature, of this formalism. They found that one could come to within ($10^{-16} \times T_c$) of the transition temperature before deviations were expected in the case of pure bulk materials.** It appears that these estimates were mistaken for criteria for observability of fluction effects themselves.*** This

---

* It should be emphasized that this expansion was valid <u>below</u> some transition temperature, T_c. Above T_c the order parameter vanished.

** This temperature interval is larger for samples of restricted dimensionality and for "dirty materials" (<u>i.e.</u> small mean free path).

*** The situation was complicated by the <u>assumption</u> that a mean field theory like Landau's was valid <u>above</u> T_c. Within this assumption the "order parameter" was reinterpreted as a probability for superfluid creating fluctuations.

interpretation was reinforced when Cochran[18] (1964) failed to see fluctuation effects in the specific heat anomaly at T_c.* There followed a number of years in which no further work was done on fluctuation effects in superconductors.

Then, perhaps encouraged by remarks by Anderson[19] (1965), Shier and Ginzburg[20] (1966) began work on thin films of amorphous materials. Although it is not clear that they were looking for fluctuation effects, and though when they saw them they blamed them on inhomogenieties and strains, these workers were the first to see fluctuation broadening of a resistive transition.

This work was taken up by Ferrel and Schmidt,[21] and Glover[22] and others, at the University of Maryland. Ferrel and Schmidt suggested that fluctuation effects might be observable, in resistance measurements similar to those of Shier and Ginzburg. They predicted a Curie-Weiss behavior of the "extra conductivity", σ', for thin films above T_c:

$$\sigma' \sim \tau^{-1}$$

$$\sigma' = \sigma - \sigma_n \qquad \tau = (T - T_c)/T_c$$

σ =conductivity enhanced by superconducting fluctuations

σ_n =normal state conductivity

* No such fluctuation effects were to be expected for reasons we will not go into here.

They also predicted $\tau^{-3/2}$ behavior close to T_c. The data of Glover was in excellent agreement with these results.

Meanwhile, but independently, Aslamasov and Larkin[23] had arrived at the same Curie-Weiss prediction for the extra conductivity in thin films, as well as a $\tau^{-1/2}$ dependence for 3D samples. This was done on the basis of a microscopic calculation.

Experimental work[24-36] continued for two years, in which the correct temperature dependence was consistently verified, with an occasional misgiving about the numerical prefactor, τ_0 , called the width parameter, that should accompany the τ^{-1} to give the expression for extra conductivity in two dimensions.* The values of τ_0 obtained from fits with data varied from ½ to 10 times the value expected on the basis of theory.

A group from the Bell labs,[34] finding the ubiquitous difficulty with the prefactor τ_0 , found also that a film of thickness sufficient to show 3D behavior did not show it. Examining data already published by Glover[22,24,25] and of Strongin <u>et al.</u>,[27] they found similar discrepencies between theory and experiment. Thus doubt arose concerning the ability of the Aslamosov-Larkin theory to account for the temperature dependences observed in these samples. Meanwhile Gittleman, Cohen and Hanak[29] claimed to see

---

* See summary of Aslamasov-Larkin theory below.

three dimensional behavior in films of tin and $Al:SiO_2$, with the expected transition to two dimensional behavior.

Values of the width parameter obtained by a steadily increasing number of workers still fell on all sides of the "Aslamasov-Larkin value". Theoreticians watching this scene began to consider corrections that would modify the prefactor to the Aslamasov-Larkin temperature dependence. This seemed often to make matters worse, for where corrections were thought to be necessary on theoretical grounds, the experiments were already in good agreement with the unmodified theory.

It was in the midst of this uncertain picture that this present work was begun. Real interest in the samples described in this thesis arose when it was found that, with a reasonable assumption concerning the normal resistance of our samples, three dimensional behavior was found. Again, however, there was trouble with the width parameter.

Since the general theoretical and experimental picture is still cloudy, we will introduce our findings with a summary of the theoretical models. Since a comparison with this theoretical situation requires a complete knowledge of sample parameters and characteristics, this matter is discussed in as much detail as possible. This is done in chapter two

Theoretical Survey

Calculations of fluctuation effects in superconductors are performed on two levels of sophistication. These are called "mean field theoretical" (MFT) and "microscopic". To supplement the discussion of the former method given above, it is convenient to make several additional comments here: 1) MFT techniques are used to account for fluctuation effects both above and below T_c. The formalism is the same in each case, but the interpretation given to the expansion parameter for the free energy is not.* The validity of MFT below T_c has been well established experimentally. Calculations performed above T_c are made with the <u>assumption</u> that this formalism can be extended into this regime also. So far as calculations of thermodynamic quantities is concerned, the feeling now is that this extension of MFT can be made. 2) It is now understood that MFT calculations are in principle valid up to quite close to T_c. This is discussed quantitatively below. 3) Within the framework of MFT it is in principle possible to consider interactions of arbitrary order, but only in a single internal (mean) field variable. Above T_c, only interactions with an external field have been considered. Below T_c it is evidently necessary to include the self interaction of the field. This has been done by Marcelja[37] in the Hartree approximation. 4) The difficulty with the MFT approach concerns the need of an equation of motion for the "order parameter". One must know the time dependence to

---

* Above T_c the order parameter is replaced by an average of the corresponding fluctuating quantity.

calculate transport properties such as the conductivity. However, the equation of motion assumed to date[38] has not been firmly established by experiment. Microscopic calculation has shown,[39] in fact, that the time dependent generalization of the Ginzburg-Landau equations now used ought to be valid only in very special circumstances.

In contrast to the phenomenological approach, with a "microscopic" calculation one can treat several interacting field variables.[40] It is possible to treat self consistently, for example, interactions between the superconducting fluctuations and the normal electrons or "quasiparticles".

We can now point out that a significance of the experimental work in this field rests in its ability to test the validity of the time dependent generalizations of MFT. This problem is in fact of major interest at this time. There is a term in the expression for the fluctuation current which appears only in microscopic calculations. This term, the Maki[41] term, is, to first order, the interaction of fluctuations with the sea of normal electrons. If this term is important, the equation for time evolution for the order parameter in the MFT is no longer simple, or even tractable.[39] The importance of the Maki term is measured by the strength of a depairing interaction,[42] invoked[43] to renormalize a divergence due to the Maki term in one and two dimensional geometries. This is discussed further below. It seems worthwhile to emphasize that the concern over the treatment of the depairing interaction, as it affects the importance of the Maki term, is intimately related to the validity of the time dependent generalization of MFT used by most theoreticians.

The choice of boundary condition used to solve the MFT equation of motion, though now also supported by microscopic calculation,[39] can also be considered to be on trial in experimental work such as this.

In calculations of fluctuation effects, a distinction is made, principly the basis of computational ease, between two regimes of behavior. When the effects of superconductivity creating fluctuations are small, it turns out that the lifetimes of superconducting regions created by these fluctuations are quite long. This allows calculation of their effects by essentially non quantum mechanical means. Thus there is an interval in reduced temperature, Υ, generally characterized by the condition $\sigma' \ll \sigma$, which has earned the name "classical regime". Where interactions between superconductivity creating fluctuations become important, the theoretical situation becomes much more difficult. Any of a large number of terms in a perturbation expansion for the fluctuation current could well contribute. Clearly the theoretical problem is to estimate the importance of these contributions. This latter regime in reduced temperature is called the critical one. Theoretical contributions to superconducting behavior at critical temperatures have most often been treatments of a "next term" giving its temperature dependence but with no hard estimates of its importance beyond an a posteriori comparison with existing data.

This distinction between classical and critical behavior is a somewhat artificial one. For instance, the Maki term is generally considered of importance in the classical region. The theoretical situation with this term is cloudy. What can be gathered from the literature will nevertheless be summarized below.

In the section below, we will begin the survey of the theoretical situation with the pioneering work of Aslamasov and Larkin. We then mention the corrections to, and elaborations on that model. The results of several calculations treating the resistive behavior in the critical region are summarized next, followed by a summary of the work that has been done on the region below T_c. A simple way to test for the commonly predicted power law dependence of extra conductivity on reduced temperature, due to Testardi *et al.*,[(34)] is then presented. We complete the theoretical survey with a discussion of the effects of magnetic and electrostatic fields on superconducting fluctuations.

Fluctuation Effects Above T_c

The first substantial theoretical contribution to the effects of fluctuations on the resistive transition of a superconductor was made by Aslamasov and Larkin[23] (AL). With a microscopic calculation which took into account the first order contributions in the pair fluctuations, they found

$$\sigma'_{AL}(3D) = \frac{e^2}{32\hbar\,\xi(0)\,\tau^{1/2}}$$ for sample thickness $d \gg \xi(T)$ (Three dimensional or 3D limit)

$$\sigma'_{AL}(2D) = \frac{e^2}{16\hbar\, d\, \tau}$$ for $d \ll \xi(T)$ (Two dimensional or 2D limit)

where $\xi(0)$ is the temperature independent part of the coherence length $\xi(T) = \xi(0)/\tau^{1/2}$, and $\tau = (T - T_c)/T_c > 0$. These results were later obtained within the framework of the Ginzburg-Landau theory by Abrahams and Woo,[44] H. Schmidt,[45] and A. Schmid.[46]

Although Abrahams and Woo obtained a factor (ln2) not gotten by the other authors,[66] they did point out correctly that, far from T_c, τ should be replaced by $\ln(T/T_c)$.

Testardi et al.[34] have evaluated the (AL) expression for σ' for films of arbitrary thickness. They get $\sigma' = \sigma'_{AL}(2D) \cdot G(T)$, where G(T) can be written as

$$G(T) = \frac{1}{2}\left(1 + \frac{d}{\xi(T)} \coth \frac{d}{\xi(T)}\right) .$$

The conditions for validity of this expression are

$$\sigma' \ll \sigma_n \quad \text{and} \quad \tau \gg \tau_0 = \frac{\sigma'(\tau = 1)}{\sigma_n}$$

These authors note that failure of the last condition has the result of renormalizing T_c and of changing the theoretically predicted value of R(T). The renormalized values become: $T_c^* = T_c(1+A\tau_0)$ and $R^*(T) = R(T)(1+A\tau_0)$, where A is the coefficient of a $\left(\frac{\tau_0}{\tau}\right)^2$ term neglected in the (AL) expression for σ'.

Testardi et al. also find that the 2D limit for σ' is obtained to within a few per cent for $(d/\xi(T)) < \frac{1}{2}$ and that the 3D limit for σ' is obtained to within a few per cent for $(d/\xi(T)) > 2$. The middle of the 2D-3D transition is at $d = \xi(T)$.

The form of the (AL) result used in comparison with the data here is:

$$\sigma' = \frac{e^2}{32\hbar d \ln\left(\frac{T}{T_c}\right)} \left(1 + \frac{d}{\xi(T)} \coth \frac{d}{\xi(T)}\right)$$

where $\xi(T) = \xi(0) \cdot \left(\frac{T}{T_c}\right) \Big/ \left(\ln\left(\frac{T}{T_c}\right)\right)^{1/2}$

and $$\xi(0) = 0.85\,(\ell \cdot \xi_0)^{1/2} \;*$$

This contains the modifications suggested by Abrahams and Woo.

We consider next the attempts to extend the above results. These take into consideration: 1) effects associated with the strong coupling(47,48) nature of some superconducting materials, 2) effects associated with depairing(42,49,43,36) interactions, and 3) corrections arising from contributions to σ' neglected by (AL) such as the "Maki term."(41) All of these corrections are in the end bound together in a way yet to be worked out. In the absence of this complete theory, we present the modifications as more or less distinct.

Maki's correction gave an extra conductivity, σ'_M, which could be simply added to the A.L. result. In Maki's original calculation, however, σ'_M diverged for temperatures above T_c for 1D and 2D geometries.

Somewhat later, Thompson(43) introduced a cutoff into the divergent momentum integrals in the Maki expressions for σ' in two dimensions. The cutoff was associated with a depairing interaction(36) intrinsic to the conduction mechanisms at force in a superconductor, or due to mag-

---

* ℓ is the mean free path for normal conduction electrons, ξ_0 is the BCS coherence length. This expression corresponds to the "dirty limit", $\ell < \xi_0$.

netic impurities or an external magnetic field. Thompson expressed the cutoff in terms of a transition temperature, T_{co}, which could be thought of as the transition temperature in the absence of the depairing interaction. The "Maki-Thompson"(MT) expressions are given below:

$$\sigma'_{MT}(\text{2D and 3D}) = \sigma'_{AL}(\text{2D \& 3D}) + \sigma'_{M}(\text{2D \& 3D})$$

$$\sigma'_{AL}(\text{2D \& 3D}) = \frac{e^2}{32 d \tau \hbar}\left(1 + \frac{d}{\xi(T)} \coth \frac{d}{\xi(T)}\right)$$

$$\sigma'_{M}(\text{2D \& 3D}) = \frac{e^2}{8 d \tau \hbar}\left(\ln\left[\frac{\xi(0)}{d\tau_c^{1/2}} \sinh \frac{d(\tau+\tau_c)^{1/2}}{\xi(0)}\right] + \frac{1}{2}\ln\left(\frac{\tau+\tau_c}{\tau_c}\right)\right)$$

$$\sigma'_{MT}(\text{2D}) \xrightarrow[\xi(T) > d]{} \frac{e^2}{16\hbar d\tau}\left(\frac{1}{1+\frac{\tau_c}{\tau}} + 2\ln\left(\frac{1+\frac{\tau_c}{\tau}}{\frac{\tau_c}{\tau}}\right)\right)$$

$$\sigma'_{MT}(\text{3D}) \xrightarrow[\xi(T) < d]{} \frac{5}{32} \cdot \frac{e^2}{\hbar \xi(0) \tau^{1/2}}$$

where $T > T_c$ and $\tau = (T - T_c)/T_c$

and $\tau_c = (T_{co} - T_c)/T_c$

Thompson's calculations were for weak depairing:

$\sigma' \ll \sigma \tau_c$ for the 2D limit,

$\sigma' \ll \sigma (\tau \tau_c)^{1/2}$ for the 3D limit,

and generally for $\tau_c \leq 0.1$.

It is not obvious that the (AL) contributions are unchanged, as indicated above, in this weak depairing limit. The 3D expression looks particularly suspicious in this respect since it is independent of the "depairing parameter" τ_c .

Hohenberg[50] has recently extended some of Thompson's calculations to situations where there is strong depairing. He finds, among other things, that the (AL) terms are changed:

$$\sigma'_M(3D) \underset{\tau_c \gg \tau}{\sim} \frac{e^2}{8\hbar\xi(0)\,\tau_c^{1/2}} \left(1 - \left(\frac{\tau}{\tau_c}\right)^{1/2} + O\left(\frac{\tau}{\tau_c}\right)\right)$$

$$\sigma'_M(2D) \qquad \text{(not calculated)}$$

$$\sigma'_{AL}(3D) \underset{\tau_c \gg 1}{\sim} \frac{3}{8\pi^3} \cdot \frac{e^2}{\hbar\xi(0)\,\tau^{1/2}} \cdot \tau_c$$

$$\sigma'_{AL}(2D) \underset{\tau_c >> 1}{\longrightarrow} \frac{3}{4\pi^3} \cdot \frac{e^2}{\hbar d \tau} \quad \tau_c$$

$$\sigma'_{TOTAL}(3D) \longrightarrow \frac{e^2}{8\hbar \xi(0) \tau^{1/2}} \left(\frac{3}{\pi^3} \tau_c + \left(\frac{\tau}{\tau_c} \right)^{1/2} \right)$$

$$\longrightarrow (.387 \, \tau_c) \frac{e^2}{32 \hbar \xi(0) \tau^{1/2}}$$

for $\tau_c >> \tau$ and $\tau_c >> 1$

$$\sigma'_{TOTAL}(2D) \qquad (\text{not calculated}) \quad .$$

Hohehberg also verifies the Thompson results, listed above, in the weak depairing limit.

For the intermediate case of $\tau_c \sim 1$, or $\tau_c \sim \tau$ the general behavior of σ'_{TOTAL} is not known. Hohenberg gives only the expression for $\sigma'_M(3D)$:

$$\sigma'_M(3D) \approx \frac{e^2}{8\hbar \xi(0)} \left(\frac{\tau^{1/2} - \tau_c^{1/2}}{\tau - \tau_c} \right) \quad .$$

It should be emphasized that the status of these results is uncertain. The major question concerns the importance of higher order terms, of which the Maki term is the first. An estimate of smallness of these terms, made by Thompson[43] and used with hesitation by Hohenberg,[50] is by no means universally accepted.[51]

We leave this topic to discuss a modification to (AL) that fares only a little better.

The Aslamasov-Larkin results are based on the weak coupling B.C.S.[52] theory of superconductivity. One might expect different results for a strong coupling[47] superconductor. Fulde and Maki[48] have shown that in the absence of a depairing interaction, the effects of strong coupling are simply a renormalization of the relaxation frequency,[38] $\Gamma(T)$, of superconducting fluctuations. $\Gamma(T)$ is increased by a factor, $\alpha \geq 1$, called the strong coupling parameter. α =1 for a B.C.S. superconductor. Thus σ' is reduced by $1/\alpha$. When there is depairing, Maki and Fulde comment only that the situation is complicated.

Eilenberger and Ambegaokar[53] offer an expression with which the strong coupling constant can be estimated. Because of the material parameters which enter this expression, the use of it is a bit messy. So we make this estimate in the next chapter and pass on to a discussion of the critical region.

The Critical Region

In the critical region, a number of different terms contributing to σ' have been treated by different authors, each with its generally distinct temperature dependence. There is no unanimity as to which is the dominant contribution beyond assurances by each author that his results give the leading corrections, only, as T approaches T_c.

Early in this game(1967) Ferrel and Schmidt(21) used scaling law arguments to arrive at a $\tau^{-3/2}$ dependence for a 2D sample. A year later, Tzusuki and Kawasaki(54) found terms in σ' going like $\tau^{-1/3}$ for 3D and like τ^{-1} for 2D.

Tzusuki,(55) in a later more detailed calculation of the dynamic conductivity, confirmed the $\tau^{-1/3}$ dependence in three dimensions in the static limit, but found terms divergent in frequency in both the classical and critical regions in 2D. The divergent terms arose from the Maki contributions to the conductivity mentioned above. Disregarding these terms in the 2D case on experimental grounds, Tzusuki found the same τ^{-1} dependence in 2D in the critical region as in the classical. The two 2D expressions for σ' differ only in their prefactor:

$$\frac{\sigma'(2D)_{critical}}{\sigma'(2D)_{classical}} \cong \frac{1}{1+\gamma}$$

where he estimates: $\gamma \cong 0.18$

If one were to introduce a cutoff, ω_c , into the Tzusuki 2D expressions , one finds contributions which go like:

$$\sigma'(2D)_{\text{critical}} \sim \tau^{-1} \ln \left| \frac{16\sqrt{2}}{21\,\zeta(3)} k_F^2 \, l \, d \, \tau^2 \frac{k_B T_c}{\hbar \omega_c} \right|$$

$$\sigma'(2D)_{\text{classical}} \sim \tau^{-1} \ln \left| \frac{8}{\pi} \tau \frac{k_B T_c}{\hbar \omega_c} \right|$$

Estimates of the extent of the critical region appear in most of the papers mentioned in the above paragraphs. With the exception of Ferrel and Schmidt, they agree with the results which we use here, which are due to Hurault and Maki:[56]

$$\tau_{\text{critical}} \begin{cases} \cong \left(k_F^4 l^3 \xi_0\right)^{-1} & \text{in } 3D \\ \cong \left(k_F^2 l d\right)^{-1} & \text{in } 2D \end{cases}$$

For convenience we pause here to estimate these numbers:

$$(T_{\text{critical}} - T_c) \begin{cases} \cong 1\,m^\circ K & \text{for } 3D \\ \cong 2\,m^\circ K & \text{for } 2D \end{cases}$$

We have used (see next chapter):

$$K_F \cong 1 Å \quad ; \quad l \cong 3 Å \quad ; \quad \xi_0 \cong 600 Å \; .$$

Hurault and Maki also estimate the effects of critical fluctuations on the conductivity in the classical region. These effects appear as a renormalization of T_c. If T_c^* is obtained by fitting a "classical" expression to data from the classical regime, and T_c the "actual" T_c, the find:

$$T_c^* - T_c = (2.4)T_c \cdot \left(\tau_{critical}^{(2D)}\right) \cdot \left(1 + \ln \tau\right)$$

in the 2D limit. Using this we expect to find $T_c^* = T_c - 30m^{o}K$ for our samples. In the 3D limit we assume the same expression holds with the replacement of $\tau_{crit.}^{(2D)}$ by $\tau_{crit.}^{(3D)}$.

There $T_c^* = T_c - 80m^{o}K$.

<u>The Conductivity Below T_c</u>

Contributions to the extra conductivity below T_c have been calculated by Marcelja <u>et al.</u>,[37,32] by Schmid[57] and by Schmidt.[58]

In the Marcelja papers and explicit result is written down only for the 2D limit. An expression is given from which the 3D behavior could be obtained numerically, but this calculation has not been done. The 2D result has the limiting form:

$$\sigma'(2D) \sim \frac{e^2}{16\hbar d} F(T) \qquad ,$$

$$F(\tau) = \frac{\left(\frac{\hbar^2}{2m\xi^2(0)}\right)}{k_B T} \exp\left\{4|\tau| \frac{U_{co}^2 d\, \xi^2(0)}{k_B T}\right\}$$

for $T \ll T_c$. Unfortunately this condition probably does not allow us to use this expression. More detailed calculations generalizing this last expression for use near T_c are still in progress.(59) The expression from which 3D behavior can be calculated is:

$$\sigma'(3D) = \frac{e^2}{32\hbar\, \xi(0)} \left(\frac{R}{\xi(0)}\right)$$

Where $1 = \frac{R^2}{\delta}\left(a + b\frac{k_B T Q}{2\pi^2\delta}\left(1 - \frac{\tan^{-1} QR}{QR}\right)\right)$ (A).

In terms of the Ginsburg-Landau parameters(15),

$$R = \left(\delta / \left(a + b \langle|\psi|^2\rangle\right)\right)^{1/2} ;$$

Q is a momentum cutoff $\sim 1/\xi(0)$. The above authors note that $a + b\langle|\psi|^2\rangle$ is nonzero (and thus $\sigma'(3D)$ finite) only for temperatures above a "new" critical temperature T^*, analogous to the Bose-Einstein condensation temperature. To find T^* they set $1/R = 0$ and $T = T^*$ in (A) to obtain

$$1 + \frac{b k_B T^* Q}{2\pi \delta^2} \xi^2(T^*) = 0$$

With an assumption regarding $\xi^2(T)$ for $T < T_c$ which is difficult to understand,[‡] they obtain(correcting some misprints):

$$\frac{T_c - T^*}{T^*} \cong b \frac{k_B T_c \xi(0)}{2\pi^2 \delta^2}$$

$$\cong \frac{k_B T_c}{2\pi H_{co}^2 \xi^3(0)}$$

‡ One must assume either $\xi^2(T)/\xi^2(0) < 0$ or $T^* > T_c$ for this expression to hold.

Marcelja's calculations have recently been criticized by Mikeska and Schmidt,[60] who point out that Marcelja has the order parameter relax to zero average value below T_c. This may be related to Marcelja's second T^* and the odd temperature dependence of $\xi(\tau)$ he must assume for $T^* < T < T_c$. but the connection is not clear. The criterion for 2D and 3D behavior ought also to be mentioned. It is not clear in Marcelja's calculation whether $\xi(\tau)$ or the length R (mentioned above) is the important parameter in this regard. Mikeska and Schmidt claim that two dimensional behavior of σ' is to be expected for $(\rho/d) \ll 1$ for $T < T_c$, where d = sample thickness and ρ = an unspecified distance in the film plane.

Test For Power Law Dependence on $(T-T_c)/T_c$

Testardi *et al.*[34] have pointed out that if σ' has a power law dependence on τ above T_c, then there is a method of analysis of the data that tests for this temperature dependence, gives the power of τ and is insensitive to the choice of T_c. A slight modification of this result is necessary for our use, where the normal resistance has a temperature dependence.

Suppose that $\sigma'(\tau) = \sigma'(1)\, \tau^{-n}$. Multiplying by the normal resistivity $\rho_n(T)$, we get:

$$\mathcal{R}_x \equiv \frac{R_n(T) - R(T)}{R(T)} = \left(\sigma'(1)\, d\, \frac{W}{X}\right) \frac{R_n(T)}{\tau^n}$$

Differentiating with respect to T and multiplying by $1/R_n(T)$, we get:

$$\frac{1}{R^2}\, \frac{dR}{dT}$$

$$= \frac{1}{R_n R}\, \frac{dR_n}{dT} - \sigma'(1)\, d\, \frac{W}{X} \left(\frac{1}{R_n \tau^n}\, \frac{dR_n}{dT} - \frac{n}{\tau^{n+1}\, T_c} \right)$$

$$= \frac{1}{R_n R}\, \frac{dR_n}{dT} - \frac{\mathcal{R}_x}{R_n^2}\, \frac{dR_n}{dT} + \frac{n}{T_c R_n} \left(\sigma'(1)\, d \cdot R_n\, \frac{W}{X}\right)^{-\frac{1}{n}} \mathcal{R}_x^{\frac{n+1}{n}}$$

$$= \frac{1}{R_n^2}\, \frac{dR_n}{dT} + \frac{n}{T_c R_n} \left(\frac{\sigma_n(\tau)}{\sigma'(1)} \right)^{\frac{1}{n}} \mathcal{R}_x^{\frac{n+1}{n}}$$

---

* d, w, and x are sample thickness, width and length respectively. The quantity $R_n w/x = \rho_n/d$ is called sample resistance per square.

If the fractional change in $R_n(T)$ is small in the temperature interval over which τ^{-r} behavior exists, then a plot of

$$\log(D) \quad \text{vs.} \quad \log(\mathcal{R})$$

where
$$D = \frac{1}{R^2}\frac{dR}{dT} - \frac{1}{R_n^2}\frac{dR_n}{dT}$$

and
$$\mathcal{R} = \frac{R_n(T) - R(T)}{R(T)}$$

produces a straight line of slope $(r+1)/r$. The coefficient of $\mathcal{R}^{\frac{r+1}{r}}$ can be evaluated at a conventient pair of values $(D, \mathcal{R})$.

The above analysis does not indicate whether one might expect other than power law dependence on τ from straight line behavior on log-log plots. To answer this question we must integrate the differential equation:

$$D = \beta \mathcal{R}^{\alpha}$$

where α is the slope of the data on the log-log plot. For simplicity, we will assume that $R_n(T)$ = const.*

Above T_c, $\frac{1}{R^2}\frac{dR}{dT} = \beta \mathcal{R}^{\alpha}$ and $\tau = \frac{T}{T_c} - 1$

lead to

$$\frac{d\mathcal{R}}{d\tau} = -R_n T_c \beta \mathcal{R}^{\alpha} \ .$$

If $\alpha = 1$, and if σ' is finite at Tc, then

$$\sigma'(\tau) = \sigma'(0)\, e^{-R_n T_c \beta \tau} .$$

If $\alpha \neq 1$, then

$$\sigma'(\tau) = \left(\sigma'(0)^{1-\alpha} - \beta R_n T_c (1-\alpha)\, \tau\, \sigma_n{}^{1-\alpha}\right)^{1/(1-\alpha)} .$$

If $\alpha > 1$, let $1/(\alpha - 1) = n > 0$. Then

$$\sigma'(\tau) = \sigma_n \left(\frac{\beta R_n T_c \tau}{n} + \left(\frac{\sigma_n}{\sigma'(0)} \right)^{\frac{1}{n}} \right)^{-n} .$$

---

* Without this assumption, the solution to the resulting Bernoulli equation is substantially more complicated. The behavior is, however, the same as that obtained above to a very good approximation in the temperature range of interest.

If furthermore, $\sigma'(\tau)$ diverges at T_c, then

$$\sigma'(\tau) = \sigma_n \left(\frac{n}{\beta R_n T_c}\right)^n \Big/ \tau^n$$

in agreement with the results of Testardi et al.

If $\alpha < 1$, let $1/(1-\alpha) = s > 0$. Then

$$\sigma'(\tau) = \left(\sigma'(0)^{1/s} - \frac{\beta R_n T_c \tau}{s} \sigma_n^{1/s}\right)^s.$$ Here either

$\sigma' = \infty$ or σ' has nonphysical τ dependence.*

It will be useful to look into the interpretation of straight line segments of data below an assumed T_c on a plot of log(D) vs. log($\mathcal{R}_x$). If we define τ' as $1-(T/T_c)$, such linear portions of data, with slope α, are equivalent to $\frac{d\mathcal{R}_x}{d\tau'} \cong R_n T_c \beta \mathcal{R}_x^{\alpha}$. If $\alpha = 1$, integration gives $\sigma'(\tau') = \sigma'(0)\, e^{R_n T_c \beta \tau'}$ for finite $\sigma'(0)$. If $\alpha \neq 1$, we obtain

$$\sigma'(\tau') = \left(\sigma'(0)^{1-\alpha} + \beta R_n T_c (1-\alpha) \tau \sigma_n^{1-\alpha}\right)^{1/(1-\alpha)}.$$

---

* σ' decreases as the temperature decreases.

When $\alpha < 1$, we can set $1/(1-\alpha) = s > 0$. Either $\sigma'(\tau')$ is infinite or finite below T_c. If $\sigma'(0)$ is finite, we find

$$\sigma'(\tau') = \left(\sigma'(0)^{1/s} + \frac{\beta R_n T_c \tau'}{s} \sigma_n^{1/s} \right)^s .$$

On the other hand, if the slope of the data, α , is greater than one, we define $1/(\alpha - 1) = n > 0$ to find

$$\sigma'(\tau') = \sigma_n \left(\left(\frac{\sigma_n}{\sigma'(0)} \right)^{1/n} - \frac{\beta R_n T_c \tau'}{n} \right)^{-n}$$

Here again, $\sigma'(\tau')$ has a nonphysical τ' dependence, ($\sigma'(\tau')$ decreases as the temperature decreases).

We gather from the observations above that on plots of log(D) vs. log($\mathcal{R}_x$) that <u>a slope of less than one is not consistent with the assumption that the data with this slope lies above T_c.</u> Similarly, <u>slopes greater than one are inconsistent with the assumptions that the data is below T_c.</u>

For later convenience we write the expression for the prefactor $\sigma_n'(1)$ in $\sigma'(\tau) = \sigma_n'(1)/\tau^n$ in terms of the constants β_n which can be gotten from the data on a log-log plot of

$$D = \beta_n \mathcal{R}_x^{(n+1)/n} :$$

$$\sigma_n'(1) = \sigma_n \left(\frac{n}{\beta_n T_c R_n} \right)^n$$

Where the data on the log-log analysis shows slope one

$$\left(D = \beta R \right) : \quad \sigma'(\tau) = \sigma'(0)\, e^{-\tau/\tau_1}$$

where $\tau_1 = 1 / (\beta T_c R_n)$.

The results of this section will be used in the analysis of the data in chapter 4.

Fluctuation Effects in a Magnetic Field

Because of experimental difficulties associated with measurements in magnetic fields oriented parallel to the sample, only results concerning perpendicular fields will be discussed.

Expressions describing the magnetic field behavior of fluctuations in the classical regime have appeared in the earliest theoretical literature.(23,41,49,61) We here quote only the most recent results, which are consistent with earlier literature.

We have chosen to compare our data with the calculations of magnetic field behavior above T_c made by Abrahams, Prange and Stephens.(62) The expression which they give for the effect of magnetic fields in the 2D limit of the classical regime is:

$$\sigma'(2D) = \sigma_{AL}'(2D)\; 8x^2 \left(\psi\left(\tfrac{1}{2}+x\right) - \psi(1+x) + 2x \right)$$

ψ = digamma function , $x = \tau/(2h)$,

$h = H \cdot \xi^2(0)/\phi_0$, ϕ_0 = flux quantum ,

H = magnetic field .

This expression is derived within the context of the Ginzburg-Landau formalism, and so does not contain the contribution due to the Maki term. The corresponding expression for the 3D limit is:(63)

$$\sigma'(3D) = \sigma'_{AL}(3D) \cdot S(x) ,$$

$$S(x) = 4x^{1/2} \sum_{m=1}^{\infty} \left(\frac{1}{\sqrt{m-\frac{1}{2}+x}} + \frac{1}{\sqrt{m+\frac{1}{2}+x}} - \frac{2}{\sqrt{m+x}} \right) ,$$

x defined as above .

These calculations have also been made by Usadel.(64) This author obtains the same results except that τ is replaced by $\ln\left(\frac{T}{T_c}\right)$.

Expressions also exist for the extra conductivity in both parallel and perpendicular magnetic fields which contain the effect of the Maki term with cutoff.(65) Since assumptions regarding the depairing parameter make these results inapplicable to our samples, they will not be reproduced here.

<u>Nonohmic Behavior of the Extra Conductivity</u>

The calculations discussed up to this point have been made with the assumption that the electric field, E , used in the measurement of the resistance, is small enough not to perturb the fluctuation lifetime. For E sufficiently large, electrons within a region of fluctuation superconductivity can be accelerated to the critical velocity before they can traverse the superfluid portion of the sample. Such events contribute to the so-called nonlinear, or nonohmic, behavior of the sample resistance in the transition region.

Hurault[60] has calculated $\sigma'(E)$ due to such effects, using the time dependent Ginzburg-Landau equation. He found for $T > T_c$, a critical value of E:

$$E_c(T) = \frac{k_B T_c}{e\,\xi(T)} \cdot \frac{4\sqrt{3}}{\pi} \cdot \tau$$

below which the Aslamasov-Larkin value of σ' , σ'_{AL} is recovered. For $E \gg E_c(T)$, Hurault finds:

$$\sigma'_{Hurault}(3D) = \sigma'_{AL}(3D) \left(\frac{E_c(T)}{E}\right)^{1/3} \left(2\sqrt{3}\right)^{-1/3}$$

$$\sigma'_{Hurault}(2D) = \sigma'_{AL}(2D) \left(\frac{E_c(T)}{E}\right)^{2/3} \left(2\sqrt{3}\right)^{-2/3} .$$

If we take, for our samples, a coherence length of 35Å and $T_c = 11$ K, we find $E_c(T) = (7 \times 10^3 \text{volts/cm}) \cdot \tau^{3/2}$

$$\approx \begin{cases} 7\text{V/cm}, \text{for } T-T_c = 0.1 \text{ K} \\ 7\text{mV/cm}, \text{for } T-T_c = 1\text{m K} \end{cases}$$

Tsuzuki,[67,68] with a microscopic calculation which disregards the Maki term (and is valid only above the critical region), found the more general expressions:

$$\sigma'(3D) = \sigma'_{AL}(3D)\left(1 + \sum_{n=1}^{\infty} (-1)^n \frac{(6n-1)!!}{2^{3n} \cdot n!} \left(\frac{E}{E_c(T)}\right)^{2n}\right)$$

$$\sigma'(2D) = \sigma'_{AL}(2D)\left(1 + \sum_{n=1}^{\infty} (-1)^n \frac{(3n)!}{n!} \left(\frac{E}{E_c(T)}\right)^{2n}\right)$$

for $E < E_c(T)$, and

$$\sigma'(3D) = \sigma'_{Hurault}(3D) \cdot \left(1 + \mathcal{S}_3(E)\right)$$

$$\mathcal{S}_3(E) = \sum_{n=1}^{\infty} \left(\frac{(-1)^n}{n!\,(2n+1)} \frac{\Gamma\left(\frac{2n+7}{6}\right)}{\Gamma(7/6)} \left(\frac{E_c(T)}{E}\right)^{2n/3}\right)$$

$$\sigma'(2D) = \sigma'_{Hurault}(2D) \cdot \left(1 + \mathcal{S}_2\right)$$

$$\mathcal{S}_2(E) = \sum_{n=1}^{\infty} \left(\frac{(-1)^n}{(n+1)!} \frac{\Gamma\left(\frac{n+4}{3}\right)}{\Gamma\left(\frac{4}{3}\right)} \left(\frac{E_c(T)}{E}\right)^{2n/3}\right)$$

for $E > E_c(T)$. The quantities $E_c(T)$ and $\sigma'_{Hurault}$ are those which appear in the Hurault results, above.

Gor'kov,[69] also with a microscopic calculation (no

Maki term), presents explicit results only for 2D behavior. These agree with the expressions gotten by Hurault for 2D and $T > T_c$. Gor'kov, however, appears to claim validity of the results for temperatures below T_c as well. He also obtains a weak field (?) expression:

$$\sigma'(2D) = \sigma'_{AL}(2D) \cdot \pi \cdot \left(\frac{\pi\sqrt{3}}{2} \frac{E_c(T)}{E} \right) \cdot e^{\frac{\pi^2}{\sqrt{3}} \frac{E_c(T)}{E}}$$

We proceed now to the important discussion of the sample parameters which appear in all the theories outlined above, and which must be known to the accuracy with which we want to make comparison with the models.

Sample Parameter Assumptions

Certain sample parameters appear in all expressions for the extra conductivity due to fluctuations. It will be necessary to make assumptions about these parameters in order to compare the above models with our data. Aside from the fairly trivial matters of geometry, the important numbers are the normal resistance, $R_n(T)$, the coherence length, $\xi(0)$, the depairing parameter τ_c and the strong coupling constant α. The most serious problem is associated with the normal resistance.

For most materials on which experimental work has been done, the normal resistance has been directly measurable. Easily obtainable magnetic fields have been sufficient to quench the superconducting fluctuations in these materials. We do not have this advantage. Attempts have been made to realize the normal resistance in our samples in fields up to 100 kOe, but these were unsuccessful. Recent work[70] has shown that the critical field H_{c2} for our material is at least 180 kOe. Other measurements[71] on very high resistivity films such as ours suggest in fact that even these fields might not be enough to quench the fluctuation conductivity near the zero field transition temperature.

We have little alternative but to extrapolate the normal resistance from high temperatures. As discussed in the next chapter, our samples have a negative temperature coefficient of resistance at high temperatures. Even though the relative change in resistance with temperature is about 0.1%/ K, the extrapolation leads to an inevitable ambiguity. So we choose as a first approximation that extrapolated $R_n(T)$ which produces the largest region of "correct" temperature dependence (some power law in τ) in the "log-log" analysis and which is reasonable as an extrapolation. Beyond this we treat $R_n(T)$ as a free parameter.

Although the present inability to measure $R_n(T)$

directly is certainly unsatisfactory, a fundamental question would still remain even if it were measurable. That is, would the measured normal conductivity, $\sigma_n^{meas.}$ be the same as the σ_n which appears in σ' ?

Our material is polycrystalline, not amorphous.* A crystallite will have some characteristic resistivity $\rho_x(T)$. One could associate a different $\rho_g(T)$ to a grain boundary between two crystallites since this at least acts as a scatterer. It could be that in a normal conduction process these two contributions to sample resistivity are averaged over in a way different from that in force in the superconducting state.

The averaging process in the superconducting state itself requires closer examination. It may be (although it seems unlikely) that the resistivity contributions of crystallites and grain boundaries are averaged over differently depending on whether $\xi(T)$ is greater than or less than an average crystallite size. It seems most likely that this sort of consideration would really become important only in the event the coherence length were less than some effective width of a grain boundary.

These problems have been discussed by Abeles, Cohen and Stowell.[72] The results of their analysis suggest

*See discussion in next chapter.

that, so long as $\xi(\tau) >$ grain size, it is possible to assign a single effective mean free path to processes involving fluctuation conductivity. We will assume, on the basis of their results, that we are justified in incorporating the granular nature of our samples into our expression for $\xi(\tau)$, so long as $\xi(\tau) >$ grain size.

To summarize, we must make the following assumptions about the normal resistance: 1) It is obtainable as a reasonable linear extrapolation from high temperatures. 2) The averaging process which yields the normal resistance at high temperatures is the same as the one which would give the normal conductivity in the theoretical expressions for σ'.

There is a similar problem with the value of the coherence length itself. In this analysis, we will assume that $\xi(\tau)$ is given by the expression $H_{c_2}(\tau) = \phi_0 / (2\pi \xi^2(\tau))$ which is essentially a mean field (Ginzburg-Landau) result.

A measurement of $\xi(0)$ is tantamount to a measurement of the mean free path. Again the important question is: Are the processes which limit conduction the same where fluctuation effects are small as they are near or below T_c where, presumably, $\xi(0)$ is measured? We shall tentatively assume that they are.

Almost nothing is known, a priori, about the depairing parameter. It is known that T_c for bulk NbN is about 18 K. So we might not be surprised if T_{co} were near this number. Only qualitative information is known about the source of the depairing interaction in our samples.* So T_c will be treated essentially as a free parameter.

There are many assumptions necessary to estimate the strong coupling parameter. It is most appropriate to discuss these in the next chapter.

* This is discussed in some detail in the next chapter.

CHAPTER TWO: SAMPLE DESCRIPTION

Considering the difficulty in preparing and characterizing disordered thin metallic films, it is important to describe our samples in some detail. We will discuss below the following topics: sample preparation and chemistry, sample selection, mounting and geometry, sample histories, and finally, microscopic and general experimental characteristics. This will be followed by several sections devoted to sample parameters that must be known or estimated before a comparison with theory can be made. This will include a discussion of the strong coupling nature of our material and a description of measurements leading to a number for the coherence length. This chapter ends with a table of characteristics of our samples.

Sample Preparation and Chemistry

The samples used in this study were thin films of $Nb_{.88}Ti_{.12}N$. All samples were fabricated by Y. M. Shy of the Metallurgy Department of the University of Minnesota. The films were prepared by a reactive sputtering technique using separate targets of Nb and Ti in an atmosphere of nitrogen and argon. Details of the sputtering process by which these and other similar samples were prepared are described in Shy's thesis[73] and elsewhere.[74]

The chemical composition of the samples was determined by choice of parameters involved in their preparation and by Auger spectrographic analysis.

Shy has made estimates(73) that indicate the Nb:Ti ratio can vary as much as 1% across the width of our samples. This is due to asymmetrical positioning of substrates with respect to the sputtering source.(75) But the variation of T_c with concentration of NbN vs. TiN is nearly minimum at the composition of these samples (see figure 1). So the estimated spread in T_c due to these nonhomogenieties can be estimated to be only a few millidegrees.

Sample Selection

In preliminary studies, in which another worker, Jon Zbasnik, played a substantial and most helpful role, large classes of samples prepared by Shy were eliminated from candidacy for careful study. These samples, and the reasons for not examining them in detail, deserve some comment. Some of the discarded films were mechanically soft, adhered poorly to the substrates and showed mechanical damage on microscopic examination. Another group of films, all those depositied on single crystal MgO, showed a broad resistence tail at low temperatures. Shy established that these films were nearly discontinuous at cleavage steps, which were about 100μ apart, on this substrate. Another group of samples lacked a characteristic negative temperature coefficient of resistance above liquid nitrogen temperatures. These had been deposited on substrates at elevated temperatures (about 800 K), or had been annealed at that temperature. Samples examined with

Figure 1. Transition Temperatures of Sputtered Thin Films of $Nb_xTi_{1-x}N$ vs. Nb:Ti Ratio. From Y. M. Shy's Thesis.[73]

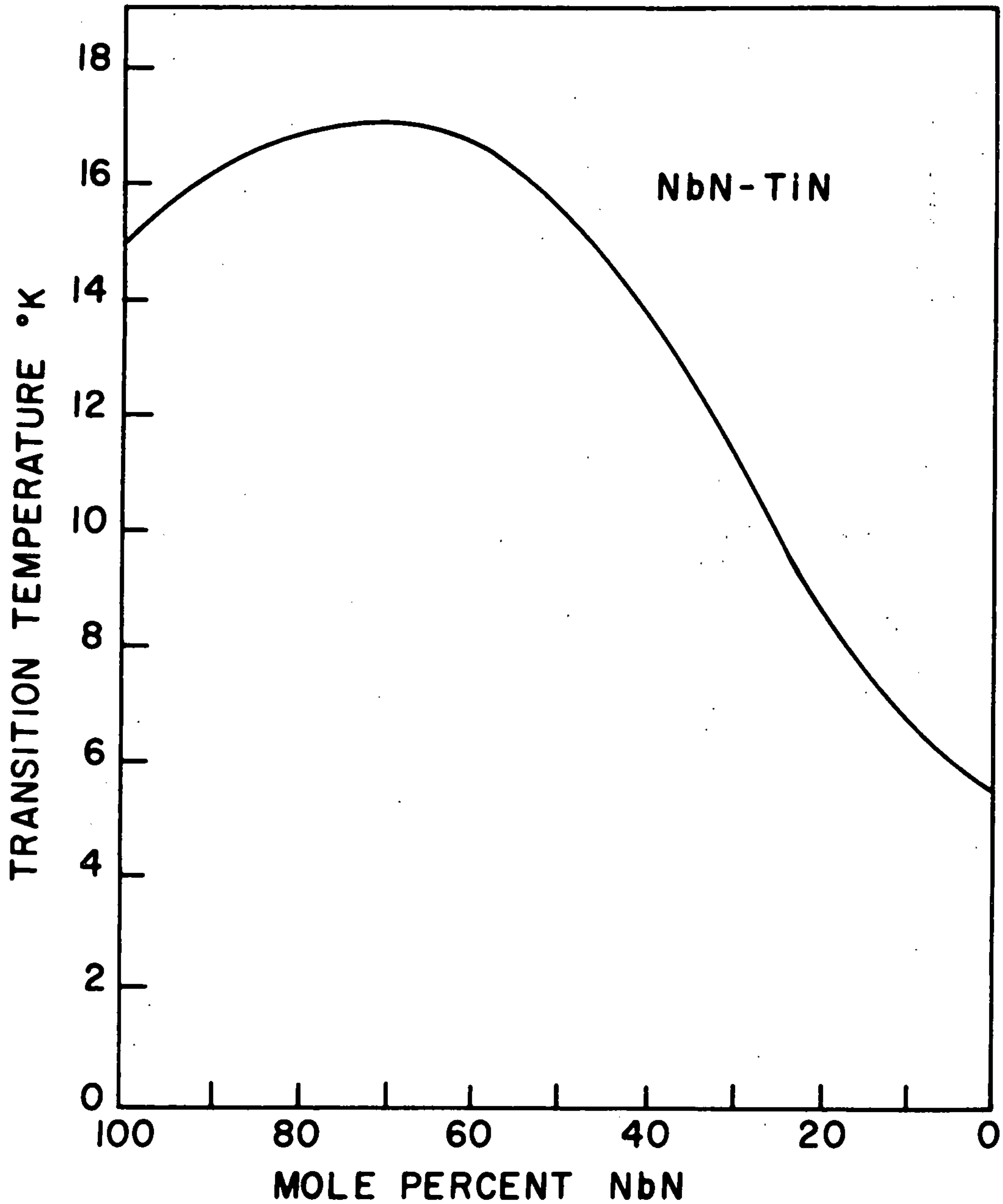

these characteristics had resistive transitions with a stair-step shape indicating regions of different transition temperature. With this process of elimination, we were left with two samples which we felt worth extensive study. It is interesting to note that these two samples had a resistivity well in excess of those eliminated. This can be noted if one compares our resistivities (about 1400 microohm cm.) with that of the samples of similar composition which Zbasnik et al.(70) used in their critical field studies (about 200 microohm cm.). The two samples for which we present data here were numbered "92A" and "92D" by Shy. One of these samples, "92D," was heated excessively in the process of preparing it for high magnetic field measurements in a special cryostat. This produced a small but noticeable change in the shape of its transition. Data taken on this sample after this mistreatment is treated separately here and is identified by means of another label: "92X".

Characteristics of Samples Selected for Study

The films used in this study were generally quite hard and brittle, adhered to the substrate remarkably well, were visibly of uniform appearance down to the scale of length accessable to an optical microscope, and had a notably high resistivity. In simple terms, a stainless steel razor would not scratch the films until damage was done to the substrate beneath the film. The resistivity of the films was the order of 10^3 microohm cm.

In addition, the following general behavior was noted during resistance measurements on the samples selected for study: 1) All had a negative temperature coefficient of resistance at high temperatures. They exhibited a definite maximum in resistance at about 20 K, about ten degrees above their approximate transition temperature. This behavior is illustrated in figures 2 through 4. 2) All samples exhibited a generally small and complicated nonohmic behavior at all temperatures and evidently at all current densities. This is discussed in greater detail in Chapter 5. 3) A monotonically downward shift in transition temperature with time and repeated thermal cycling which accumulated to about a millidegree was also noted. 4) The samples appear to show a negative magnetoresistance above 50 K.

Finally, Shy's[(73)] work on samples similar to these indicates they can be characterized microscopically as granular on the scale of 200Å, with insulating grain boundaries probably containing paramagnetic oxygen impurities. These general characteristics will now be discussed in more detail.

The phenomenon of negative temperature coefficients of resistance in thin films is well known and has been associated with films of granular structure.[(76)] Electron microscope examination[(73)] of films similar to the ones studied here show ours to be similarly granular in structure with an average grain size of 200Å. A typical electron micrograph is shown in figure 5. Presumably this microscopic

Figures 2 through 4.

High Temperature Behavior of Samples Showing Linear Extrapolations to Approximate the Normal Resistance in the Transition Region.

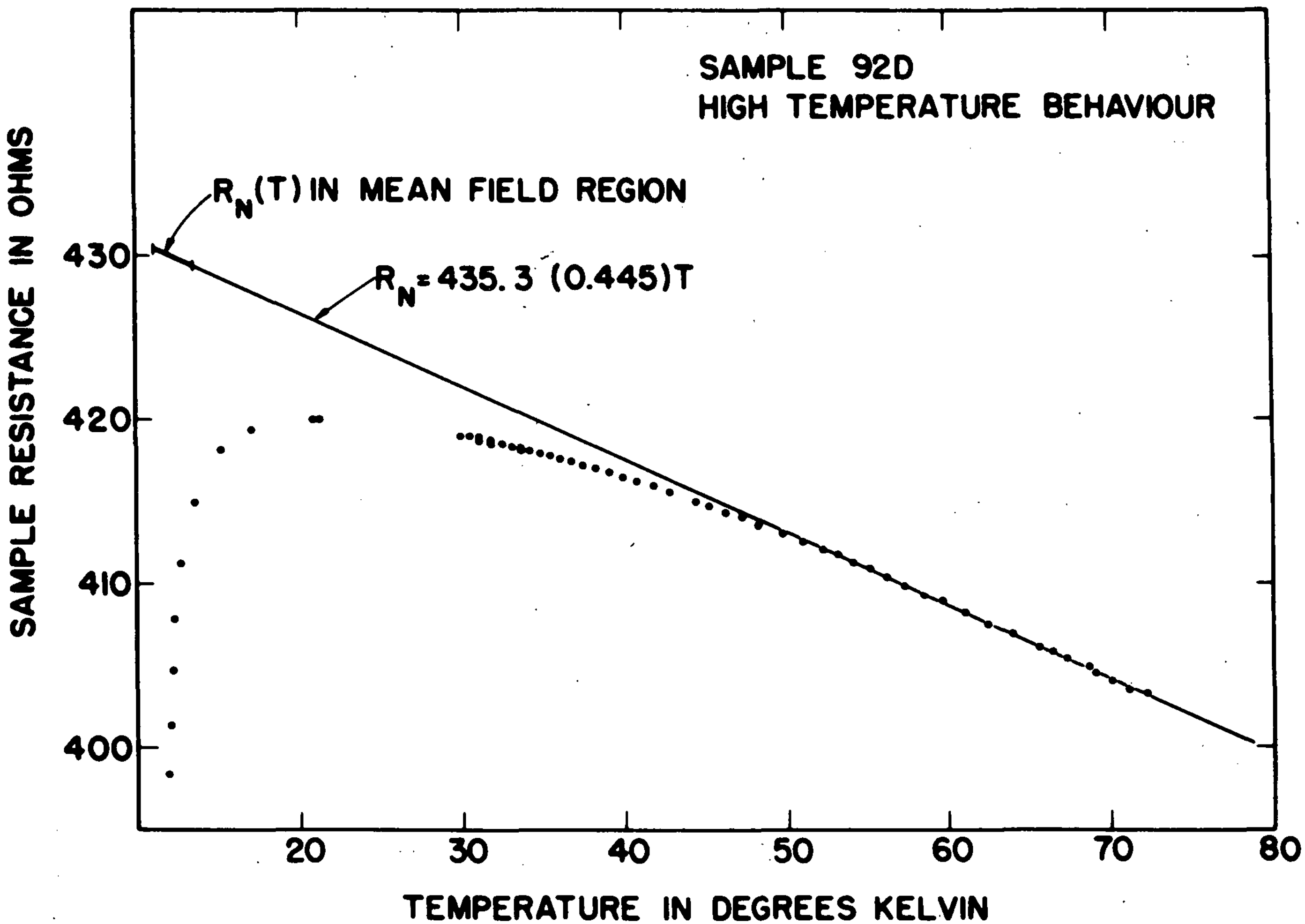
SAMPLE 92D
HIGH TEMPERATURE BEHAVIOUR
R_N(T) IN MEAN FIELD REGION
R_N = 435.3 (0.445)T
430
420
410
400
SAMPLE RESISTANCE IN OHMS
20
30
40
50
60
70
80
TEMPERATURE IN DEGREES KELVIN

FIGURE 2

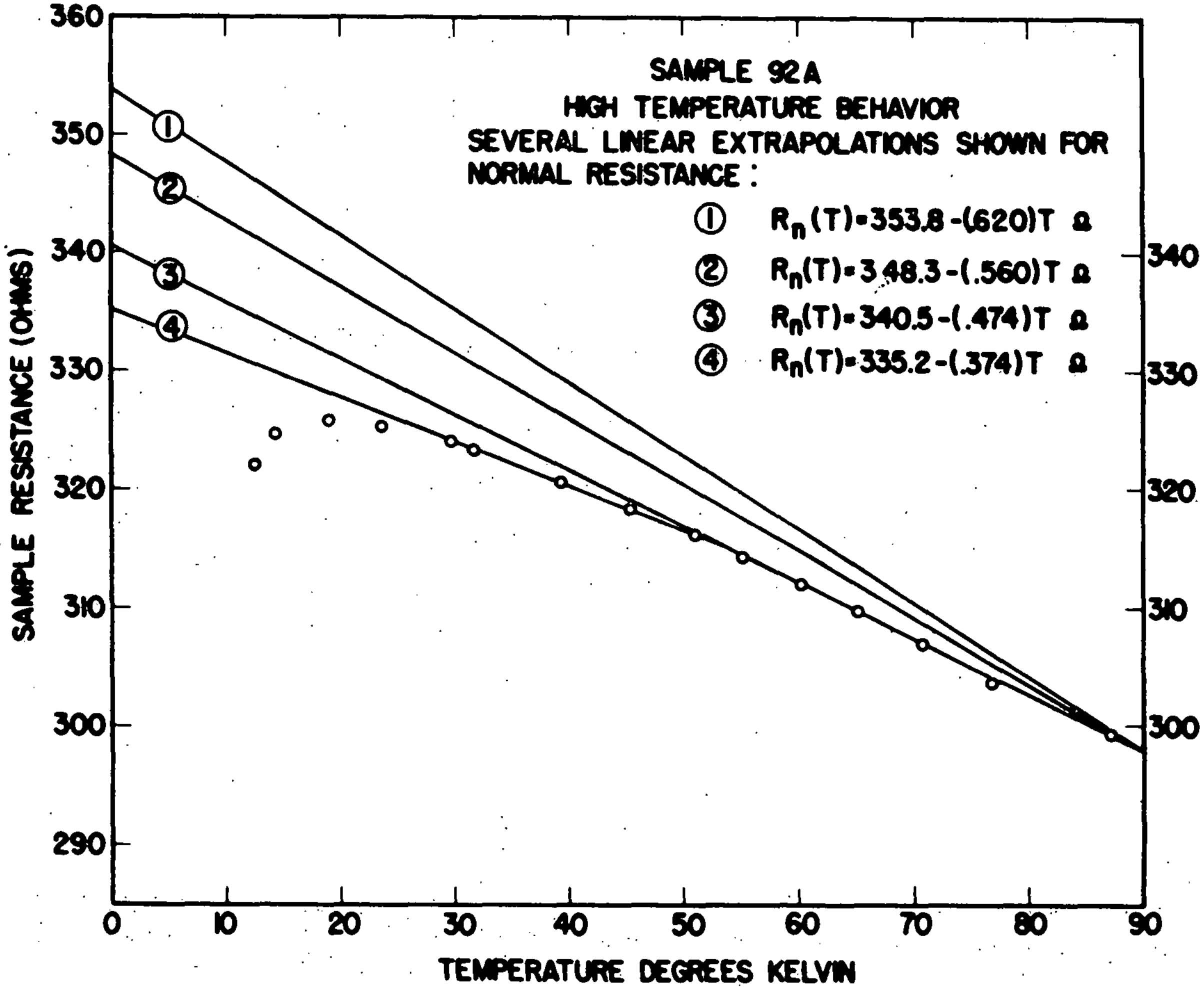
SAMPLE 92A
HIGH TEMPERATURE BEHAVIOR
SEVERAL LINEAR EXTRAPOLATIONS SHOWN FOR
NORMAL RESISTANCE :
① $R_n(T)=353.8-(.620)T$ Ω
② $R_n(T)=348.3-(.560)T$ Ω
③ $R_n(T)=340.5-(.474)T$ Ω
④ $R_n(T)=335.2-(.374)T$ Ω
SAMPLE RESISTANCE (OHMS)
TEMPERATURE DEGREES KELVIN

FIGURE 3

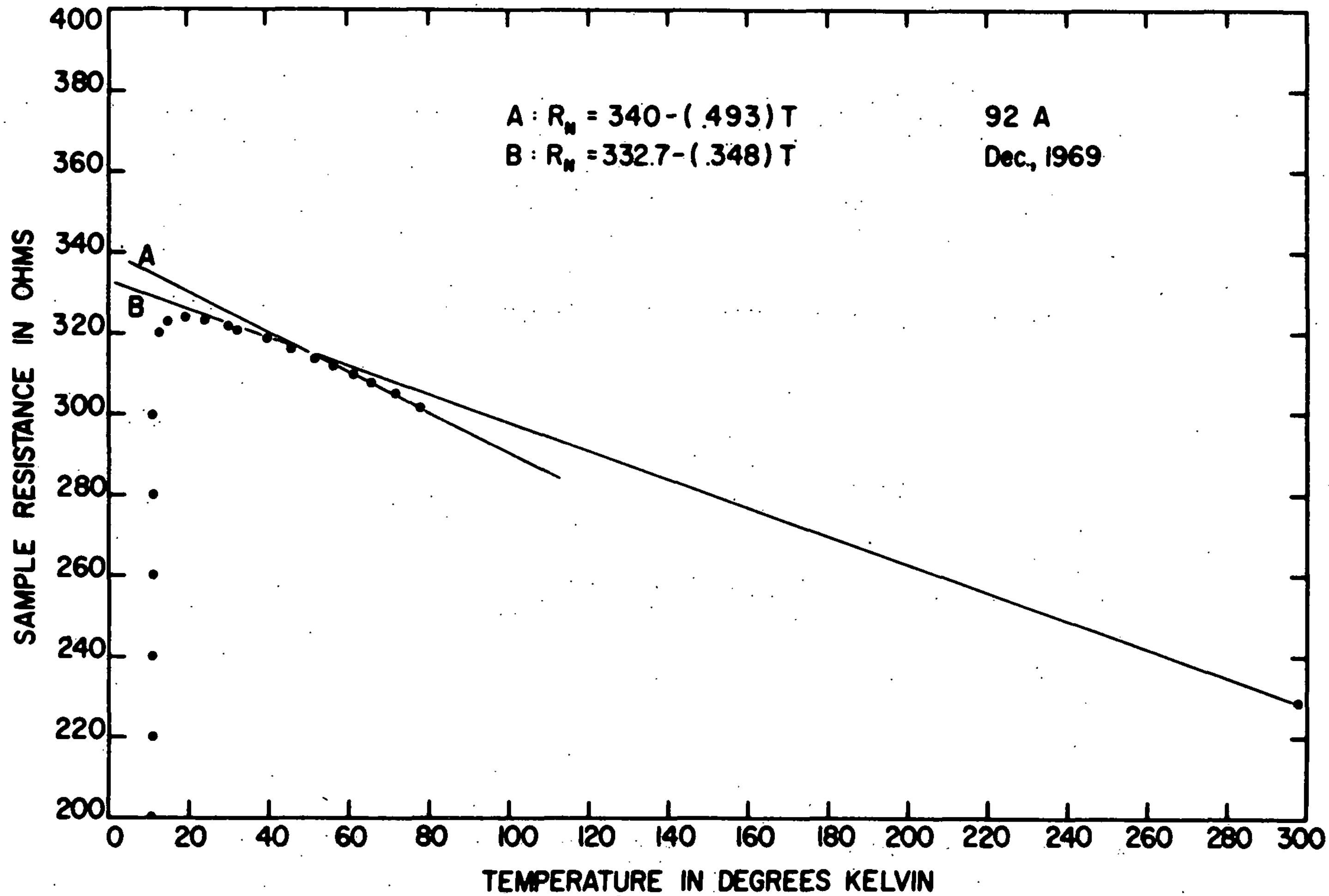

A : R_N = 340-(.493) T
B : R_N = 332.7-(.348) T
92 A
Dec., 1969
SAMPLE RESISTANCE IN OHMS
TEMPERATURE IN DEGREES KELVIN
A
B
400
380
360
340
320
300
280
260
240
220
200
0
20
40
60
80
100
120
140
160
180
200
220
240
260
280
300

FIGURE 4

structure is averaged over in the superconducting transition region as discussed in Chapter 1 (pages 36 and 37). We here want to relate this granular structure to the negative temperature coefficient of resistance and to an impurity to be discussed in the next paragraph.

Auger spectrographic studies on films sputtered in atmospheres identical to those used for our samples have indicated oxygen impurities in these films. A typical Auger spectrum is shown in figure 6. Shy[73] has made the following observations which relate this impurity to the microscopic granular structure. Films sputtered in an atmosphere from which oxygen had been preferentially removed by presputtering with Ti did not have the negative temperature coefficient of resistance at high temperatures. Their resistive transitions were quite narrow. On the other hand, films deposited, as ours were, where oxygen contamination was allowed, all showed a negative temperature coefficient of resistance. They also had at least an order of magnitude higher resistivity and a rounded resistive transition depressed by a few degrees. Annealing of these films at temperatures above 800°C generally resulted in these films assuming the properties of those deposited in the absence of oxygen. These observations led Shy to associate the oxygen content of the films with the grain boundaries and the grain boundaries with the negative temperature coefficient of resistance. This author concurs in

Figure 5.

Electron Diffraction Pattern and Electron Micrograph of $Nb_{.9}Ti_{.1}N_x$ on MgO Substrate. After Shy.[73]

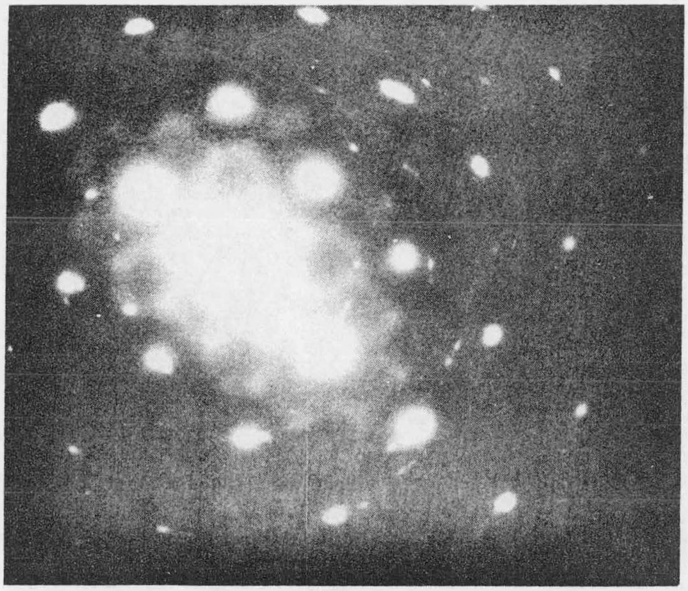

(a)

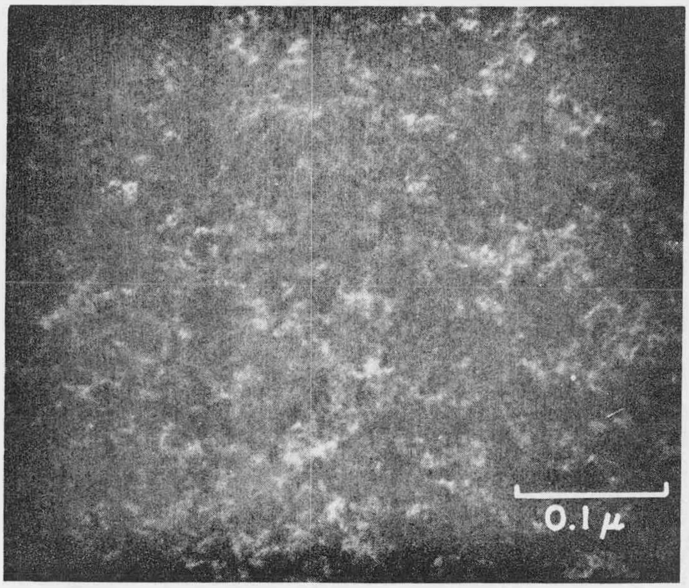

(b)

Electron diffraction pattern and corresponding electron micrographs for a sputter deposited $Nb_{.9}Ti_{.1}N_x$ film (Substrate - MgO, thickness-1500 Å)

(a) NaCl pattern on (100) plane; traces of the diffractions from precipitates are shown.

(b) Electron micrographs corresponding to (a). The dislocation structure is obscure.

<u>Figure 6.</u> Auger Spectrum Showing Oxygen Content Typical of the Sputtered Films Used in This Study. After Shy.(73)

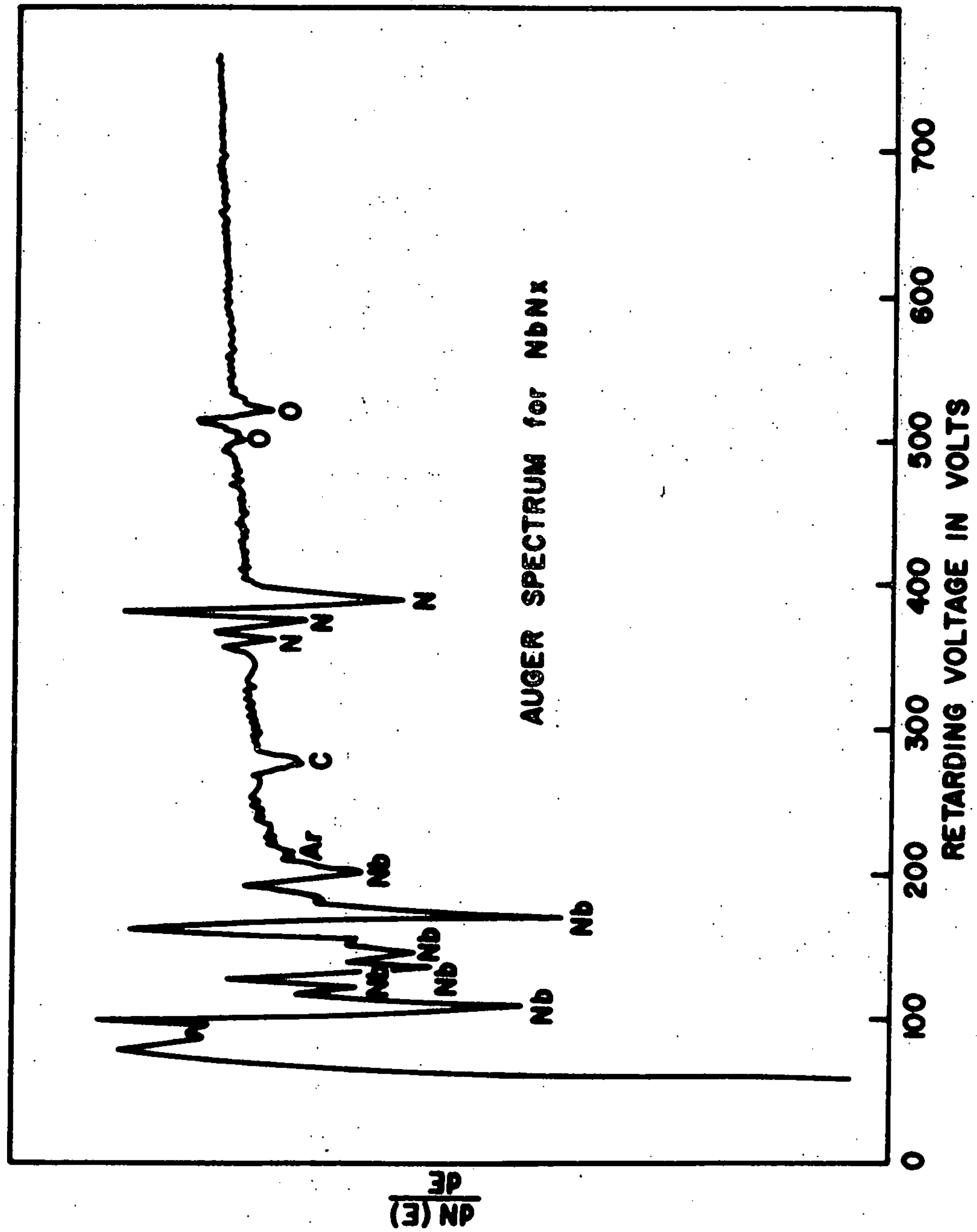

this interpretation. The additional assumption inherent in this study is that this grain structure is averaged over so long as (T) is larger than this grain structure (Chapter 1, pages 36 and 37).

We now discuss the magnetoresistance. This was noticed during an attempt to quench conjectured high temperature superconducting effects with high magnetic fields. During these measurements, increases in resistance at fixed temperatures up to 30 K were noticed in 100 kOe fields. The increases were small enough, however, to be a magnetoresistive effect in the normal sample. Measurements at even higher temperatures showed in fact a change in resistance in the opposite direction in high fields. This is the negative magnetoresistance spoken of above. Although magnetoresistance in the temperature controlling thermometer as a cause of this observed behavior cannot be ruled out entirely, it is highly unlikely. The observed thermometer magnetoresistance at 4.2 K is too small(see Chapter 3). Also changes in heater quiescent current were suspiciously unnecessary if this were to have been thermometer magnetoresistance.* It has been pointed out[77] that a negative magnetoresistance, aside from being

---

* Suppose a thermometer with finite magnetoresistance is used to control sample temperature. If a magnetic field is turned on and if one waits for effects of eddy current heating to disappear, the temperature at which the thermometer holds the sample will change. A new value of sample heater quiescent current will be necessary to maintain the sample at this new temperature. Magnetoresistance in the heater will have no effect so long as the dynamic range of heater current above quiescent value is sufficient to offset the resistive change in heater power.

unusual, has been associated with magnetic impurities such as paramagnetic oxygen, when it has been observed.

This all leads to the conclusion that the 200Å grains of which our samples are composed are separated by thin insulating grain boundaries composed probably of nonstochiometric TiO. Thus electrical conduction at high temperature is viewed as a thermal activation process with the grain boundaries dominating the normal resistance at temperatures below 100 K.

The existence of the unpaired electrons of the oxygen atoms in the grain boundary will have a depairing effect[42] on the superconductivity of the grains or of the sample as a whole. The net effect of the paramagnetic impurity on the superconducting behavior of the samples would be a reduction of the transition temperature. The observation by other workers[78] that an increased oxygen content of films of NbN and NbTiN results in drastic decreases in transition temperature supports this hypothesis.

Sample Geometry and Mounting

Sample thickness was determined by sputtering rates and times. Thickness determinations were checked and calibrated with a quartz crystal oscillator thickness monitor and with multiple beam interferometric measurements.*

---

* Varian Å-scope multiple beam interferometer, model 980-4000.

Sample thickness is presumed known to $\pm 2\%$.

Indium was used to solder the electrical leads to the samples. With some patience and cleanliness, contacts could be made which withstood indefinite numbers of thermal cyclings. In the high field measurements, in fact, where abrupt thermal cycling was necessary, the leads failed in an epoxy feed through while the contacts remained intact. The care necessary to get the indium to wet the samples precluded the use of narrow contacts. Thus the sample length, X, is only approximately known. In the classical Aslamasov-Larkin regime, where resistivity of the sample exceeds that of the contacts, X is the minimum distance between the contacts. Where the resistivity of the sample is less than that of the indium, X is taken to be the distance between the points where the voltage lead wires made contact with the indium. The uncertainty in X is $\pm 5\%$.

Samples were trimmed along their edges with a diamond scribe to avoid edge effects. The unavoidable roughness of the trimmed edges produced an uncertainty in sample width of $\pm 5\%$.

Sample Histories

Sample history particularly between runs was evidently of importance. The most important item of sample treatment was probably the heating necessary to make the indium contacts to the sample. The temperature used for this purpose generally did not exceed 200°C. This heating however was done in air. Since the samples used in this study were heated at least as severely as this in air prior to our acquiring them, no care beyond that mentioned above was taken in making contacts.

The high magnetic field measurements required samples of smaller length than that used in the zero field measurements. The alumina substrates could not be scribed and broken without danger of completely shattering them. The samples were instead shortened by abrading them manually against coarse emery paper. Even when this was done slowly, quite a bit of heat was generated. To avoid this it was necessary to do the grinding under water. The samples were covered with silicone grease when in contact with the water.

Sample Parameters

The Energy Gap*

Quasiparticle tunneling junctions were made with sample "92A". The junction barrier was grown on the $Nb_{.88}Ti_{.12}N$ film by heating it in air to 250°C for 2 hours. The film edges were covered with a thin layer of G.E.7031 varnish. A 1000Å layer of aluminum was evaporated over this to produce a junction of $1(mm)^2$ area. The most distinct current voltage characteristic obtained from such a junction is shown on figure 7. All junctions showed the excessive

* The experimental work reported in this paragraph was done by James Solinsky.

FIGURE 7

QUASIPARTICLE TUNNELING CURRENT - VOLTAGE CHARACTERISTIC OF A JUNCTION FORMED* WITH SAMPLE 92A & (NORMAL) ALUMINUM FILM

T = 4.2 K

VERTICAL SCALE IS 10 A/cm.

HORIZONTAL SCALE IS 1 mV/cm.

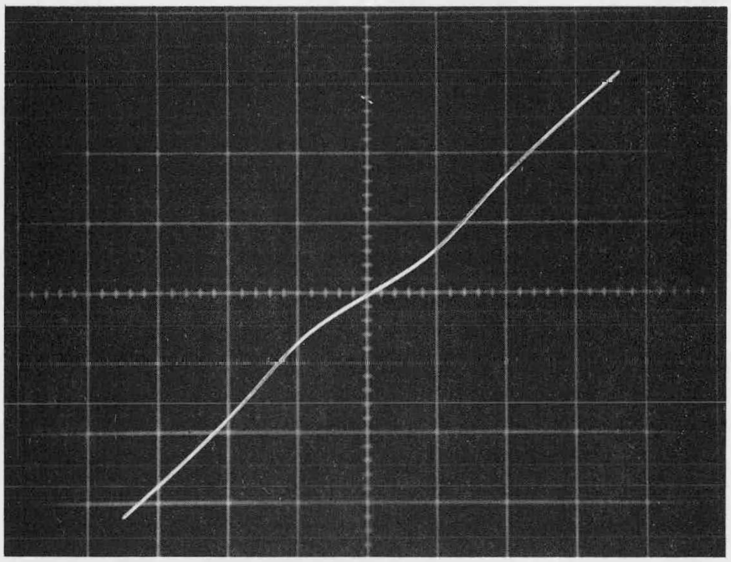

* The junction was fabricated and I-V characteristic obtained by James Solinsky.

leakage current and rounded features exhibited in the above photograph. These made estimates of the energy gap difficult. However all I-V characteristics obtained were consistent with $2 \cdot \Delta = 4.2$ meV. This corresponds to $2\Delta/(k_B T_c) = 4.1$.

The Strong Coupling Parameter

In view of the importance of the possible strong coupling nature of $Nb_{.88}Ti_{.12}N$ to any comparison between theory and experiment, some estimates of this quantity must be made. Measurements, phenomenological estimates, and theoretical calculations suggest, but not consistently, that $Nb_{.88}Ti_{.12}N$ is a strong coupling superconductor. The measurements are those of the ratio $\frac{2\Delta}{k_B T_c}$ and of C_p for NbN. A phenomenological estimate of $\frac{2\Delta}{k_B T_c}$ for $Nb_{.88}Ti_{.12}N$ can be obtained from an empirical relationship between this ratio and Θ_D noted by Laibowitz, Sadagopan, and Seiden.[79] A direct estimate of the strong coupling parameter, α , can also be made.

Komenou, Yamashita and Onodera[80] oxidized a thin film of NbN of uncertain stochiometry and overcoated it with a layer of Pb to form a quasiparticle tunneling junction. Estimating the energy gap for their NbN from current-voltage characteristics, they arrive at $2\Delta = 4.50$ meV and $\frac{2\Delta}{k_B T_c} = 4.08$. They point out that this is very close to the corresponding value for lead.

Geballe et al.[81] report measurements of specific heat on bulk $NbN_{.91}$ and $NbN_{.84}$ which show the same deviations from weak coupling B.C.S. behavior that lead does. Their observations led them to their occasionally quoted statement that NbN behaves like "stiff lead". Differences in composition aside, in contrast to our samples, the work above was done on bulk NbN and need not reflect thin film behavior. However other specific heat measurements[82] on both micron thick films and bulk NbN indicate there may be no great difference in the behavior of these two geometries so far as deviations from B.C.S. behavior is concerned.

Laibowitz, Sadagopan and Seiden[79] propose the empirical relationship: $2\Delta/k_B T_c = 3.5(1+b\exp(cT_c/\Theta_d))$ where b and c are determined by fitting this expression to their tunneling data on Nb_xN_{1-x} and to some data on other (elemental) superconductors. Using the values for Θ_D for NbN obtained by Geballe, et al.[81], and the T_c's of our samples, we obtain $2\Delta/k_B T_c$ between 3.6 and 3.7, not at all like lead. It should be noted however that the data of Komenou et al.[80] does not fall on the above empirical curve.

The most direct expression relating the strong coupling constant to material properties is due to Eilenberger and Amboegoakar[53] (EA):

$$\alpha = \left[\left(\frac{\Delta_{BCS}}{\Delta_{obs.}}\right)^2 \left(\frac{H_c^{obs}}{H_c^{BCS}}\right)\right]_{T \to T_c}$$

EA observe that if $\Delta(T)$ has B.S.C. behavior, then

$$\left(\frac{\Delta_{obs.}}{\Delta_{BCS}}\right)_{T\to T_c} = \left(\frac{\Delta_{obs.}}{\Delta_{BCS}}\right)_{T\to 0}$$

Komenou finds that $\Delta(T)$ for his films follows the B.C.S. curve closely. Assuming that our films behave in the same way, we can use the above expression with the observed quantities $2\Delta = 4.2$meV, $T_c = 10.5^{\circ}$K for sample "92A" to obtain:

$$\left(\frac{\Delta_{obs.}}{\Delta_{BCS}}\right)_{T\to T_c} = \frac{\Delta_{obs}(0)}{(1.76)\,k_B T_c} = 1.3$$

This number, for lead, turns out to be 1.52.

To estimate the ratio $\left(H_c^{obs}/H_c^{BCS}\right)_{T\to T_c}$ we observe that:

$$\left(\frac{H_c^{\,obs}}{H_c^{\,BCS}}\right)_{T\to T_c} \cong \left(\frac{dH_c^{obs}}{dT}\Big/\frac{dH_c^{BCS}}{dT}\right)_{T\to T_c} \cong \left(\frac{C_S^{obs} - C_N^{obs}}{C_S^{BCS} - C_N}\right)^{1/2}_{T\to T_c}$$

The above relations become equalities as $T \to T_c$. We recall that Geballe found the same deviations from B.C.S. in the specific heat of bulk NbN as in lead. We recall also that the Westinghouse group noted the same specific heat behavior in bulk and micron film NbN. If we assume that our material behaves like NbN in this respect, and if we assume that there is little change in going from bulk to thin films, then we can approximate the ratio $\left(H_c^{obs}/H_c^{BCS}\right)_{T\to T_c}$ for our films by that of lead. EA find this ratio to be 1.36 for lead. When we put these numbers together, we find for our films $\alpha = 1.1$.

EA obtain $\alpha = 1.2$ for lead. This latter number, however is inconsistent with other experimentally determined properties of lead.[53]

The Coherence Length

The quantity $\xi(0) = .85(\ell_{eff}\cdot\xi_o)^{1/2}$ * plays a central role in any model of fluctuations in superconductors as the characteristic distance over which nonhomogenieties are averaged in a sample. We made early attempts to obtain this quantity using the mean field expression

$$H_{c_2}(T) = \phi_o/2\pi\xi^2(T)$$ in the form

$$\xi^2(o) = \phi_o \Big/ \left(2\pi T_c \left[\frac{dH_{c_2}}{dT}\right]_{T_c}\right) .$$

T_c was associated with some fixed sample resistance and the slope $(dH/dT)_R$ was measured up to fields of 10KOe. The initial results were confusing because this slope depended on the magnitude of field except for one particular value of

* ℓ_{eff} is an effective mean free path (see discussion at end of chapter 1). ξ_o is the B.C.S. coherence length.

fixed sample resistance. Furthermore, near H=0, it depended on the value chosen for sample resistance. This behavior was assumed due to fluctuation effects on the shape of the resistive transition in the relatively small fields used.

The necessity of obtaining a value for the normal resistance of our samples in the zero field transition region led us to use the 100 KOe magnet available at the U.S.A.E.C. laboratory at the University of Iowa at Ames. Together with the attempted measurements of normal resistance, described in another chapter, measurements were made of $(dH/dT)_R$ at R=half the maximum sample resistance. Unlike the relatively lower field measurements, these higher field measurements gave a slope independent of magnetic field at $R=(½)R_{max}$. It is interesting that the slope obtained in higher fields, evidently uncomplicated by fluctuation effects, coincided with the slope obtained in lower fields at the one fixed value of sample resistance which prodeced the linear behavior of $(dH/dT)_R$.

The data obtained for $(dH/dT)_R$ vs. H are shown in figure 8. The corresponding values for $\xi(0)$ are:

Sample	$\left(\frac{dH}{dT}\right)_{R=½R_{max}}$	$\xi(0)$	T_c (assumed)
92D (92DX)	$2.40\pm.05\times10^4$ Oe/°K	$34.5\pm.4$Å	$11.55\pm.05$°K
92A	$2.68\pm.05\times10^4$ Oe/°K	$34.4\pm.4$Å	$10.42\pm.02$°K

A measurement of $\xi(0)$ can be interpreted as a measurement of the effective mean free path ℓ_{eff} (72) if one knows the

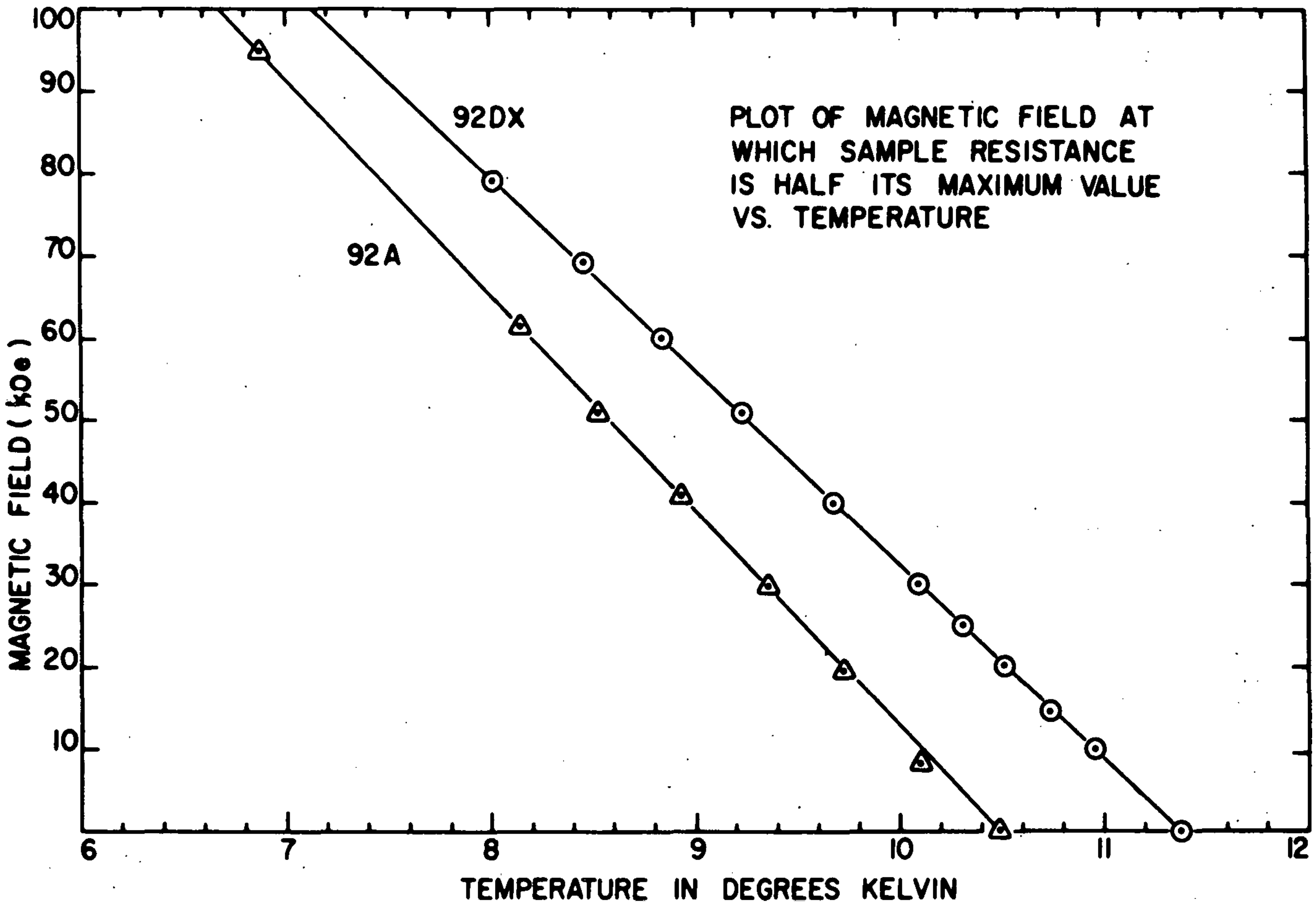
92DX
92A
PLOT OF MAGNETIC FIELD AT
WHICH SAMPLE RESISTANCE
IS HALF ITS MAXIMUM VALUE
VS. TEMPERATURE
MAGNETIC FIELD (kOe)
TEMPERATURE IN DEGREES KELVIN
100
90
80
70
60
50
40
30
20
10
6
7
8
9
10
11
12

Figure 8

B.C.S. value of the coherence length, ξ_0 . If one takes as ξ_0 the value suggested by Haake[83] for NbN, ξ_0 = 560Å, then ℓ_{eff} = 3Å.

We end this chapter with a table of properties of our samples which are useful in interpreting and analyzing the data to be presented. In this table, R_{max} is the resistance at the resistance maximum (at 19-21 K). Resistivities have been calculated using R_{max}.

TABLE ONE

GENERAL SAMPLE PROPERTIES

	SAMPLE 92D	SAMPLE 92A	SAMPLE 92DX
Geometry:			
length(cm.)	0.9 (1.1)*	0.7 (0.9)*	0.7 (0.9)*
width(cm.)	0.2	0.2	0.2
thickness(Å)	1500	1500	1500
Resistances:			
Rm. Temp.** (ohms)	315.33	229.57	248.53
R_{max}**(ohms)	422.320	325.863	339.060
resistivity (microohm cm.)	1400.	1400.	1400.
Temperatures:			
$T(R=.5R_{max})$ (°K)	11.471	10.374	11.318
$T(R=.7R_{max})$ (°K)	11.564	10.420	11.493
$T(R=R_{max})$ (°K)	20.9	18.9	20.8
$(dH/dT)_{R=.5R_{max}}$ (kOe/°K)	24.0±.5	26.8±.5	24.0±.5
3(6) (Å)	34.5±.4	34.4±.4	34.5±.4

* See discussion of sample geometry in chapter two.

** This is a typical pair of resistances at these two temperatures for a given run. These resistances occasionally changed proportionately by about 1:10^4 on cycling. This is thought to have been caused by small changes in sample electrical contacts.

CHAPTER 3: METHOD

Our primary interest, experimentally speaking, is in resistance measurements. Since these measurements are to be probes of fluctuation effects, we want the depairing effects of current, ambient magnetic and R.F. fields kept at a minimum. Resistance measurements in magnetic fields are of additional interest. These latter measurements require some care in the thermometry.

The apparatus and methods used in taking these measurements will now be discussed in some detail.

Stray Magnetic and R.F. Electromagnetic Fields

Efforts were made to minimize effects of stray radio frequency signals and to shield the samples from the earth's magnetic field.

All measurements except those performed at the Ames laboratory were done in an R.F.I. shielded environment.* Electrical signals between 14kHz and 1000MHz were attenuated by at least 100 decibels. Several tests were made for sensitivity of sample resistance to the improbable coupling of radio frequency signals to the sample. No such effects were detected.

Measurements done before the date 1/10/70 were performed with the cryostat shielded from the earth's magnetic

* An "R.F.I. Solid Metal Shielded Enclosure" manufactured by Ace Engineering and Machine Co., Inc., Huntington, Pa.

field with a single mu metal shield.* A maximum field of 10 mOe could be measured at the position of the sample with a flux gate magnetometer.** A pair of magnetic shields of Moly Permalloy*** were used during the measurements on and after the date 1/10/70. This shield pair reduced stray fields to less than 0.3mOe. No magnetic shielding was available at the Ames laboratory, where the large magnetic field work was done.

Cryostat for "Zero Field" and Small Magnetic Field Measurements

The cryostat used for most measurements of the resistive transitions of the samples is shown in figures 9 through 12.

The copper sample block was provided with slots for samples and a hole for the CryoCal thermometer. A 150 ohm heater was wound noninductively around the bottom of the sample block. The elements mounted in the sample block were greased to provide optimum thermal contact. Electrical leads were wound noninductively around the sample block to avoid heat leaks from the elements in the block.

The sample block was enclosed in an inner pot called the exchange gas can. This pot was furnished with its own

---

* Magnetic Radiation Lab Inc., Chicago, Ill.
** Magnetometer Probe Model 3529A used with Milliammeter Model 428B, Hewlett Packard Co., Loveland, Colorado
*** Williams Manufacturing Corp., San Jose, Calif.

Figure 9. Cross-section of the "Business End" of the Cryostat Used for "Zero" and Small Magnetic Field Measurements

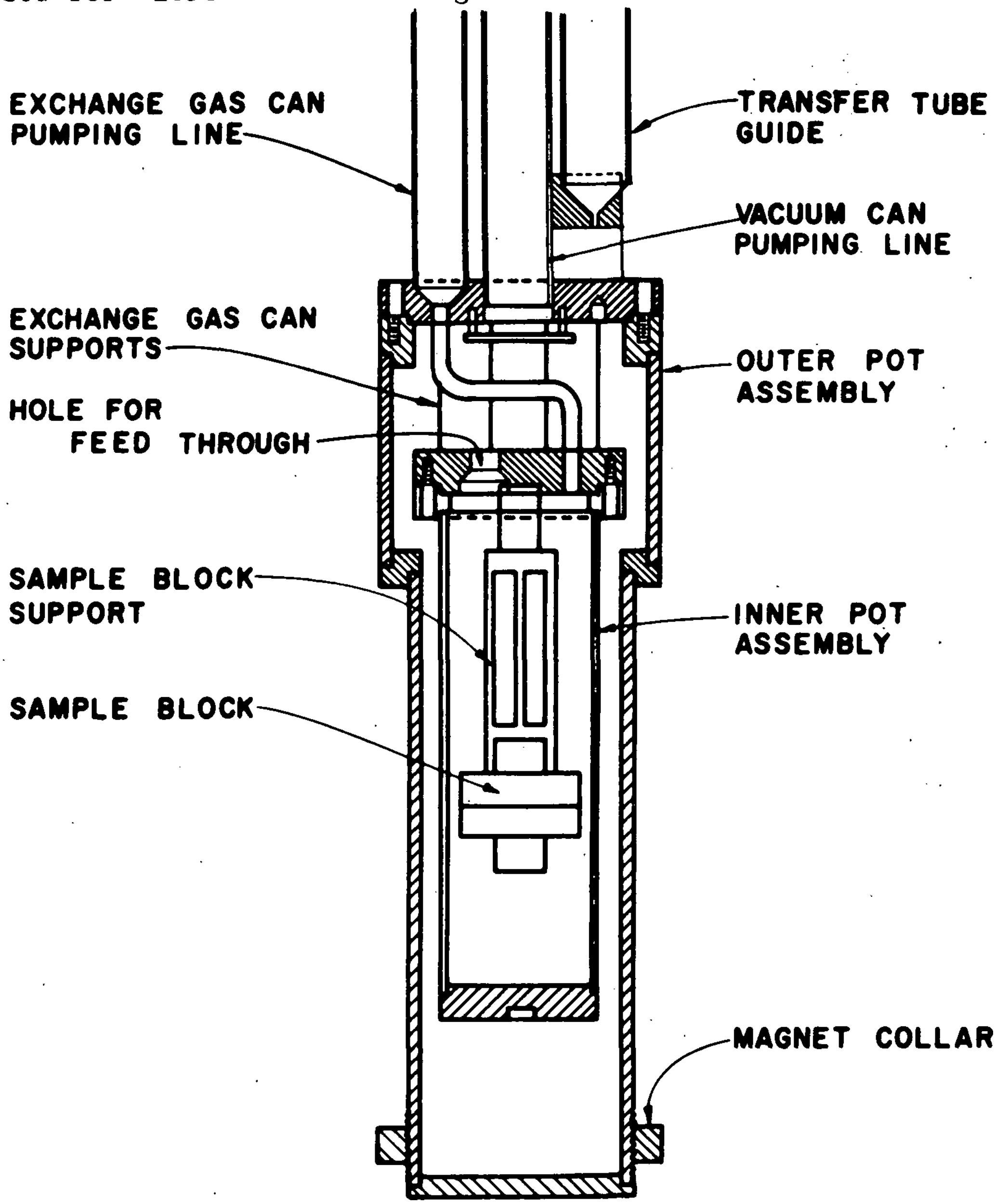

BOTTOM OF CRYOSTAT
ASSEMBLED EXCEPT FOR MAGNET

Figure 10

BOTTOM OF CRYOSTAT FOR MEASUREMENTS IN SMALL MAGNETIC FIELDS WITH VACUUM CAN AND EXCHANGE GAS CAN REMOVED

(The leads and cryogenic capacitors are held in place above the sample block with nylon twine and masking tape.)

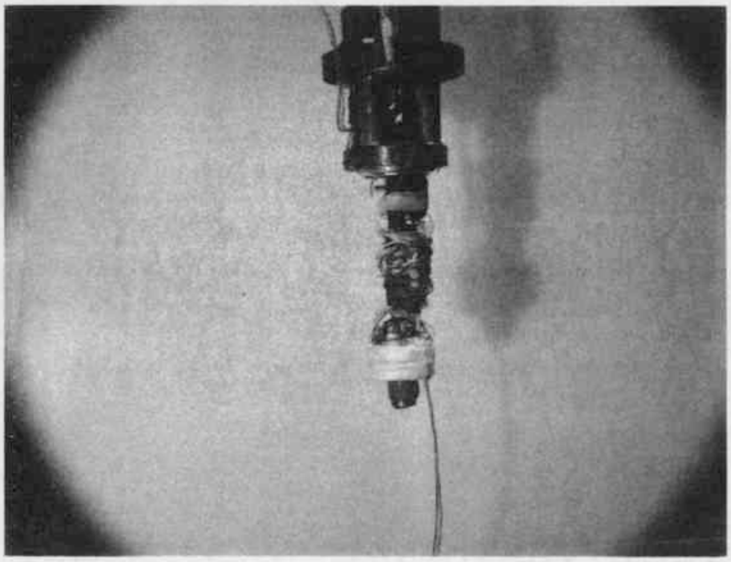

Figure 11

BOTTOM OF CRYOSTAT FOR MEASUREMENTS IN SMALL MAGNETIC FIELDS WITH VACUUM CAN REMOVED

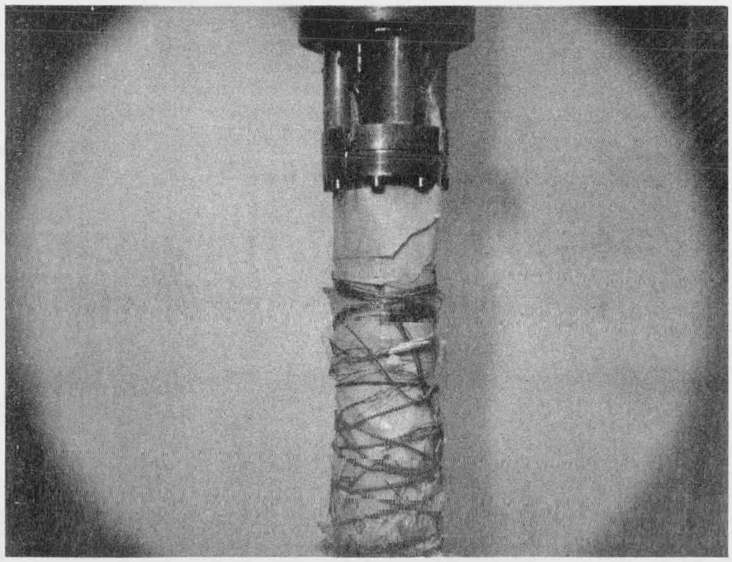

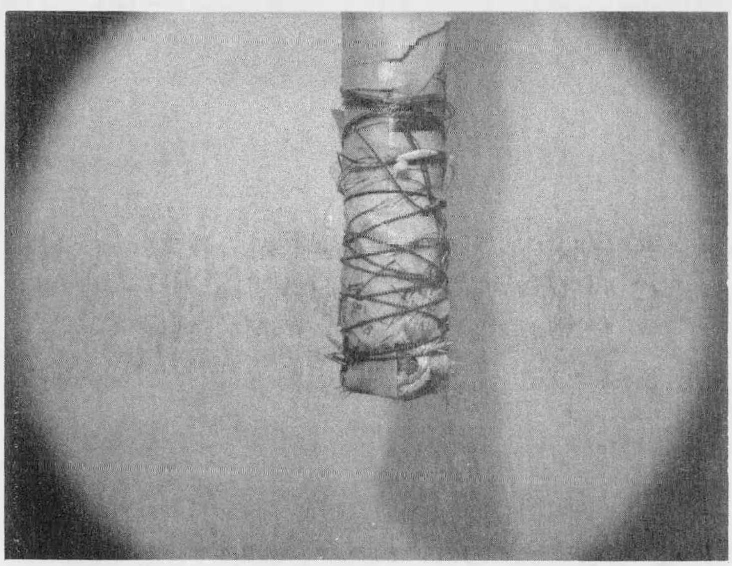

Figure 12

CRYOSTAT AND BODY GUARD

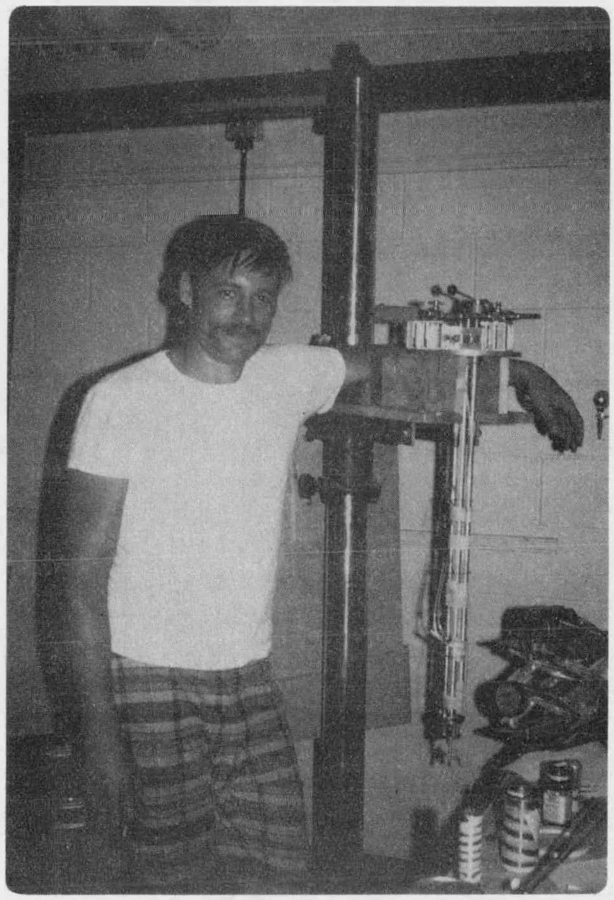

150 ohm heater, carbon resistor thermometer and temperature regulator. 100 microns of helium in the exchange gas can was found to provide optimal thermal time constant (1 sec.) for smooth temperature regulation of the sample block. The sample block was supported mechanically inside the exchange gas can by a nylon member of minimal cross-sectional area, attached to the top of the can.

A vacuum feed-through for the electrical leads into the exchange gas can was of copper and a one inch length of 1/8 inch diameter stainless steel. A stycast 2850 GT epoxy* seal for the wires was made at one end of the stainless steel tube. The assembly could be soldered into place with low temperature melting solder** by means of a copper bushing at the end opposite the epoxy seal.

The electrical leads outside the inner pot were wrapped around the pot in a manner to compensate for magnetic pickup for some 10" of length. Miniature electrical connectors allowed the pot to be removed completely from the cryostat during sample mounting. The connectors were heat sunk to the outer shield by means of silicone grease.

The inner pot was housed in a vacuum can with the intention of keeping the inner pot as close in temperature as possible to the sample block. Mechanical support for the inner pot was provided by four lengths of 12 mil wall by

---

* Emerson & Cuming, Inc., Gardena, Calif.
** Indalloy #13 M.P. 125 degrees C.

3/8" diameter by 2.7 cm length stainless steel tubes. It was found that this also furnished a thermal connection to the 4.2 K bath of such a size that no additional exchange gas was necessary in the "vacuum can".

Access to the inner pot was provided by a length of 1/8" diameter stainless steel tube between inner pot and outer pot, and by 3/8" diameter stainless steel tube from outer pot to a manifold on the cryostat top. The manifold allowed simultaneous measurement of, and change of, exchange gas pressure during a run.

Access to the vacuum can was provided by a 1/2" stainless steel tube sealed at the cryostat top by a 1/2" Circle Seal valve. A solenoid capable of producing 10 KOe, fit over the vacuum can. The whole cryostat was so designed that it fit into a 2" dewar.

Feed throughs between top of the cryostat and vacuum can were of a design due to Stephen Kral. They amounted to lengths of 1/8" stainless steel tube with 1/4" cylinders of Hughes #22 epoxy at each end. A fraction of the tube volume was filled with oil. Bushings were provided along the tubing length for solder or o-ring seals at the vacuum can top and cryostat top.

Sample and Thermometer Resistance Measurements

The resistance of both the thermometer and sample were measured with a four terminal method. A.C. bridges of basic design due to Kierstead[84] were used. These bridges used ratio transformers to compare the unknown resistances with resistance standards. The standard resisters were 5 ppm General Resistance Corp. "Econisters". The bridge circuit diagrams are shown in figures 13 and 14.

The characteristics of the 1:1 transformers used to couple the sample voltage to the detector made ecessary the use of a detector preamplifier of 10 megohm input resistance and required the use of frequencies above 10^3 Hz. A frequency of 1.5×10^3 Hz. was chosen for the sample bridge. The thermometer bridge was operated at 1.0×10^3 Hz.

A lock-in amplifier* was used for the detector to obtain the nanovolt sensitivity necessary to resolve a few milliohms at a sample current of a microamp. The noise figure of the lock-in amplifier plus preamplifier, at the frequencies used, leads to a minimum detectable signal of 5 nanovolts at 6 db rolloff for the largest sample resistances measured.

When working with these nanovolt level signals it was found necessary to make the ground connections shown with care, and to make all connections to the bridge in such a way that ground loops were avoided. Pickup was reduced to a point where a 1 sec. integration time for 10 microamp sample current, (or 10 sec. for 1 microamp) sufficed to resolve the minimum detectable signal mentioned above.

Since manganin leads were used, lead resistance pre-

---

*The lock-in amplifier was the model HR8 (with type C preamp) of Princeton Applied Research Corp., Princeton, N.J.

Figure 13. Sample A. C. Resistance Bridge

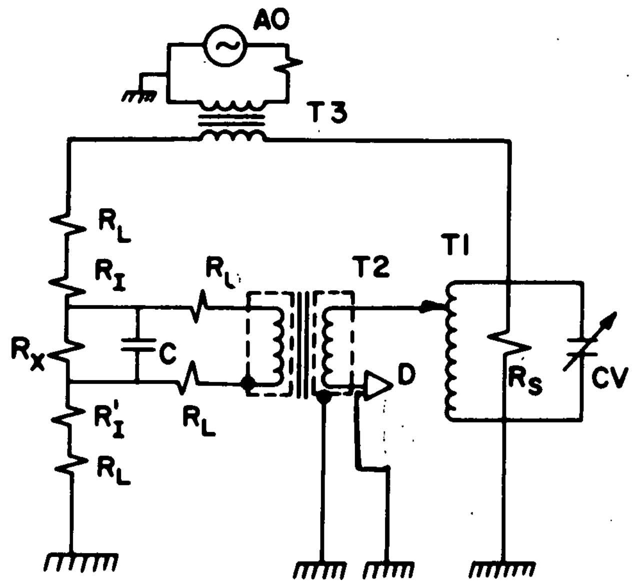

D = PHASE SENSITIVE DETECTOR: PRINCETON APPLIED RESEARCH HR8 LOCKIN AMPLIFIER WITH TYPE A 10 Meg Ω INPUT IMPEDANCE PREAMP

T_1 = RATIO TRANSFORMER: GERTSCH MODEL 1011

T_2 = 1:1 TRANSFORMER: TYPE NA1 117-2.000-30 3Q27

T_3 = 6:1 TRANSFORMER: TRIAD TYPE G-59 TF 10X 16YY

AO = AUDIO OSCILLATOR: INTERNAL OSCILLATOR OF HR8

R_X = SAMPLE RESISTANCE

R_S = STANDARD RESISTOR

R_L = LEAD RESISTANCE: 68 Ω/LEAD AT CRYOGENIC TEMPERATURES

R_I = RESISTANCE OF SAMPLE BETWEEN CURRENT & VOLTAGE CONTACTS: $\lesssim$ 20 Ω

C = CAPACITANCE ACROSS SAMPLE IN CRYOSTAT: .0105 μf SILVER MICA

CV = DECADE CAPACITOR

Figure 14. Thermometer A. C. Resistance Bridge

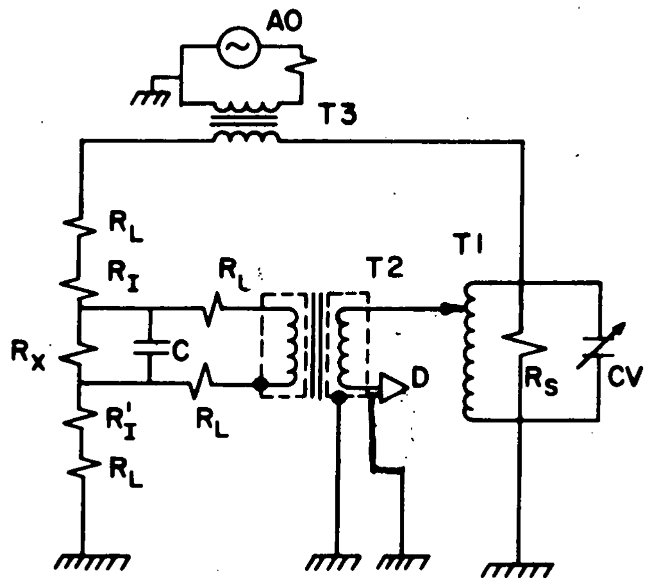

D = PHASE SENSITIVE DETECTOR: PRINCETON APPLIED RESEARCH HR8 LOCKIN AMPLIFIER WITH TYPE A 10 Meg INPUT IMPEDANCE PREAMP

T_1 = RATIO TRANSFORMER: DEKATRON TYPE DT 72A

T_2 = 1:1 TRANSFORMER NORTH ATLANTIC T-109

T_3 = 6:1 TRANSFORMER: JANES 8314

AO = AUDIO OSCILLATOR: INTERNAL OSCILLATOR HR8

R_X = THERMOMETER RESISTANCE

R_S = STANDARD RESISTOR

R_L = LEAD RESISTANCE: 68 Ω/LEAD AT CRYOGENIC TEMPERATURES

R_I = RESISTANCE OF THERMOMETER BETWEEN CURRENT AND VOLTAGE LEADS

C = CAPACITANCE ACROSS THERMOMETER IN CRYOSTAT: TRW .01 μf MYLAR

CV = DECADE CAPACITOR

sented a problem in the use of the bridges. The capacitance of the 1:1 transformer was about 1000 pf. This reactance could draw enough current through the sample voltage leads to produce an error signal of $2R_L wC_{1:1} = 10^{-3}$. In addition, at frequencies above about 400 hertz, additional capacitance must be placed across the sample to reactively balance the ratio transformer interwinding capacitance. This would make matters even worse. It was therefore necessary to put substantial capacitance across the voltage leads of the resistance unknown in the cryostat. Having done this, it was possible to put across the standard resistor a decade capacitor with which a reactive balance could be made at each resistance measurement.

The method for achieving bridge balance needs some discussion. For reasons of simplicity, the "in-phase" balance was made at that relative phase setting (via the phase shifter in the HR8) at which null was least sensitive to changes in capacitance placed across the standard resistor. Analysis of the bridge equations show that with this criterion for balance, reactive terms enter into the "in phase" balance equations. Thus a calibration of the bridge was found to be necessary leading to a "bridge factor" that could be used, to suitable accuracy, to adjust the value of the standard so that the ratio read on the ratio transformer gave the correct resistance.

The bridges were calibrated by a substitution method.

A small box was made reproducing the lead resistances, sample resistance and cryostat capacitor. Standard resistors were put in place of the sample resistance. For fixed bridge standard resistance, corrections to the ratio transformer reading were noted for various values of sample resistance. The error in ratio transformer reading was linear in transformer ratio to $3:10^4$. This corresponds to 1×10^{-1} ohm for largest sample resistances and to 1 millidegree error at 10°K. Although these numbers are relatively large, they represent accumulated errors over a substantial part of the resistive transition, e.g. 0.1 ohm over a 300 ohm interval or 0.001 degree over a 10 degree interval.

Measurement of small resistances presented some difficulty. For sample resistances about 10 ohms or less, the balance is so insensitive to reactive components that a phase setting for minimum sensitivity to changes in them is impossible to determine. It was found, however, using a substitution circuit for the cryostat environment of the sample, that for all but one relative phase setting, a finite ratio transformer setting was necessary to produce a null signal for 0(±5 milliohm) resistance in the substitution circuit. That phase setting was chosen for these low resistance measurements which allowed zero ratio transformer setting to produce a null signal. This results in a zero (resistance) error of 5 milliohms. Thus a residual resistance of 10 milliohm could have persisted below the transition undetected.

Temperature Control

The off-null signal from the thermometer resistance measurement was usually used to control the temperature of the sample block. When $\frac{1}{R}\cdot\frac{dR}{dT}$ of the sample exceeded that of the thermometer, the sample resistance then servoed the temperature. With the thermometer currents used (see below) temperature changes of 10 microdegrees could be resolved in the vicinity of the samples' resistive transition.

The error signal from the detector of the thermometer bridge was fed to two operational amplifiers in a buffer and summing configuration shown in figure 15. This circuit and the thermometer bridge was built by John T. Anderson.

The temperature regulator for the exchange gas can was a Wheatstone bridge with a phase sensitive detector. This temperature regulator was capable of resolving a 100 microdegree temperature change. A simple calculation shows however that there is a 10 millidegree temperature drop across the exchange gas can in a typical running situation. This is due to heater power necessary to make it function as a heat shield. The function of a heat shield in this case is, of course, to prevent such a temperature drop across a sample block.

The output of the phase sensitive detector for the Wheatstone bridge went to a pair of Kepco* operational amp-

* These were "Operation Power Supplies OPS 40-0.5(C) and PBX 40-0.5(C) of Kep o, Inc., Flushing, N.Y.

TEMPERATURE CONTROL POWER SUPPLY

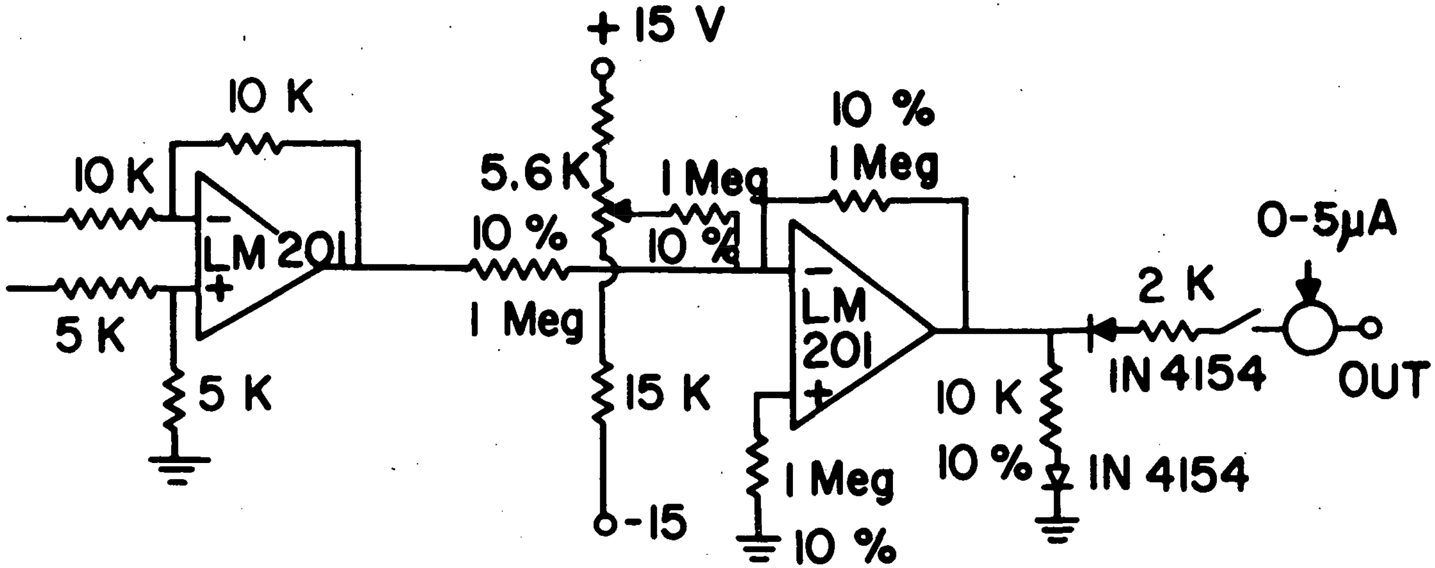

POT IS 10 TURN

LM 201 COMPENSATED WITH 30pf, SUPPLIED WITH ± 15 V BY POWER TRAN SUPPLY MM-15

ALL RESISTORS ARE 1% UNLESS OTHERWISE NOTED

Figure 15

lifiers in a summing configuration. These provided sufficient current to bring the temperature of the exchange gas can from 4.2 K to 90 K within a half hour. Typical heater currents at 10 K were 5 to 6 milliamps. The Wheatstone bridge was operated at 1 x10^3hertz.

Electrical leads to the exchange gas can were isolated from those to the sample block. Several tests showed there was no cross talk between these two sets of leads.

Cryostat Performance

During preliminary runs, a sample was used as a thermometer to determine optimum values for heater currents, exchange gas pressures and wait times for thermal equilibrium. A point was chosen on the sample resistance vs. temperature curve where the slope amounted to 1.3m K/Ω. Changes in power fed to the various elements in the cryostat produced the following changes in temperature difference between sample and thermometer:

Element	Current induced change in sample-thermometer temperature separation
Sample(R=200Ω)	0.3μ°K/(μA)^2
Thermometer(R=100Ω)	0.2μ°K/(μA)^2
Sample Heater(R=150Ω)	1 mK/(mA)^2

A choice of appropriate sample current was complicated by nonohmic behavior of samples. Despite this difficulty, sample currents of generally 4μA RMS were used, since this permitted resolution of sample resistance changes of a few milliohms in reasonable times. Nonohmic behavior produced resistance changes of up to several tens of milliohms. This effect was noted in such a way that corrections can be made for it if necessary. The stability of the sample current source was better than 0.1%.

The CryoCal thermometer was used at constant power. The value of 1 μwatt is that recommended by the manufacturer and used here. Over the portion of the samples' resistive transition where resistance changes most rapidly (a few tenths of a degree wide) constant current was used for the thermometer. At this temperature the thermometer is about 100 ohms. The 100 microamp thermometer current used here produces a millidegree temperature difference between itself and the sample. Thus it was necessary to use a 0.1% power supply for the thermometer current also.

A sample block heater current of 300 microamps was the smallest current consistent with reasonable time between data points. Enough resistance was put in series with the sample block servo signal source to limit the heater current excursions to ten microamps. Monitoring and holding this heater current to the nominal 300 microamps at each data point insured that relative temperature errors were at most a microdegree due to this cause.

Method of Taking Data

For each data point, the temperature controlling bridge was set to the desired resistance. The exchange gas can heater current and other bridge was adjusted to bring the sample heater current to 300 microamps.

The time necessary for thermal equilibrium for temperature steps of 5 millidegrees was a few minutes. This was about the time necessary to check reactive balance and estimate changes in quiescent currents and bridge settings for the next data point. Thermal equilibrium was judged to have been established when no further changes in bridge settings were necessary for fixed values of quiescent current.

For temperature changes larger than 5 millidegrees, correspondingly longer waits were necessary. In fact, after the initial transfer of liquid helium, a three hour wait was necessary for thermal equilibrium even with quiescent currents preset to desired values.

With this sort of care, reproducibility within a given run, cycling between 4.2 K and 90 K, was better than 0.01 ohm or 10 microdegrees on the most sensitive part of the transition.

Thermometry

A precalibrated CryoCal germanium resistance thermometer* was used to determine the temperature of the sample. The calibration is traceable to the National Bureau of Standards Provisional Scale of 1965 with an accuracy of 0.01 K in the temperature range 5 K to 20 K. In the range from 20 K to

*CryoCal, Inc., Riviera Beach, Fla, unit #825.

90 K the calibration is traceable to the Bureau of Standards Provisional Scale of 1955 with an accuracy of 0.04 K from 20 K to 40 K, and of 0.1 K form 40 K to 90 K. Interpolation* was done with the expression

$$T \ln R = \sum_{n=0} A_n (\ln R)^n$$

It was found that a reasonable fit to the calibration points could only be made in sections of the thermometer resistance vs. temperature curve and using four terms in the above series. These fitted sections of curves failed to coincide by at most 3 millidegrees at the high temperature end. This discrepancy is not significant in this work since it occurs at temperatures where the sample resistance is only weakly temperature dependent.

The CryoCal thermometer was used for measurements in magnetic fields up to 10 kOe except for those measurements dated 1/10/70. When the CryoCal was used, adjustments were made for its magnetoresistance using data furnished by Cryo-Cal, Inc. A check of this magnetoresistance data using the National Carbon Co. thermistor (discussed below) later showed the corrections to be in error by +11 %. This amounts to an essentially constant error in the data presented, of 11 m K for the 10 kOe data presented in the fourth chapter and an essentially constant error of 0.4m K for the 2 kOe

* The coefficients in this expression appear in the subroutine for calculation of temperatures from thermometer resistances listed in appendix I.

data. The listed temperatures for the above mentioned data are too high by the stated amounts. Magnetic field data taken on 1/10/70 were taken with a thermistor.

A National Carbon Co., Inc. thermistor was used as a thermometer in the measurements that involved fields up to 100kOe. Use of this thermistor for these measurements was suggested by Schlosser and Munnings(85), who reported at most a 0.2% change in its resistance at 4.2 K in a field of 19kOe. We checked this measurement with our own unit in fields up to 10kOe and found no change in a resistance of 81 kilohms at 4.2 K within 50 milliohms. This amounts to a temperature error of less than 10 microdegrees. This was taken as evidence that the thermistor was a dependable thermometer in high magnetic fields so long as the CryoCal was used as a transfer standard in zero field.

In some of the high field measurements it was not possible to mount the CryoCal in the sample block with the thermistor. Thus tests had to be made to determine the cyclability of the thermistor. Comparison of the thermistor with the CryoCal over five cyclings between room and liquid helium temperatures over a five month period showed a shift in the thermistor's resistance vs. temperature curve of 1.2 millidegree toward lower temperatures.

The thermistor was calibrated in zero field with the CryoCal as transfer standard. The calibration is shown in appendix II. Interpolation was done with the same fitting program used for the CryoCal.

Magnetic Field Measurements

Magnetic fields up to 10kOe were available with the cryostat described above. They were produced by a solenoid wound with 3 mil core Supercon* T48B copper clad and formvar coated wire. Solenoid geometry was: mean winding diameter= 1.835"; winding length= 3.65". With 9218 turns, the solenoid formula gives 1.117 kOe/ampere. This number was roughly verified with room temperature measurements using a flux-gate magnetometer. The solenoid was wound by Bob Riess.

The samples were centered geometrically with respect to the solenoid to within a few millimeters. Uniformity of the magnetic field over the samples is estimated to have been 1%. Because the sample block support was not rigid, sample alignments were to within a few degrees of arc. Because of this alignment problem, magnetic fields were only applied perpendicular to the samples.

A second cryostat (figure 16) was necessary for the measurements made in conjunction with the 100 kOe magnet at University of Iowa at Ames, Iowa. The inner diameter of the 100 kOe magnet did not allow room for a temperature shield between the vacuum can and sample block. The electrical leads to the sample block in this case passed through the 4.2 degree bath and were wound around the sample block. Sample and thermometer resistances were measured as des-

---

* Supercon division of National Research Corporation, Natick, Mass.

Figure 16

BOTTOM OF CRYOSTAT FOR MEASUREMENTS IN 100KOe FIELDS WITH VACUUM CAN REMOVED

(The sample block is supported with a threaded nylon rod. Connectors are heat sunk to copper holders near the flange.)

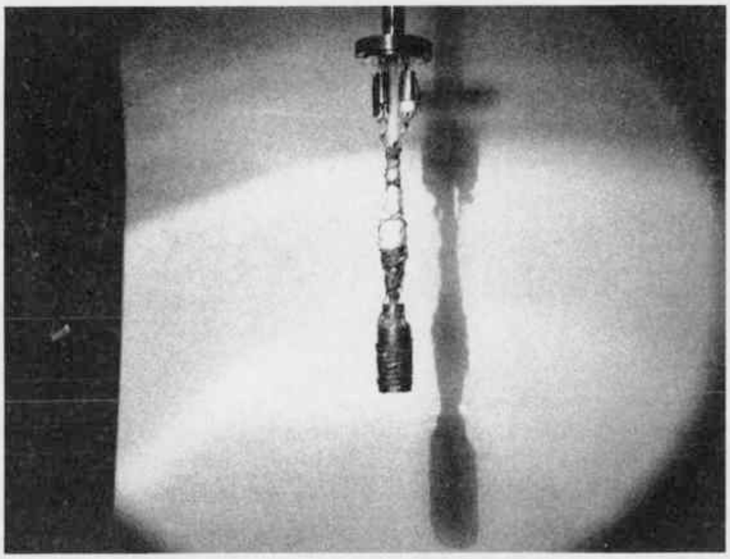

cribed above. Sample resistance measurements were of the same accuracy as those gotten with the small field cryostat. Thermometry was less precise. It is estimated that a 0.1 K error could have accumulated over the temperature range covered in these measurements(4.2 K to 60 K).

High field measurements were made at the U.S.A.E.C. Laboratory, University of Iowa, Ames, Iowa. The 100 kOe magnet there was made available to us through the courtesy of Profs. Samuel Legvold and Douglas Fennemore of that laboratory.

The magnet was a 1" bore Nb_3Sn ribbon-wound 100 kOe solenoid manufactured by RCA with serial #SM2804. Solenoids wound with Nb_3Sn ribbon show considerable hysterisis and long term relaxation effects in their magnetic field vs. magnet current characteristics. It was therefore necessary to measure magnetic field directly. This was done with a magnetoresistance probe, astatically wound, of #36 thermocouple grade Cu wire. The probe was secured rigidly to the bore of the solenoid and communicated directly with the 4.2 K bath. Calibration of the probe was done against a smaller probe of 99.999%pureCu wire calibrated with an NMR Gaussmeter in a high homogeniety 60 kilogauss field.

The writer would like to express sincere gratitude to Professors Douglas Finnemore, Helmut Gartner and to Albert Harvey for their help in the use of this magnet.

CHAPTER 4: DATA

We present in this chapter the data taken on the three samples described in the previous chapter. At the heading of each page are the sample name, date of run, sample measuring current (I_s, measured peak to peak), and type of measurement (R(T) means resistance vs. temperature at constant magnetic field and R(H) means resistance vs. magnetic field at constant temperature).

Printed above listings of resistance vs. temperature are, in addition, the magnetic field and maximum sample resistance. The data listed in this case is the CryoCal thermometer resistance in ohms (corrected for the bridge factor and for any magnetic field), sample resistance in ohms (corrected for bridge factor, but not adjusted for any nonohmic effects), sample resistance normalized to maximum sample resistance, and temperature.

The maximum sample resistance was found to differ by a few tenths of an ohm from run to run for each sample. No such changes were noted so long as the sample was kept at liquid nitrogen temperatures. So this is thought to be due to small changes in the contacts on cycling.

Magnetic field data at constant temperature on sample 92D was taken at equally spaced intervals of sample resistance: R/R_{max} = 0.3, 0.4,...., 0.8. The data on 92A was taken at several fixed temperatures in the region where Aslamasov

Larkin behavior was observed. The initial value of magnetic field listed for each temperature is a "fake" value for computational purposes. This number is supposed to correspond to zero applied magnetic field (see first part of chapter three).

Larkin behavior was observed. The initial value of magnetic field listed for each temperature is a "fake" value for computational purposes. This number is supposed to correspond to zero applied magnetic field (see first part of chapter three).

SAMPLE 92D   10/29/69 I_s = 14 microamps P.P.

R(T)   H = 0 R_{max} = 422.320 ohms

HIGH TEMPERATURE DATA*; ABOVE RESISTANCE MAXIMUM

(PART 1)

THERMOM.R	SAMPLE R	SAMPR/RM	TEMP.
20.0999	421.4000	.997822	29.7484
19.5974	421.2794	.997536	30.2838
19.0949	421.1637	.997262	30.8442
18.4919	420.9928	.996857	31.5523
17.8889	420.8219	.996453	32.3033
17.4869	420.6862	.996131	32.8299
17.0849	420.5454	.995798	33.3790
16.6829	420.3745	.995393	33.9524
16.2809	420.2186	.995024	34.5518
15.8789	420.0628	.994655	35.1794
15.4769	419.8818	.994227	35.8372
15.0749	419.6857	.993762	36.5278
14.6729	419.4696	.993251	37.2539
14.2709	419.2433	.992715	38.0184
13.8689	418.9870	.992108	38.9246
13.4669	418.7155	.991465	39.6759
13.0649	418.4289	.990786	40.5763
12.6629	418.1122	.990037	41.5299
12.2609	417.7855	.989263	42.5173
11.6579	417.2224	.987930	44.1629
11.3564	416.9057	.987180	45.0527
11.0549	416.5538	.986346	45.9919
10.7534	416.1667	.985430	46.9847
10.4519	415.7796	.984513	48.0361
10.0499	415.2065	.983156	49.5386
9.7485	414.7339	.982037	50.7499
9.4470	414.2061	.980787	52.0422
9.2460	413.8290	.979895	52.9535
9.0450	413.4319	.978954	53.9084
8.8440	413.0046	.977942	54.9104
8.6430	412.5572	.976883	55.9638
8.4420	412.0746	.975740	57.0732
8.2410	411.5467	.974490	58.2440

* This data was taken during initial cooldown while temperature was drifting slowly downward.

SAMPLE 92D 10/29/69 I_s = 14 microamps P.P.

R(T) H = 0 R_{max} = 422.320 ohms

HIGH TEMPERATURE DATA*; ABOVE RESISTANCE MAXIMUM

(PART 2)

THERMOM.R	SAMPLE R	SAMPR/RM	TEMP.
8.0400	410.9937	.973181	59.4823
7.8390	410.3604	.971729	60.7951
7.6380	409.7419	.970217	62.1905
7.4370	409.1487	.968812	63.6776
7.2360	408.3393	.966896	65.2672
7.1355	407.9925	.966074	66.1043
7.0350	407.5903	.965122	66.9719
6.9345	407.1529	.964086	67.8719
6.8340	406.7005	.963015	68.8063
6.7335	406.2128	.961860	69.7774
6.6330	405.7252	.960706	70.7875
6.5325	405.2175	.959503	71.8394
6.4320	404.6795	.958230	72.9359
6.3315	404.0863	.956825	74.0801
6.2310	403.5082	.955456	75.2756
6.1305	402.8798	.953968	76.5259
6.0300	402.2112	.952385	77.8353
5.9295	401.5074	.950718	79.2083
5.8290	400.7835	.949004	80.6497
5.7285	399.9791	.947100	82.1652
5.6280	399.1597	.945159	83.7608
5.5275	398.1392	.942743	85.4430
5.4370	397.2493	.940636	87.0373
5.3466	396.3696	.938553	88.7137
5.2260	395.0876	.935517	91.0882
5.1355	394.0319	.933017	92.9830
5.0451	392.9008	.930339	94.9845
4.9245	391.2670	.926470	97.8353
4.8340	389.9599	.923375	100.1232
4.7335	388.4015	.919685	102.8315
4.6431	386.5917	.915400	105.4330
4.6431	386.5917	.915400	105.4330

* This data was taken during initial cooldown while temperature was drifting slowly downward.

SAMPLE 92D 11/3/69 I_s = 14 microamps

R(T) H = 0 R_{max} = 422.586 ohms

HIGH TEMPERATURE DATA*; NEAR RESISTANCE MAXIMUM

(PART 1)

THERMOM.R	SAMPLE R	SAMPR/RM	TEMP.
19.5974	421.3397	.997051	30.2838
20.0999	421.4503	.997312	29.7484
20.6024	421.5559	.997562	29.2362
21.1049	421.6514	.997788	28.7456
21.6074	421.7469	.998014	28.2751
22.1099	421.8374	.998228	27.8235
22.6124	421.9178	.998419	27.3898
23.1149	421.9882	.998585	26.9728
24.1199	422.1139	.998883	26.1858
25.1249	422.2245	.999144	25.4565
25.6274	422.2647	.999240	25.1119
26.1299	422.3099	.999347	24.7830
27.1349	422.3853	.999525	24.1528
27.6374	422.4205	.999608	23.8536
28.1399	422.4457	.999668	23.5642
28.6424	422.4758	.999739	23.2842
29.1449	422.4959	.999787	23.0131
29.6474	422.5161	.999834	22.7505
30.1499	422.5311	.999870	22.4960
30.6523	422.5462	.999906	22.2493
31.1548	422.5613	.999942	22.0100
31.6573	422.5663	.999953	21.7777
32.1598	422.5764	.999977	21.5523
32.6623	422.5814	.999989	21.3333
33.1648	422.5864	1.000001	21.1206
33.6673	422.5814	.999989	20.9138
34.1698	422.5864	1.000001	20.7127
34.6723	422.5764	.999977	20.5172
35.1748	422.5764	.999977	20.3269
35.6773	422.5714	.999965	20.1417
36.1798	422.5563	.999930	19.9613
36.6823	422.5462	.999906	19.7857
37.1848	422.5362	.999882	19.6146
37.6873	422.5211	.999846	19.4478
38.1898	422.5060	.999811	19.2853
38.6923	422.4909	.999775	19.1267
39.1948	422.4708	.999727	18.9721
39.6973	422.4507	.999680	18.8213
40.1998	422.4205	.999608	18.6741

* This data was taken during initial cooldown while temperature was drifting slowly downward.

SAMPLE 92D   11/3/69 I_s = 14 microamps

R(T)   H = 0 R_{max} = 422.586 ohms

HIGH TEMPERATURE DATA* NEAR RESISTANCE MAXIMUM

(PART 2)

THERMOM.R	SAMPLE R	SAMPR/RM	TEMP.
40.7023	422.4055	.999573	18.5304
41.2048	422.3803	.999513	18.3901
42.2098	422.3150	.999359	18.1193
43.2148	422.2546	.999216	17.8608
44.2198	422.2546	.999216	17.6139
45.2248	422.1139	.998883	17.3778
46.2298	422.0334	.998692	17.1518
47.2348	421.9430	.998478	16.9355
48.2398	421.8575	.998276	16.7281
49.2448	421.7569	.998038	16.5310
50.2497	421.6463	.997776	16.3387
51.2547	421.5458	.997538	16.1539
52.2597	421.4302	.997265	15.9760
53.2647	421.3095	.996979	15.8047
54.2697	421.1788	.996670	15.6396
55.2747	421.0431	.996349	15.4804
56.2797	420.9023	.996016	15.3267
57.2847	420.7515	.995659	15.1783
58.2897	420.6007	.995302	15.0349
59.2947	420.4499	.994945	14.8961
60.2997	420.2739	.994529	14.7619
61.3047	420.0980	.994112	14.6319
62.3097	419.9069	.993660	14.5059
63.3147	419.7159	.993208	14.3838
64.3197	419.5048	.992709	14.2653
65.3247	419.3087	.992245	14.1504
66.3297	419.0674	.991674	14.0387
67.3347	418.8311	.991115	13.9303
68.3397	418.5898	.990543	13.8248
69.3447	418.3234	.989913	13.7223
70.3496	418.0418	.989247	13.6226
71.3546	417.7553	.988569	13.5255

* This data was taken during initial cooldown while temperature was drifting slowly downward.

SAMPLE 92D 10/22/69 R_{max} = 422.320 ohms

R(T) H = 0 I_s = 14 microamps P.P.

UPPER HALF OF RESISTIVE TRANSITION

(PART 1)

THERMOM.R	SAMPLE R	SAMPR/RM	TEMP.
102.3587	166.9935	.395419	11.4083
102.1075	175.6252	.415858	11.4208
101.9567	180.6977	.427869	11.4283
101.7055	189.4148	.448510	11.4409
101.5547	194.9247	.461557	11.4484
101.4040	200.4847	.474722	11.4560
101.2532	206.0649	.487936	11.4636
101.1025	211.7557	.501411	11.4712
100.9517	217.6375	.515338	11.4789
100.8010	223.3987	.528980	11.4865
100.6502	229.1699	.542645	11.4942
100.4995	235.4740	.557573	11.5019
100.3488	241.9239	.572845	11.5096
100.1980	248.7207	.588939	11.5174
100.0473	255.6030	.605235	11.5251
99.8965	262.5455	.621674	11.5329
99.7458	269.6087	.638399	11.5407
99.5950	277.5215	.657136	11.5485
99.4443	284.5998	.673896	11.5564
99.2935	294.3074	.696882	11.5642
99.1428	304.2160	.720345	11.5721
98.9920	314.3207	.744271	11.5800
98.8413	323.4651	.765924	11.5880
98.6905	331.3880	.784685	11.5959
98.5398	338.9992	.802707	11.6039
98.3890	345.3184	.817670	11.6119
98.2383	350.9136	.830919	11.6199
98.0875	355.8504	.842608	11.6279
97.9368	360.2089	.852929	11.6360
97.7860	363.9441	.861773	11.6440
97.6353	367.2621	.869630	11.6521
97.4845	370.1980	.876582	11.6603
97.3338	372.9177	.883022	11.6684

SAMPLE 92D 10/22/69 I_s = 14 microamps P.P.

R(T) H = 0 R_{max} = 422.320 ohms

UPPER HALF OF RESISTIVE TRANSITION

(PART 2)

THERMOM.R	SAMPLE R	SAMPR/RM	TEMP.
97.1328	376.0547	.890450	11.6793
96.9318	378.7492	.896830	11.6902
96.6805	381.7153	.903853	11.7039
96.3790	384.7316	.910995	11.7205
95.9770	388.0194	.918781	11.7427
95.4745	391.2821	.926506	11.7707
94.8715	394.3738	.933827	11.8046
94.1178	397.3248	.940814	11.8476
93.0625	400.4366	.948183	11.9087
91.6555	403.4780	.955385	11.9923
89.4446	406.8614	.963396	12.1282
86.4296	410.0034	.970836	12.3237
81.4046	413.4621	.979025	12.6786
72.3596	417.1872	.987846	13.4309
58.2897	420.3393	.995310	15.0349
47.2348	421.6866	.998500	16.9355
34.1698	422.3200	1.000000	20.7127
33.1648	422.3200	1.000000	21.1206
20.0999	421.2090	.997369	29.7484
19.0949	420.9576	.996774	30.8442
17.0849	420.3795	.995405	33.3790

SAMPLE 92D 12/12/69 I_s = 14. microamps P.P.

R(T) H = 0 R_{max} = 422.586 ohms

LOWER PORTION OF TRANSITION

(PART 1)

THERMOM.R	SAMPLE R	SAMPR/RM	TEMP.
98.8614	323.7517	.766120	11.5869
98.8925	321.7408	.761362	11.5853
98.8965	321.7408	.761362	11.5850
98.9759	316.7136	.749465	11.5809
99.0523	311.6864	.737569	11.5769
99.1277	306.6592	.725673	11.5729
99.2031	301.6320	.713777	11.5690
99.2010	301.6320	.713777	11.5691
99.2774	296.6048	.701880	11.5651
99.3578	291.5776	.689984	11.5609
99.4433	286.5504	.678088	11.5564
99.5357	281.5232	.666191	11.5516
99.6342	276.4960	.654295	11.5465
99.7387	271.4688	.642399	11.5411
99.8463	266.4416	.630503	11.5355
99.9578	261.4144	.618606	11.5297
100.0684	256.3872	.606710	11.5240
100.1819	251.3600	.594814	11.5182
100.2975	246.3328	.582918	11.5123
100.4181	241.3056	.571021	11.5061
100.5457	236.2784	.559125	11.4995
100.6754	231.2512	.547229	11.4929
100.8080	226.2240	.535332	11.4862
100.9407	221.1968	.523436	11.4794
101.0734	216.1696	.511540	11.4727
101.2080	211.1424	.499644	11.4659
101.3447	206.1152	.487747	11.4590
101.4834	201.0880	.475851	11.4520
101.6231	196.0608	.463955	11.4450
101.7668	191.0336	.452059	11.4378
101.9125	186.0064	.440162	11.4305
102.0603	180.9792	.428266	11.4231
102.2100	175.9520	.416370	11.4157

SAMPLE 92D 12/12/69 I_s = 14 microamps P.P.

R(T) H = 0 R_{max} = 422.586

LOWER PORTION OF TRANSITION

(PART 2)

THERMOM.R	SAMPLE R	SAMPR/RM	TEMP.
102.3597	170.9248	.404473	11.4083
102.5085	165.8976	.392577	11.4009
102.6552	160.8704	.380681	11.3937
102.7989	155.8432	.368785	11.3866
102.9376	150.8160	.356888	11.3798
103.0723	145.7888	.344992	11.3732
103.2009	140.7616	.333096	11.3669
103.3245	135.7344	.321199	11.3609
103.4441	130.7072	.309303	11.3550
103.5597	125.6800	.297407	11.3494
103.5597	125.7353	.297538	11.3494
103.5607	125.6750	.297395	11.3494
103.6733	120.6480	.285499	11.3439
103.7828	115.6210	.273603	11.3386
103.8904	110.5940	.261708	11.3334
103.9969	105.5670	.249812	11.3283
104.1024	100.5400	.237916	11.3232
104.2069	95.5130	.226020	11.3182
104.3125	90.4860	.214124	11.3131
104.4210	85.4590	.202229	11.3079
104.5335	80.4320	.190333	11.3025
104.6541	75.4050	.178437	11.2968
104.7878	70.3780	.166541	11.2904
104.9355	65.3510	.154645	11.2834
104.9406	65.3510	.154645	11.2831
104.9406	65.4908	.154976	11.2831
104.9446	65.3601	.154667	11.2830
105.1044	60.3324	.142770	11.2754
105.2762	55.3047	.130872	11.2673
105.4602	50.2770	.118975	11.2586
105.6612	45.2493	.107077	11.2491
105.8823	40.2216	.095180	11.2388
106.1194	35.1939	.083282	11.2277
106.3717	30.1662	.071385	11.2160
106.6400	25.1385	.059487	11.2036
106.9325	20.1108	.047590	11.1901

SAMPLE 92D   12/12/69 I_s = 14 microamps P.P.

R(T)   H = 0 R_{max} = 422.586

LOWER PORTION OF TRANSITION

(PART 3)

THERMOM.R	SAMPLE R	SAMPR/RM	TEMP.
106.9325	20.1428	.047666	11.1901
106.9335	20.1227	.047618	11.1901
107.2681	15.0920	.035713	11.1747
107.6902	10.0614	.023809	11.1555
107.6902	10.0674	.023823	11.1555
107.6902	10.0715	.023833	11.1555
107.9827	7.5536	.017875	11.1423
108.2872	5.5393	.013108	11.1285
108.5716	4.0286	.009533	11.1158
108.8038	3.0215	.007150	11.1054
108.9435	2.5179	.005958	11.0992
109.1133	2.0143	.004767	11.0916
109.2168	1.7625	.004171	11.0870
109.3354	1.5107	.003575	11.0818
109.4852	1.2589	.002979	11.0752
109.6942	1.0071	.002383	11.0659
109.6942	1.0071	.002383	11.0659
109.7171	1.0071	.002383	11.0649
109.6684	1.0575	.002502	11.0671
110.0311	.7554	.001787	11.0512
110.3928	.5539	.001311	11.0354
110.7219	.4029	.000953	11.0211
110.9718	.3021	.000715	11.0103
111.3235	.2014	.000477	10.9951
111.6663	.1511	.000357	10.9805
112.7314	.1007	.000238	10.9365
114.1129	.0755	.000179	10.8791
115.6477	.0554	.000131	10.8167
117.0443	.0403	.000095	10.7611
117.7476	.0302	.000071	10.7335
118.3505	.0201	.000048	10.7101
119.0187	.0101	.000024	10.683

SAMPLE 92A 12/28/69 I_s = 12 microamps P.P.

R(T) H = 0 R_{max} = 325.863 ohms

UPPER PART OF RESISTIVE TRANSITION

THERMOM.R	SAMPLE R	SAMPR/RM	TEMP.
125.4868	251.3600	.771367	10.4465
125.2733	256.3872	.786794	10.4541
125.0296	261.4144	.802222	10.4627
124.7583	266.4416	.817649	10.4723
124.4318	271.4688	.833076	10.4840
124.0525	276.4960	.848504	10.4975
123.5978	281.5232	.863931	10.5139
123.0101	286.4247	.878973	10.5352
122.4474	290.2957	.890852	10.5557
121.8270	293.7896	.901574	10.5786
121.1990	296.6551	.910367	10.6019
120.5710	299.0681	.917773	10.6254
119.8174	301.2801	.924561	10.6538
118.8127	303.8942	.932583	10.6922
117.5567	306.2570	.939834	10.7410
116.0496	308.5193	.946776	10.8006
113.7889	311.0329	.954490	10.8925
110.5234	313.6973	.962666	11.0297
105.4996	316.4120	.970997	11.2567
96.9592	319.4283	.980253	11.6887
84.3243	322.0927	.988430	12.4677
62.8122	324.6566	.996298	14.4444
39.2953	325.8631	1.000000	18.9417
28.1091	325.2598	.998149	23.5816
20.1641	324.1036	.994601	29.6817
18.4498	323.3999	.992441	31.6033
13.6792	320.5845	.983802	39.2205
11.2818	318.3223	.976859	45.2804
9.7251	316.0601	.969917	50.8472
8.7950	314.2000	.964209	55.1620
7.9458	311.9378	.957267	60.0874
7.2584	309.7258	.950479	65.0843
6.6417	307.0111	.942148	70.6977
6.1151	303.6429	.931811	76.7228
5.4286	299.4703	.919007	87.1891

SAMPLE 92A 12/24/69 I_s = 12 microamps P.P.

R(T) H = 0 R_{max} = 325.863 ohms

MIDDLE OF RESISTIVE TRANSITION

THERMOM.R	SAMPLE R	SAMPR/RM	TEMP.
123.7792	279.1001	.856495	10.5074
124.0156	276.4960	.848504	10.4989
124.4044	271.4688	.833076	10.4849
124.7340	266.4416	.817649	10.4732
125.0156	261.4144	.802222	10.4632
125.2672	256.3872	.786794	10.4543
125.4747	251.3600	.771367	10.4470
125.6802	246.3328	.755940	10.4397
125.8593	241.3056	.740512	10.4335
126.0231	236.2784	.725085	10.4277
126.1743	231.2512	.709658	10.4224
126.3132	226.2240	.694230	10.4176
126.4443	221.1968	.678803	10.4130
126.5674	216.1696	.663376	10.4087
126.6835	211.1424	.647948	10.4047
126.7940	206.1152	.632521	10.4009
126.8977	201.0880	.617094	10.3973
126.9974	196.0608	.601666	10.3938
127.0924	191.0336	.586239	10.3906
127.1841	186.0064	.570812	10.3874
127.2720	180.9792	.555384	10.3844
127.3576	175.9520	.539957	10.3814
127.4410	170.9248	.524530	10.3786
127.5214	165.8976	.509102	10.3758
127.6018	160.8704	.493675	10.3730
127.6794	155.8432	.478248	10.3704
127.7570	150.8160	.462820	10.3677
127.8342	145.7888	.447393	10.3651
127.9125	140.7616	.431966	10.3624
127.9911	135.7344	.416538	10.3597
128.0720	130.7072	.401111	10.3570
128.1574	125.6800	.385684	10.3541
128.2456	120.6528	.370256	10.3511
128.3408	115.6256	.354829	10.3478
128.4408	110.5984	.339402	10.3444

SAMPLE 92A 2/28/70

R(T) H = 0

R_{max} = 325.863 ohms

$I_s = 0.5 \times 10^{-6}$A to 20 ohms
$I_s = 1 \times 10^{-6}$A to 7.5 ohms
$I_s = 5 \times 10^{-6}$A to 0.02 ohms
$I_s = 50 \times 10^{-6}$A to 1 milli-ohm

LOWER PART OF RESISTIVE TRANSITION

(PART 1)

THERMOM.R	SAMPLE R	SAMPR/RM	TEMP.
127.8065	150.8160	.462820	10.3660
127.8103	150.8160	.462820	10.3659
127.8110	150.8160	.462820	10.3659
128.3026	120.6528	.370256	10.3491
128.3993	115.6256	.354829	10.3458
128.5011	110.5984	.339402	10.3424
128.5083	110.6094	.339435	10.3421
128.6191	105.5817	.324006	10.3384
128.7372	100.5540	.308578	10.3344
128.7322	100.5540	.308578	10.3346
128.8578	95.5263	.293149	10.3303
128.9884	90.4986	.277720	10.3259
128.9984	90.4986	.277720	10.3256
129.0813	85.4709	.262291	10.3228
129.2245	80.4432	.246862	10.3180
129.3677	75.4155	.231433	10.3132
129.5209	70.3878	.216004	10.3080
129.6791	65.3601	.200575	10.3027
129.8525	60.3324	.185147	10.2969
130.0308	55.3047	.169718	10.2910
130.2217	50.2770	.154289	10.2847
130.4327	45.2493	.138860	10.2777
130.6437	40.2216	.123431	10.2707
130.8622	35.1939	.108002	10.2635
131.0933	30.1662	.092573	10.2559
131.3295	25.1385	.077144	10.2481
131.5857	20.1108	.061716	10.2398
131.5894	20.1108	.061716	10.2396
131.5681	20.1227	.061752	10.2403
131.7439	17.1043	.052489	10.2346
131.9348	14.0859	.043226	10.2284
132.0755	12.0736	.037051	10.2238
132.2312	10.0614	.030876	10.2188

SAMPLE 92A 2/28/70 I_s = 1 x10^{-6}A to 7.5ohms
I_s = 5 x10^{-6}A to 0.02ohms
R(T) H = 0 I_s = 50 x10^{-6}A to 1 milli-ohm

R_{max} = 325.863 ohms

LOWER PART OF RESISTIVE TRANSITION

(PART 2)

THERMOM.R	SAMPLE R	SAMPR/RM	TEMP.
132.2262	10.1722	.031216	10.2189
132.4573	7.5536	.023180	10.2115
132.7060	5.5393	.016999	10.2034
132.9597	4.0286	.012363	10.1953
133.2109	3.0215	.009272	10.1872
133.3967	2.5179	.007727	10.1813
133.6454	2.0143	.006181	10.1734
133.7911	1.7625	.005409	10.1687
133.9996	1.5107	.004636	10.1621
134.2458	1.2589	.003863	10.1543
134.5020	1.0071	.003091	10.1462
134.7783	.7554	.002318	10.1375
135.0219	.5539	.001700	10.1299
135.2631	.4029	.001236	10.1224
135.4992	.3021	.000927	10.1150
135.7002	.2518	.000773	10.1087
135.9438	.2014	.000618	10.1012
136.1247	.1763	.000541	10.0956
136.3080	.1511	.000464	10.0899
136.5843	.1259	.000386	10.0814
136.9913	.1007	.000309	10.0689
137.4911	.0755	.000232	10.0537
138.0036	.0554	.000170	10.0381
138.3050	.0403	.000124	10.0290
138.8953	.0201	.000062	10.0113
139.1214	.0101	.000031	10.0045
139.1214	.0111	.000034	10.0045
139.3851	.0055	.000017	9.9966
139.5107	.0030	.000009	9.9929
139.5936	.0010	.000003	9.9904

SAMPLE 92DX 5/23/70 I_s = 2 microamps P.P.

R(T) H = 0 R_{max} = 339.081 ohms

FULL TRANSITION UP TO RESISTANCE MAXIMUM (PART 1)

THERMOM.R	SAMPLE R	SAMPR/RM	TEMP.
33.7259	338.9591	.999640	20.8901
33.8063	339.0094	.999789	20.8576
33.8717	339.0596	.999937	20.8313
34.0175	338.8083	.999196	20.7731
84.1181	331.7702	.978439	12.4821
91.3339	326.7430	.963613	12.0117
94.5740	321.7158	.948787	11.8215
96.2584	316.6886	.933962	11.7271
97.1016	311.6614	.919136	11.6810
97.6162	306.6342	.904310	11.6532
97.9337	301.6070	.889484	11.6361
98.1930	296.5798	.874658	11.6223
98.4091	291.5526	.859832	11.6108
98.6131	286.5254	.845006	11.6000
98.8041	281.4982	.830180	11.5899
99.0011	276.4710	.815354	11.5796
99.2010	271.4438	.800528	11.5691
99.2774	269.5837	.795042	11.5651
99.4051	266.4166	.785702	11.5584
99.6262	261.3894	.770876	11.5469
99.8563	256.3622	.756050	11.5350
100.0875	251.3350	.741224	11.5231
100.3196	246.3078	.726398	11.5111
100.5548	241.2806	.711572	11.4991
100.7970	236.2534	.696746	11.4867
101.0512	231.2262	.681920	11.4738
101.3186	226.1990	.667094	11.4603
101.5959	221.1718	.652268	11.4464
101.8804	216.1446	.637442	11.4321
102.1728	211.1174	.622616	11.4176
102.4592	206.0902	.607790	11.4034
102.7406	201.0630	.592965	11.3895
103.0070	196.0358	.578139	11.3764
103.2552	191.0086	.563313	11.3642
103.4924	185.9814	.548487	11.3527
103.7285	180.9542	.533661	11.3412
103.9667	175.9270	.518835	11.3297
104.2059	170.8998	.504009	11.3182
104.4532	165.8660	.489163	11.3064
104.7044	160.8390	.474338	11.2944
104.9597	155.8120	.459513	11.2822
105.2129	150.7850	.444687	11.2702
105.4672	145.7580	.429862	11.2583
105.7114	140.7310	.415037	11.2468
105.9586	135.7040	.400211	11.2352

SAMPLE 92DX 5/23/70 I_s = 2. microamps P.P.

R(T) H = 0 R_{max} = 339.081 ohms

FULL TRANSITION UP TO RESISTANCE MAXIMUM (PART 2)

THERMOM.R	SAMPLE R	SAMPR/RM	TEMP.
106.1998	130.6770	.385386	11.2240
106.4471	125.6500	.370560	11.2125
106.7134	120.6230	.355735	11.2002
106.8712	115.5960	.340910	11.1929
107.0681	110.5690	.326084	11.1839
107.2521	105.5420	.311259	11.1755
107.4370	100.5290	.296475	11.1670
107.8309	90.4736	.266820	11.1491
107.6279	95.5013	.281647	11.1583
108.0571	85.4459	.251993	11.1389
108.2983	80.4182	.237165	11.1280
108.5596	75.3905	.222338	11.1163
108.8460	70.3628	.207510	11.1035
109.1344	65.3351	.192683	11.0907
109.4138	60.3074	.177855	11.0783
109.6681	55.2797	.163028	11.0671
109.8992	50.2600	.148224	11.0569
110.1123	45.2315	.133394	11.0476
110.3113	40.2030	.118565	11.0389
110.4972	35.1745	.103735	11.0308
110.7319	30.1460	.088905	11.0207
110.9768	25.1175	.074075	11.0101
111.3184	20.0890	.059245	10.9954
111.5081	17.5747	.051831	10.9872
111.7141	15.0605	.044416	10.9784
111.9313	12.5462	.037001	10.9692
112.1587	10.0465	.029629	10.9606
112.4099	7.5286	.022203	10.9500
112.6435	5.5143	.016263	10.9401
112.6585	5.5143	.016263	10.9395
112.8947	4.0036	.011807	10.9296
113.1207	2.9964	.008837	10.9202
113.2915	2.4929	.007352	10.9131
113.5553	1.9893	.005867	10.9021
113.7060	1.7375	.005124	10.8959
113.8843	1.4857	.004382	10.8885
114.0325	1.2339	.003639	10.8824
114.2008	.9821	.002897	10.8755
114.3968	.7304	.002154	10.8675
114.6354	.5289	.001560	10.8577
115.0247	.3779	.001114	10.8419
117.6647	.2771	.000817	10.7368

SAMPLE 92DX 5/22/70

R(T) H = 0 R_{max} = 339.081 ohms

LOW RESISTANCE PORTION OF R(T)

THERMOM.R	SAMPLE R	SAMPR/RM	TEMP.
112.2545	10.0746	.029711	10.9565
112.5191	7.5567	.022286	10.9454
112.7733	5.5353	.016324	10.9347
113.0117	4.0246	.011869	10.9247
113.2260	3.0174	.008899	10.9158
113.3692	2.5139	.007414	10.9098
113.5633	2.0103	.005929	10.9018
113.6814	1.7585	.005186	10.8969
113.8196	1.5067	.004444	10.8912
113.9628	1.2549	.003701	10.8853
114.1261	1.0031	.002958	10.8786
114.3044	.7514	.002216	10.8713
114.4828	.5499	.001622	10.8640
114.6561	.3989	.001176	10.8569
114.8069	.2981	.000879	10.8507
114.9048	.2478	.000731	10.8468
114.9777	.1974	.000582	10.8438
115.1711	.1723	.000508	10.8360
115.2816	.1471	.000434	10.8315
115.4600	.1219	.000359	10.8243
115.9549	.0967	.000285	10.8044
117.2059	.0715	.000211	10.7547
117.9621	.0514	.000152	10.7252
118.5575	.0363	.000107	10.7021
119.4518	.0161	.000048	10.6677
120.1150	.0061	.000018	10.6426
122.6171	.0010	.000003	10.5495

SAMPLE 92D   11/10/69 I_s = 12 microamps P.P.

R(T)   H = 2 kOe R_{max} = 422.586 ohms

MAGNETIC FIELD PERPENDICULAR TO SAMPLE

TEMPERATURE CORRECTED FOR THERMOMETER MAGNETORESISTANCE*

THERMOM.R	SAMPLE R	SAMPR/RM	TEMP.
72.8809	417.2576	.987391	13.3828
83.8182	412.2304	.975495	12.5033
84.3825	407.2032	.963598	12.4636
92.5006	402.1760	.951702	11.9418
94.4494	397.1488	.939806	11.8286
95.5467	392.1216	.927910	11.7666
96.3792	387.0944	.916013	11.7205
96.9872	382.0672	.904117	11.6872
97.4769	377.0400	.892221	11.6607
97.8702	372.0128	.880324	11.6395
98.2096	366.9856	.868428	11.6214
98.5007	361.9584	.856532	11.6059
98.7631	356.9312	.844636	11.5921
98.9942	351.9040	.832739	11.5799
99.2113	346.8768	.820843	11.5685
99.4126	341.8496	.808947	11.5580
99.5946	336.8224	.797051	11.5486
99.7686	331.7952	.785154	11.5395
99.9297	326.7680	.773258	11.5312
100.1001	321.7408	.761362	11.5224
100.2527	316.7136	.749465	11.5146
100.3985	311.6864	.737569	11.5071
100.5499	306.6592	.725673	11.4993
100.6902	301.6320	.713777	11.4922
100.8268	296.6048	.701880	11.4852
100.9477	291.5776	.689984	11.4791
101.0920	286.5504	.678088	11.4718
101.2255	281.5232	.666191	11.4650
101.3492	276.4960	.654295	11.4588
101.4704	271.4688	.642399	11.4527
101.6039	266.4416	.630503	11.4460
101.7261	261.4144	.618606	11.4398
101.8545	256.3872	.606710	11.4334
101.9780	251.3600	.594814	11.4272
102.1065	246.3328	.582918	11.4208
102.2319	241.3056	.571021	11.4146
102.3594	236.2784	.559125	11.4083
102.4869	231.2512	.547229	11.4020
102.6163	226.2240	.535332	11.3956
102.7408	221.1968	.523436	11.3895
102.8703	216.1696	.511540	11.3831
102.9997	211.1424	.499644	11.3767
103.1273	206.1152	.487747	11.3705
103.2657	201.0880	.475851	11.3637

* See chapter three for discussion of this correction.

SAMPLE 92D   11/10/69 I_s = 12. microamps P.P.

R(T)   H = 2. kOe R_{max} = 422.586 ohms

MAGNETIC FIELD PERPENDICULAR TO SAMPLE

TEMPERATURE CORRECTED FOR THERMOMETER MAGNETORESISTANCE*

THERMOM.R	SAMPLE R	SAMPR/RM	TEMP.
103.4002	196.0608	.463955	11.3572
103.5365	191.0336	.452059	11.3506
103.6732	186.0064	.440162	11.3439
103.8107	180.9792	.428266	11.3373
103.9481	175.9520	.416370	11.3306
104.0896	170.9248	.404473	11.3238
104.2333	165.8976	.392577	11.3169
104.3768	160.8704	.380681	11.3100
104.5203	155.8432	.368765	11.3032
104.6352	150.8160	.356888	11.2977
104.8234	145.7888	.344992	11.2887
104.9691	140.7616	.333096	11.2818
105.1174	135.7344	.321199	11.2748
105.2548	130.7072	.309303	11.2683
105.4275	125.6800	.297407	11.2601
105.5801	120.6528	.285511	11.2530
105.7406	115.6256	.273614	11.2454
105.8992	110.5984	.261718	11.2380
106.0598	105.5712	.249822	11.2305
106.1813	100.5540	.237949	11.2249
106.3758	95.5263	.226052	11.2158
106.5484	90.4986	.214154	11.2078
106.7191	85.4709	.202257	11.2000
106.8985	80.4432	.190359	11.1917
107.0801	75.4155	.178462	11.1834
107.2717	70.3878	.166564	11.1746
107.4684	65.3601	.154667	11.1656
107.6711	60.3324	.142770	11.1564
107.8898	55.3047	.130872	11.1465
108.1165	50.2770	.118975	11.1362
108.2099	45.2493	.107077	11.1320
108.6242	40.2216	.095180	11.1134
108.9051	35.1939	.083282	11.1009
109.2036	30.1662	.071385	11.0876
109.5581	25.1385	.059487	11.0719
109.9761	20.1108	.047590	11.0536
110.4868	15.0831	.035692	11.0313
110.6885	10.0554	.023795	11.0225
112.2683	5.0277	.011897	10.9559

* See chapter three for discussion of this correction.

SAMPLE 92D 11/10/69 I_s = 12. microamps P.P.

R(T) H = 10 .kOe R_{max} = 422.586 ohms

MAGNETIC FIELD PERPENDICULAR TO SAMPLE

TEMPERATURE CORRECTED FOR THERMOMETER MAGNETORESISTANCE*

THERMOM.R	SAMPLE R	SAMPR/RM	TEMP.
32.6784	422.5663	.999953	21.3264
72.4571	417.2576	.987391	13.4219
84.5392	412.2304	.975495	12.4527
90.4757	407.2032	.963598	12.0641
93.9821	402.1760	.951702	11.8554
96.2403	397.1488	.939806	11.7281
97.8001	392.1216	.927910	11.6433
98.9649	387.0944	.916013	11.5815
99.8000	382.0672	.904117	11.5379
104.1476	336.8224	.797051	11.3210
106.2139	296.6048	.701880	11.2233
109.3957	211.0145	.499341	11.0791
109.9312	195.9420	.463674	11.0555
107.9646	251.3600	.594814	11.1431
113.2013	110.5314	.261560	10.9168
114.3788	85.4709	.202257	10.8682
117.2400	40.2216	.095180	10.7534
121.4635	10.0544	.023793	10.5920
127.5537	1.0054	.002379	10.3747
134.0095	.1005	.000238	10.1618
140.6000	.0101	.000024	9.9607

* See chapter three for discussion of this correction.

SAMPLE 92D

SMALL PERPENDICULAR MAGNETIC FIELDS AT CONSTANT TEMPERATURE

10/22/69 I_s = 14 microamps P.P.

H (Oe)	T (K)	RS EXP (ohms)
.223E-02	11.6103	344.263
3.24	11.6103	344.122
11.6	11.6103	344.052
32.6	11.6097	344.122
110.	11.6097	344.926
337.	11.6095	347.741
684.	11.6089	351.693

H (Oe)	T (K)	RS EXP (ohms)
.223E-02	11.5663	298.214
2.66	11.5665	298.726
12.0	11.5667	300.149
34.6	11.5667	302.361
112.	11.5666	307.026
337.	11.5668	315.557
682.	11.5668	324.767

H (Oe)	T (K)	RS EXP (ohms)
.223E-02	11.5256	255.256
3.80	11.5251	255.784
12.4	11.5246	256.799
22.7	11.5246	257.729
112.	11.5241	264.431
223.	11.5241	270.488
760.	11.5228	288.963

SAMPLE 92D

SMALL PERPENDICULAR MAGNETIC FIELDS AT CONSTANT TEMPERATURE

10/22/69 I_s = 14 microamps P.P.

H (Oe)	T (K)	RS EXP (ohms)
.223E-02	11.4758	214.677
4.78	11.4758	215.280
1.43	11.4758	214.933
11.7	11.4758	215.994
34.5	11.4758	217.778

H (Oe)	T (K)	RS EXP (ohms)
.223E-02	11.4758	214.822
3.02	11.4758	215.194
22.3	11.4758	218.552
152.	11.4758	224.314
689.	11.4750	246.398

H (Oe)	T (K)	RS EXP (ohms)
.223E-02	11.4484	195.146
5.90	11.4482	195.784
10.9	11.4482	196.171
33.5	11.4480	197.735
116.	11.4479	201.958
335.	11.4479	210.906
677.	11.4473	223.565

H (Oe)	T (K)	RS EXP (ohms)
.223E-02	11.3414	116.530
3.93	11.3414	116.782
12.5	11.3412	117.435
35.0	11.3411	119.245
112.	11.3409	123.579
335.	11.3405	132.175
677.	11.3398	143.235

SAMPLE 92A

PERPENDICULAR MAGNETIC FIELDS AT CONSTANT TEMPERATURE

1/10/70 I_s = 14 microamps P.P.

H (Oe)	T (K)	RS EXP (ohms)
.223E-02	11.1376	315.205
.200E+04	11.1376	315.205
.401E+04	11.1376	315.306
.601E+04	11.1376	315.457
.800E+04	11.1376	315.708
.101E+05	11.1376	315.960

H (Oe)	T (K)	RS EXP (ohms)
.223E-02	10.8424	309.927
.100E+04	10.8424	309.927
.200E+04	10.8424	309.927
.399E+04	10.8424	310.329
.602E+04	10.8424	310.681
.800E+04	10.8424	311.184
.916E+04	10.8424	311.536
.101E+05	10.8424	311.787

H (Oe)	T (K)	RS EXP (ohms)
.223E-02	10.5614	291.578
.100E+04	10.5614	292.080
.201E+04	10.5614	293.287
.299E+04	10.5614	294.544
.400E+04	10.5614	296.002
.501E+04	10.5614	297.409
.601E+04	10.5614	298.666
.697E+04	10.5614	299.772
.800E+04	10.5614	300.828
.901E+04	10.5614	301.934

SAMPLE 92A

PERPENDICULAR MAGNETIC FIELDS AT CONSTANT TEMPERATURE

1/10/70 I_s = 14 microamps P.P.

H (Oe)	T (K)	RS EXP (ohms)
.223E-02	10.4610	261.113
.100E+04	10.4610	266.442
.201E+04	10.4610	272.273
.399E+04	10.4610	281.171
.501E+04	10.4610	284.690
.600E+04	10.4610	287.707
.700E+04	10.4610	290.271
.800E+04	10.4610	292.533

H (Oe)	T (K)	RS EXP (ohms)
.223E-02	10.3956	200.887
.100E+04	10.3956	228.989
.201E+04	10.3956	244.573
.299E+04	10.3956	255.130
.401E+04	10.3956	263.827
.501E+04	10.3956	270.514
.601E+04	10.3956	275.893
.700E+04	10.3956	280.116
.800E+04	10.3956	283.735
.903E+04	10.3956	287.154

SAMPLE 92A

SAMPLE RESISTANCE VS. PERPENDICULAR MAGNETIC FIELD AT HIGH CONSTANT TEMPERATURES

R_{max} = 448.725 ohms I_s = 12 microamps P.P.

MAGNETIC FIELD (kOe)	SAMPLE RESISTANCE (ohms)	TEMPERATURE (°K)
0	448.725	19.097
39.65	448.790	"
61.55	448.937	"
81.00	449.077	"
94.45	449.148	"
0	445.810	30.506
39.65	445.774	"
61.55	445.729	"
81.00	445.674	"
94.45	445.644	"
0	441.305	41.050
39.65	441.285	"
60.55	441.270	"
81.00	441.215	"
94.45	441.195	"
0		55.96
39.65	431.864	"
81.00	431.834	"
94.45	431.784	"

SAMPLE 92DX

RESISTANCE VS. TEMPERATURE IN A PERPENDICULAR MAGNETIC FIELD OF 69.30 KOe.

R_{max} = 336.628 ohms I_s = 12 microamps P.P.

THERMISTOR RESISTANCE (ohms)	TEMPERATURE (K)	SAMPLE RESISTANCE (ohms)
13.394	19.935	336.859
280.445	9.762	321.718
384.651	9.173	301.611
493.531	8.757	251.342
563.605	8.554	201.074
627.646	8.397	150.805
699.298	8.247	100.537
800.769	8.069	50.268

TEMPERATURE VS. MAGNETIC FIELD AT CONSTANT SAMPLE RESISTANCE

$R/R_{max} = 0.5$ $I_s = 12$ microamps P.P.

THERMISTOR RESISTANCE (ohms)	TEMPERATURE (K)	MAGNETIC FIELD (kOe)
SAMPLE 92DX	SAMPLE RESISTANCE = 168.314 ohms	
133.849	11.385	0
160.327	10.961	9.725
175.542	10.754	14.55
191.742	10.557	19.78
210.731	10.351	24.41
234.330	10.126	30.13
291.430	9.687	40.65
370.847	9.237	51.40
458.241	8.877	59.80
603.216	8.454	69.30
836.661	8.014	79.15
SAMPLE 92A	SAMPLE RESISTANCE = 224.192 ohms	
198.530	10.481	0
233.813	10.131	8.26
287.278	9.715	19.57
352.501	9.329	30.19
439.181	8.946	40.75
564.811	8.550	50.7
742.961	8.166	61.65

SAMPLE 92A

RESISTANCE VS. TEMPERATURE AT A PERPENDICULAR MAGNETIC FIELD

OF 94.95 kOe

I_s ≈ 12 microamps P.P.

THERMISTOR RESISTANCE (ohms)	TEMPERATURE (K)	SAMPLE RESISTANCE (ohms)
15.186	19.097	448.807
614.275	8.428	437.335
1006.365	7.791	423.210
1343.079	7.472	402.147
1608.933	7.285	377.013
1819.154	7.161	351.879
2149.746	6.995	301.611
2440.815	6.870	251.342
3037.361	6.653	150.805
3425.386	6.533	100.537
4025.734	6.371	50.268
4203.036	6.327	40.200
4447.178	6.269	30.150
4792.778	6.193	20.100
5388.52	6.074	10.050
6023.09	5.960	5.025
6342.18	5.908	3.517
6917.01	5.821	2.010
7648.83	5.722	1.005
8425.	5.629	.502
11421.	5.357	.050

SAMPLE RESISTANCE VS. PERPENDICULAR MAGNETIC FIELD AT THE TEMPERATURE FOR MAXIMUM RESISTANCE IN ZERO FIELD

I_s = 12 microamps P.P.

SAMPLE	MAGNETIC FIELD (kOe)	SAMPLE RESISTANCE (ohms)	TEMPERATURE (K)
92DX	0	336.628	19.935
"	14.55	336.648	"
"	19.78	336.653	"
"	19.935	336.668	"
"	30.13	336.688	"
"	40.65	336.728	"
"	51.40	336.773	"
"	59.80	336.814	"
"	69.30	336.859	"
"	79.15	336.914	"
92A	0	448.384	19.097
"	8.26	448.384	"
"	15.186	448.384	"
"	30.19	448.430	"
"	40.75	448.480	"
"	50.7	448.550	"
"	61.65	448.606	"
"	79.8	448.716	"
"	94.95	448.807	"

Voltage Dependence of Resistance for Sample 92D

Temperature (K)	Sample Resistance (ohms)	Sample Current (μA rms)	Sample Voltage (μV rms)
10.037	.10072	4.95	.495
	.10072	9.90	.990
	.10575	24.7	2.62
	.11179	49.5	5.53
	.12086	99.0	11.96
	.13868	247	34.3
11.067	1.0072	4.95	4.99
	1.0243	9.90	10.14
	1.0681	24.7	26.4
	1.1275	49.5	55.9
	1.2265	99.0	121.4
	1.5115	247	374

Voltage Dependence of Resistance for Sample 92A

Temperature (K)	Sample Resistance (ohms)	Sample Current (μA rms)	Sample Voltage (μV rms)
10.146	1.0072	.172	.173
	.9064	.339	.308
	.8259	.862	.712
	.8158	1.72	1.40
	.8259	3.39	2.803
	.8661	8.62	7.47
	.9145	17.2	15.7
10.219	10.0715	.173	1.73
	9.9909	.339	3.39
	9.9506	.862	8.58
	10.0161	1.72	17.21
	10.1823	3.39	34.6
	10.6083	8.62	91.5
	11.0847	17.2	191
10.335	100.272	.182	18.3
	100.172	.357	35.8
	100.162	.913	91.4
	100.320	1.82	183
	100.715	3.57	360
	101.730	9.13	928
	102.907	18.2	1874
10.368	150.866	.172	25.9
	150.816	.339	51.2
	150.731	.862	130
	150.751	1.72	259
	150.871	3.39	512
	151.304	8.62	1305
10.397	201.038	.172	34.5
	200.937	.339	68.2
	200.862	.862	173
	200.862	1.72	345
	200.897	3.39	682
	201.063	8.62	1735
	201.359	48.6	3460

Voltage Dependence of Resistance for Sample 92A

Temperature (K)	Sample Resistance (ohms)	Sample Current (μA rms)	Sample Voltage (μV rms)
10.654	300.978	.172	51.7
	300.878	.339	102
	300.803	.862	259
	300.797	1.72	517
	300.777	3.39	1021
	300.772	8.62	2600
	300.774	17.2	5170
31.603	323.450	.172	55.6
	323.350	.339	109.7
	323.249	.862	279
	323.229	1.72	555
	323.214	3.39	1097
	323.204	8.62	2790
	323.202	17.2	5550
76.72	303.844	.172	52.2
	303.643	.339	103
	303.593	.862	262
	303.578	1.72	522
	303.542	3.39	1030
	303.517	8.62	2620
	303.500	17.2	5220
296	234.469	.172	40.3
	234.368	.339	79.5
	234.268	.862	202
	234.182	1.72	402
	234.167	3.39	795
	234.147	8.62	2020
	234.137	17.2	4023

CHAPTER 5: ANALYSIS OF DATA

In this chapter, we will compare the data with some of the models for fluctuation broadening of resistive transitions summarized in chapter 1. We will begin with the "zero magnetic field" data. In this case, the Aslamasov-Larkin (AL) temperature dependence of σ' is obtained in the upper portion of the transition for an extrapolated normal resistance suggested by high temperature and magnetic field data. There is, however, no quantitative agreement between our data and this model. The material parameters such as strength of depairing interaction and strong coupling nature of our samples will be invoked to improve this situation. These parameters will thus be introduced as adjustable constants. As will be discussed below, the normal resistance will also appear as a parameter, adjustable, however, only within rather narrow limits. We will also find interesting behavior in the lower part of the transition which suggests a second T^*_c.

Data taken in magnetic fields will be used to support our assumptions on the normal resistance. A model of fluctuation effects in magnetic fields is still lacking for three dimensional samples with intermediate or strong depairing. For this reason, our magnetic field data will be presented unanalyzed except for a phenomenological search for power law dependence.

Analysis of "Zero Magnetic Field" Data

It was noted in chapter 1 that for broad ranges of sample parameters the theoretical picture is incomplete. In spite of this, there appear to be limits in these sample parameters for which the conductivity due to fluctuation effects, σ', ought to obey a power law in the reduced temperature, τ. We will see below that the most reasonable assumption for normal resistance leads to extensive regions of power law behavior.

We choose the method of Testardi et al.[34] discussed in chapter 1 to exhibit the power law behavior ($\sigma' \sim \tau^{-n}$). We call this method the "log-log" analysis. An outline of it follows in the next paragraphs.

We saw in chapter 1 that if data is plotted as log (D) vs. log($\mathcal{R}$), where

$$D = \frac{1}{R^2}\frac{dR}{dT} - \frac{1}{R_n^2}\frac{dR_n}{dT}$$

$$\mathcal{R} = (R_n - R)/R ,$$

then power law (τ^{-n}) or exponential (e^{τ}) dependence of σ' will appear as straight line segments of the data. Slopes, α, of the data greater than or equal to one are associated with data above T_c. In the analysis to follow in the sections below, we will interpret $\alpha \to 1$ as the approach to T_c.

Above T_c, straight line portions of data on a plot of log(D) vs. log($\mathcal{R}$) are equivalent to $D \cong \beta \cdot \mathcal{R}^{\alpha}$.

Slope $\alpha = 1$ corresponds to

$$\sigma'(\tau) = \sigma'(0) \cdot e^{-\beta R_n T_c \tau}$$

Slopes $\alpha > 1$ correspond to

$$\sigma'(\tau) = \sigma_n \left(\frac{\beta_n R_n T_c \tau}{n} + \left(\frac{\sigma_n}{\sigma'(0)} \right)^{1/n} \right)^{-n}$$

where $n = (\alpha - 1)^{-1}$.

The "log-log" analysis tells us nothing about $\sigma_n / \sigma'(0)$, so we will assume it to be zero consistent with the models of extra conductivity discussed in chapter 1.

<u>Zero Magnetic Field Data Above T_c</u>

For all reasonable values of $R_n(T)$, we find $\alpha > 1$ in the log-log analysis in the high resistance portion of the transition. In this region, the log-log analysis is most sensitive to errors in $R_n(T)$. Expressed as an error in the exponent of τ, this sensitivity to $R_n(T)$ can be estimated to be:

$$\frac{\delta n}{n} \cong \frac{1}{\textcircled{R}_x} \frac{\delta R_n}{R_n} \qquad (\text{above } T_c)$$

for our samples.

As discussed at the end of chapter 1, we cannot measure $R_n(T)$. In spite of this, it still turns out to be possible to make rather strong statements regarding comparison of our data to power law dependence of σ' on τ.

We began early in our use of the "log-log" analysis by trying linear extrapolations for $R_n(T)$ from above the main portion of the transition. It became clear, however, that only two linear extrapolations produced any power law behavior at all, as exhibited on a "log-log" plot. Surprisingly, one choice, from below the peak in measured R(T), produced τ^{-1} behavior. The other, from well above the peak, produced both $\tau^{-1/2}$ and τ^{-1}. Furthermore, changes in $R_n(T)$ from these optimum extrapolations had the effect of reducing the region of data on the "log-log" plots that showed any power law behavior at all.

The extrapolation for $R_n(T)$ which produced $\sigma' \sim \tau^{-1}$ has been discussed elsewhere.[86] The linear extrapolations which produce $\sigma' \sim \tau^{-1/2}$ are shown in figures 2,3,and4 (chapter 2). Figures 3 and 17 illustrate the optimum nature of the choice of $R_n(T)$ which produces $\tau^{-1/2}$ behavior.

Further considerations make one of these choices of $R_n(T)$ by far the more reasonable one. The extrapolation that gives r=1 implies that there is a peak in the normal resistance at about 16 K to 20 K. We do not know how to account for such nonmonotonic behavior of $R_n(T)$. In addition, if one were to believe the AL <u>temperature</u> <u>dependence</u> of σ', then this choice of $R_n(T)$ is inconsistent with what we know of sample thickness and coherence length. AL predict that r=1 if sample thickness, d, is less than $\xi(T)$. For our samples, d=1500Å, but $\xi(0)$ =35Å. On the other hand, the choice of $R_n(T)$ which produces $\tau^{-1/2}$ behavior of σ' corres-

Figure 17

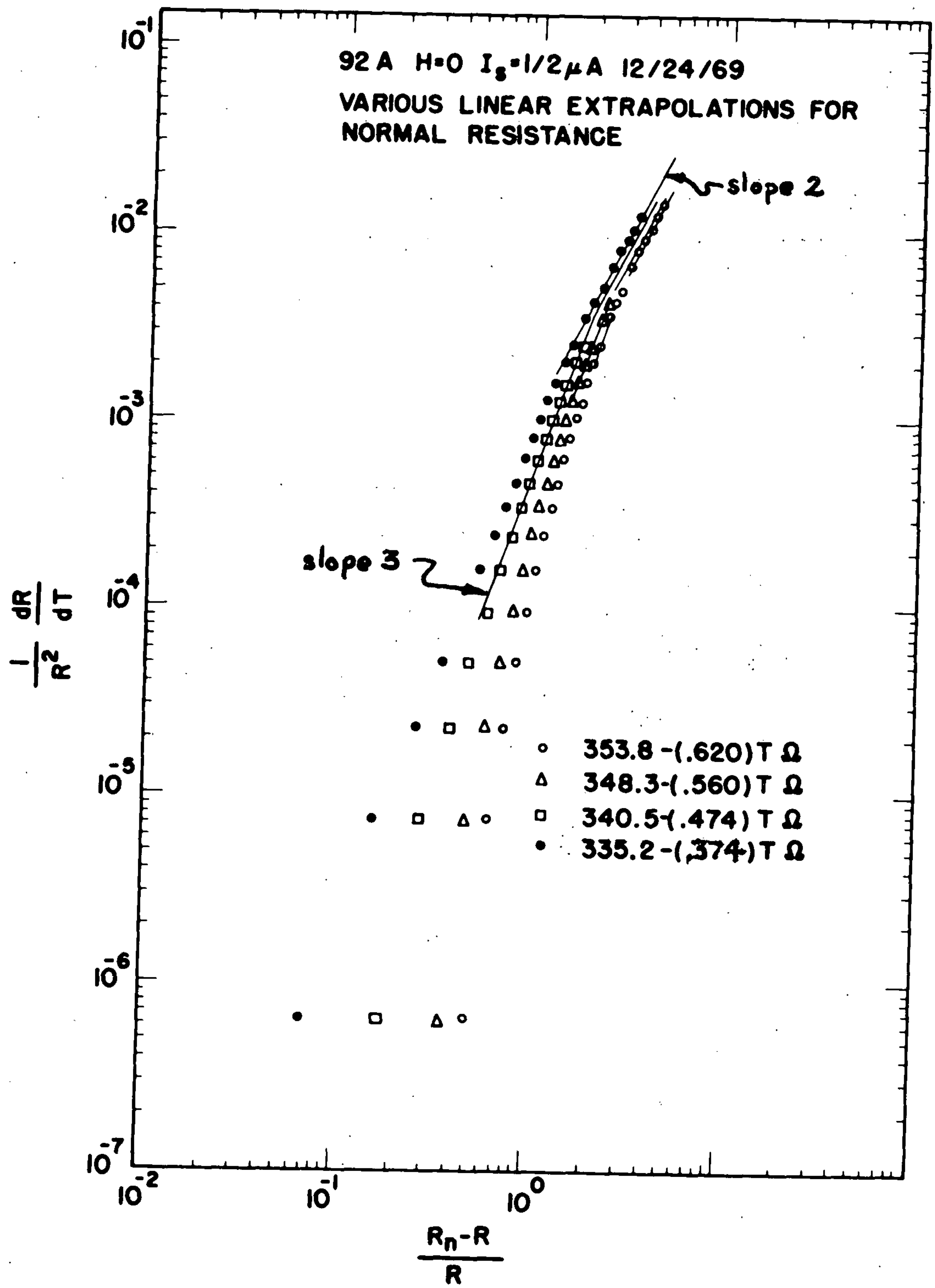

Log-Log Plot of Data for Sample 92A Showing Effects of Various Choices of Extrapolated $R_n(T)$. (Extrapolations are Shown on Figure 3.)

ponds to the aesthetically more pleasing extrapolation from temperatures well above the peak in measured R(T). (See figures 3 and 17.)

Besides producing a power law consistent with what we know of sample geometry, this choice is further supported by magnetic field data. Measurements in large magnetic fields indicate that there is fluctuation conductivity above the peak in measured R(T). At the maximum value of sample resistance in zero field (20 K), both samples show an <u>increase</u> in resistance of a few tenths of an ohm in a field of 80kOe. At higher temperatures, resistance <u>decreases</u> by a few tenths of an ohm in these fields. Moreover, the position of the resistance maximum is displaced downward in temperature by one degree in 80 kOe.

The extrapolation for $R_n(T)$, which produced ,
is used in the analysis to follow below. It should be noted that for each sample it was necessary to adjust this $R_n(T)$ by a factor (within $1{:}10^{-4}$ of unity) corresponding to small changes in R_{max}. (See comments beginning chapter 4.)

Figures 18, 19 and 20 show the "log-log" plots corresponding to this choice of $R_n(T)$. The regions of the data corresponding to r=½ (slope 3) and r=1 (slope 2) are listed in table 2 and illustrated in figure 21.

The temperature intervals over which the two power laws

Figure 18

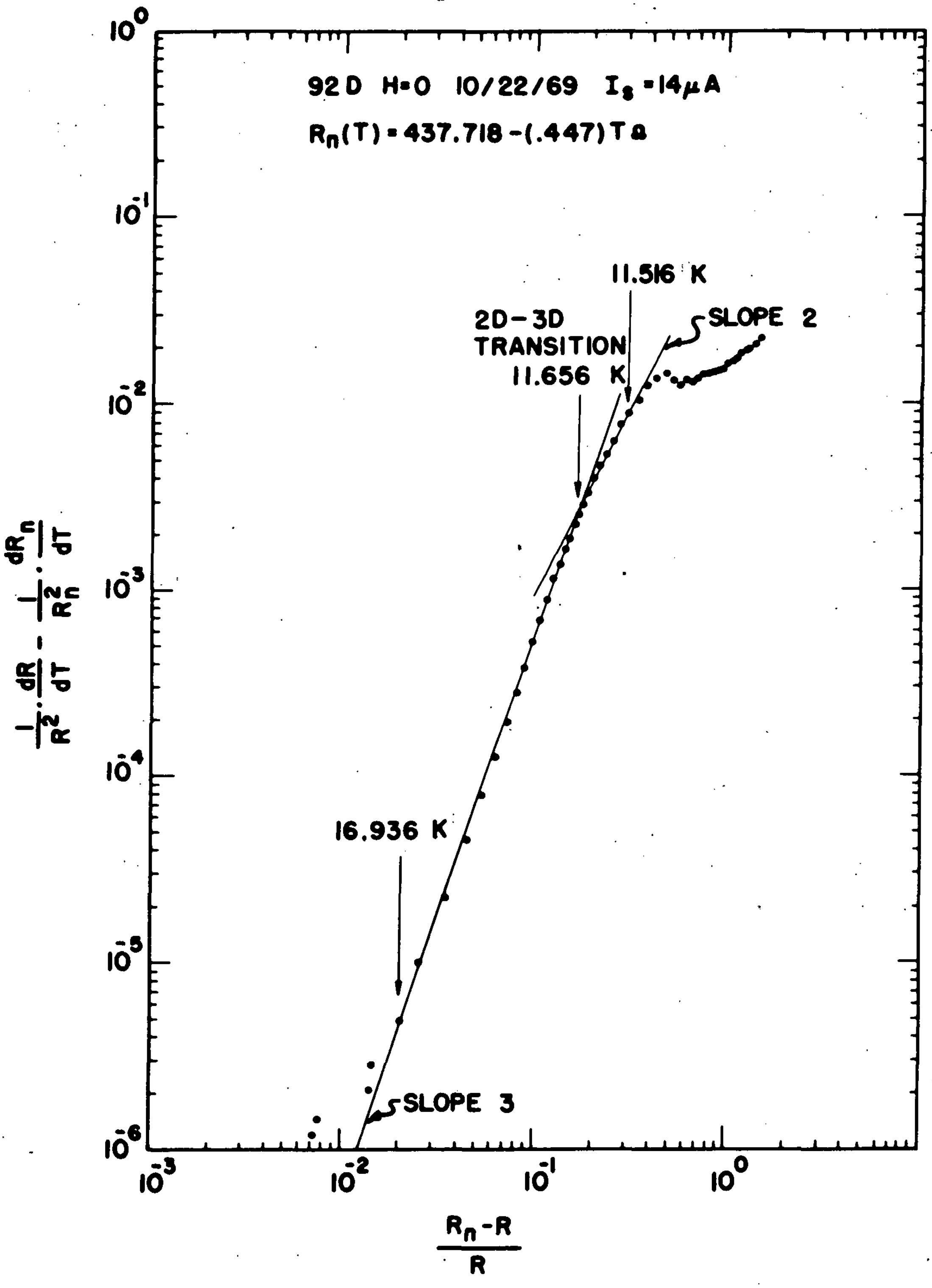

Log-Log Plot of Data for Sample 92D: Upper Portion of Transition

Figure 19

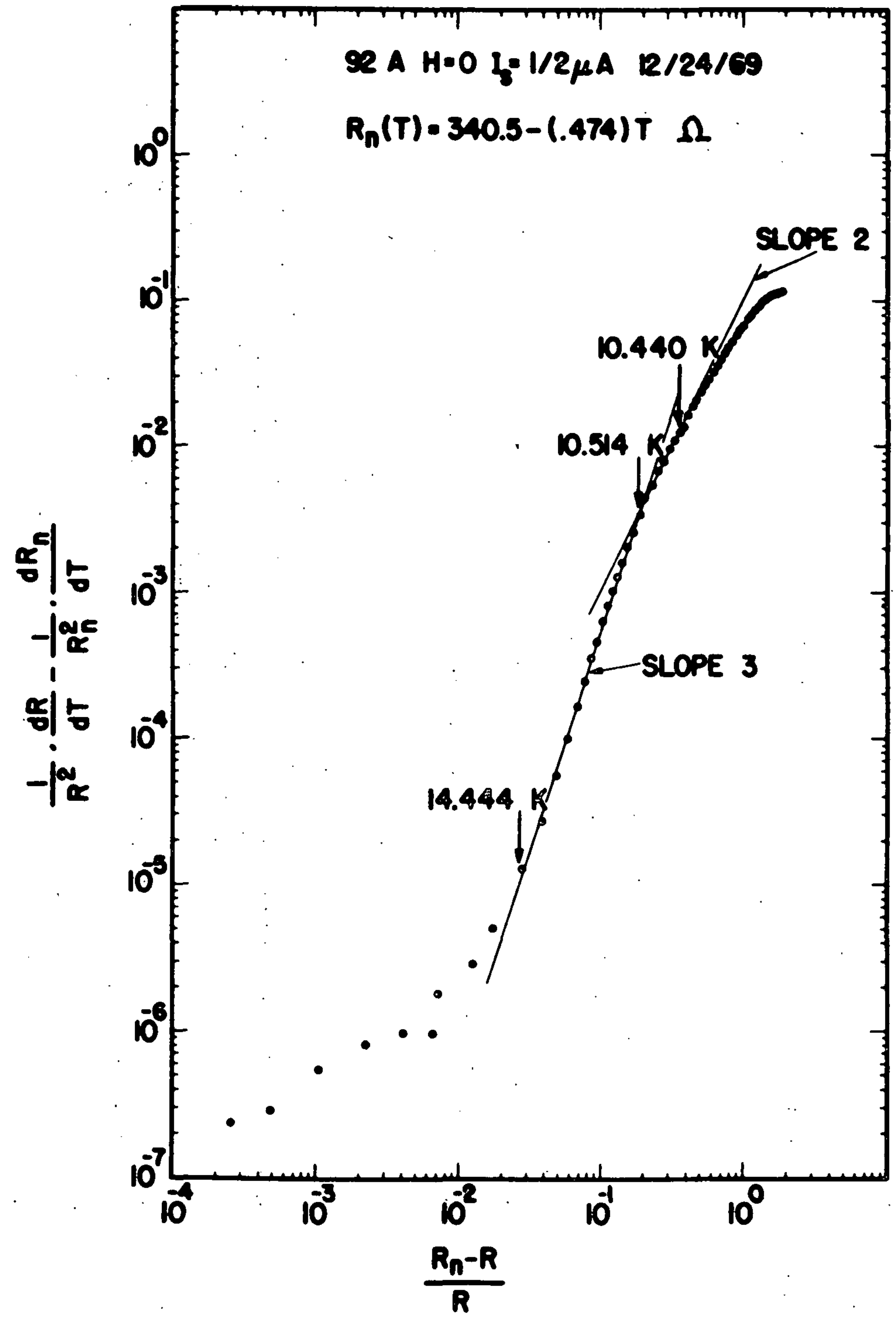

Log-Log Plot of Data for Sample 92A: Upper Portion of Transition

Figure 20

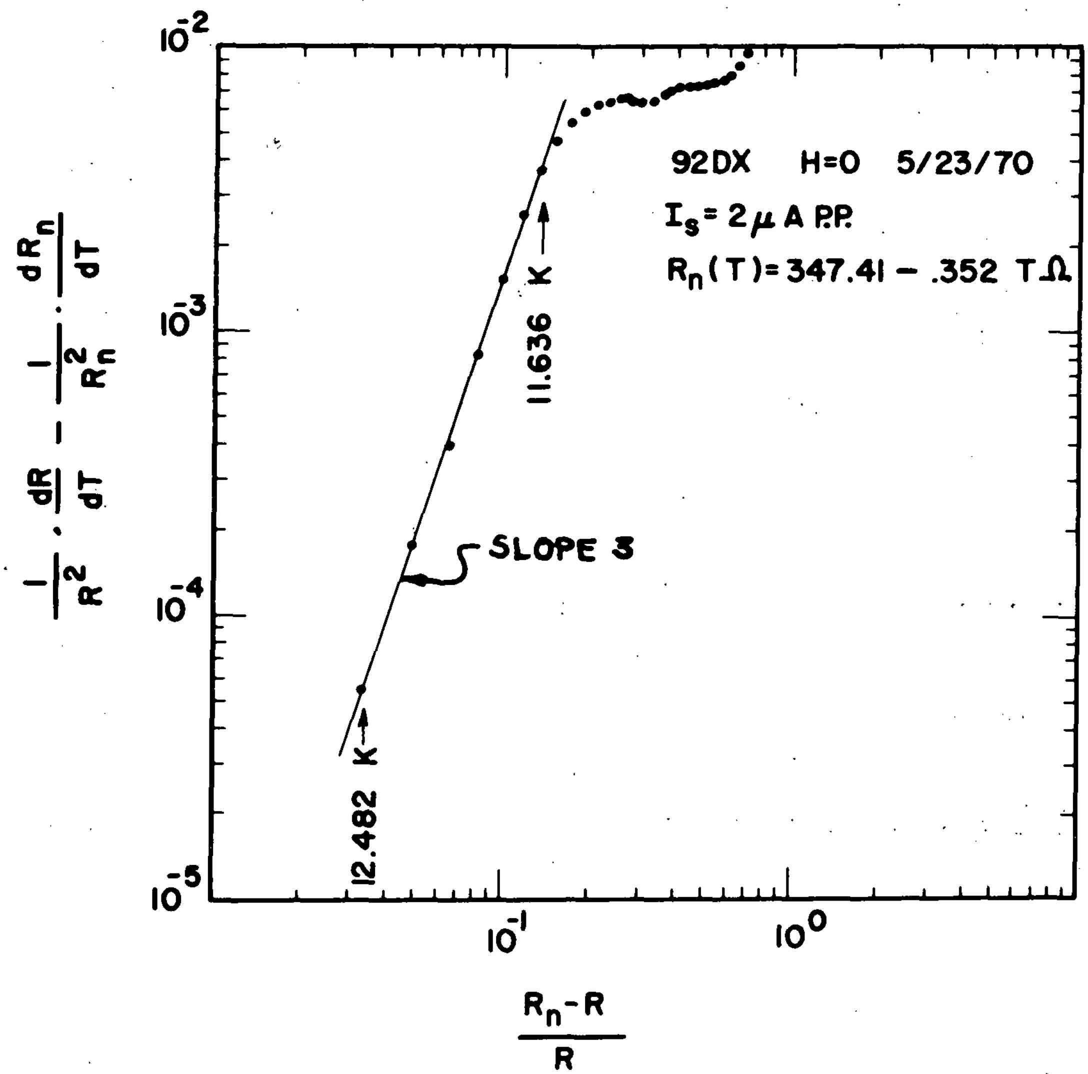

Log-Log Plot of Data for Sample 92DX: Upper Portion of Transition

Figure 21

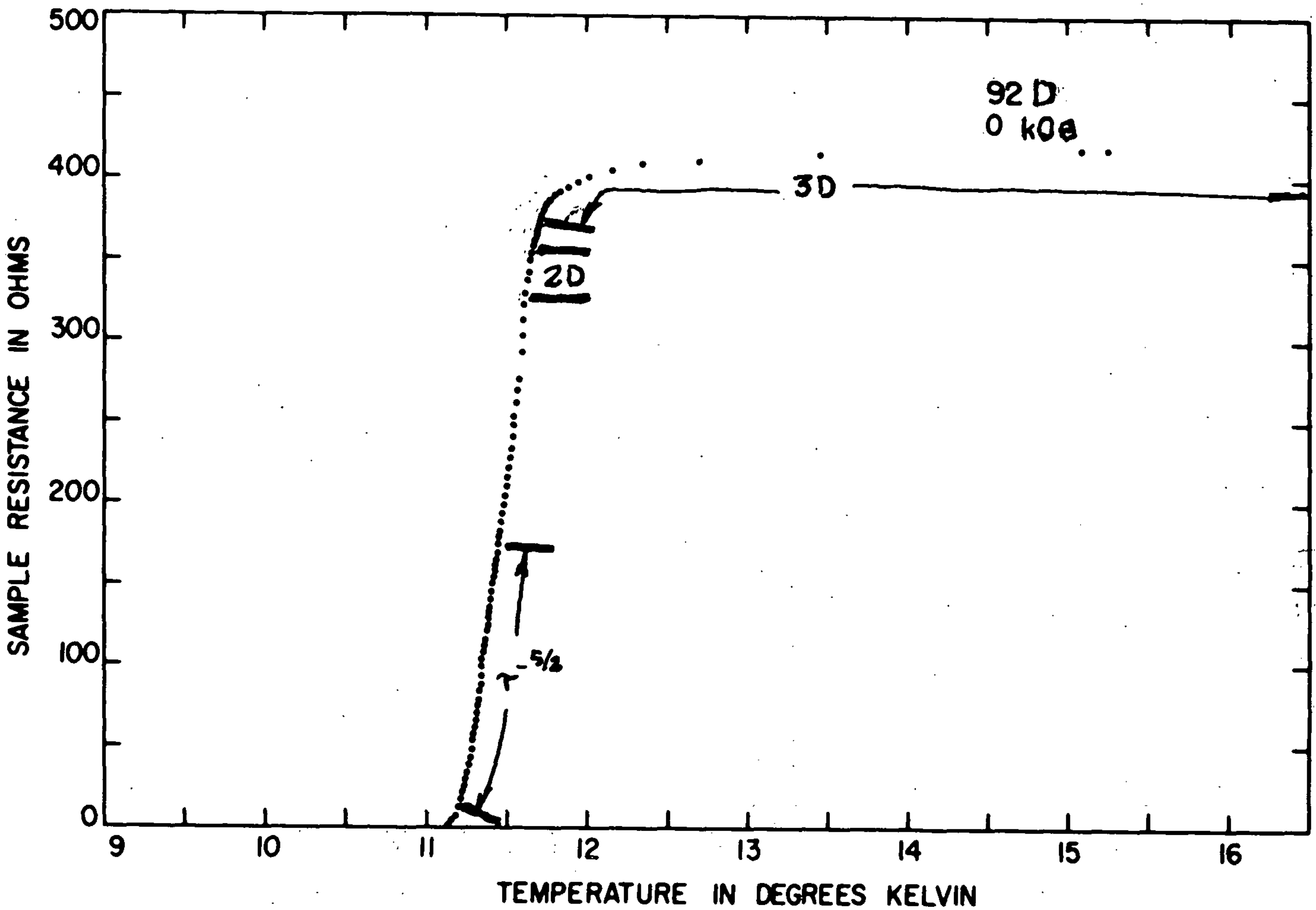

Parts of the Resistive Transition Corresponding To $\tau^{-1/2}$, τ^{-1} and $\tau^{-5/2}$

Table 2.

Extent of Regions of Power Law Behavior Found in the Upper Portion of the Resistive Transition

Sample	Temperature Interval Over Which There Is: $\tau^{-1/2}$ Behavior	Temperature Interval Over Which There Is: τ^{-1} Behavior	Sample Resistance Interval Over Which There Is: $\tau^{-1/2}$ Behavior	Sample Resistance Interval Over Which There Is: τ^{-1} Behavior
92D	16.936 K to 11.679 K (T=5.26 K)	11.636 K to 11.596 K (T=40 mK)	421.69Ω to 376.05Ω	360.21Ω to 331.39Ω
92A	14.444 K to 10.514 K (T=3.93 K)	10.514 K to 10.440 K (T=74 mK)	324.66Ω to 281.52Ω	281.52Ω to 246.33Ω
92DX	12.482 K to 11.662 K (T=.846 K)	11.662 K to 11.636 K (T=26 mK)*	331.77Ω to 301.61Ω	301.61Ω* to 296.58Ω*

Sample	Interval in (R/R_{max}) Over Which There Is: $\tau^{-1/2}$ Behavior	Interval in (R/R_{max}) Over Which There Is: τ^{-1} Behavior	Interval in [illegible] Over Which There Is: $\tau^{-1/2}$ Behavior	Interval in [illegible] Over Which There Is: τ^{-1} Behavior
92D	0.999 to 0.890	0.853 to 0.785	0.02 to 0.15	0.2 to 0.3
92A	0.996 to 0.864	0.864 to 0.756	0.03 to 0.19	0.19 to 0.36
92DX	0.978 to 0.889	0.889* to 0.875*	0.03 to 0.14	0.14* to 0.16

* These numbers correspond to only two data points on the "log-log" plot.

are observed can be compared with the corresponding temperature ranges for which three dimensional (3D) and two dimensional (2D) behavior is predicted by AL. We recall that 2D behavior is expected when $d/\xi(T) < 1.$, where d = sample thickness. 3D behavior is expected when $d > \xi(T) > \delta$, where δ = length associated with granular structure of the films. We list these temperature intervals below. We have used $d = 1500 Å$, $\delta = 200 Å$, $\xi(0) = 35 Å$, $T_c = 11.0$ K and the approximate relation: $\xi(0)/\xi(T) = \tau^{1/2}$.

Temperature Interval Over Which 2D Behavior Is Predicted		Temperature Interval Over Which 3D Behavior Is Predicted
$0 < d/\xi(T) < 1.$	$0 < \frac{d}{\xi(T)} < 0.5$	$\delta < \xi(T) < d$
6 mK	1.5mK	0.34 K

We see from table 2 that the experimental temperature intervals are larger than the predictions of AL. The empirical observation can be made, at this point, that the replacement of $\xi(T)$ with $2\xi(T)$ improves the situation:

Predicted 2D Temperature Interval Using $2\xi(T)$		Predicted 3D Temperature Interval Using $2\xi(T)$
$0 < d/2\xi(T) < 1.$	$0 < d/2\xi(T) < 0.5$	$\delta < 2\xi(T) < d$
24 mK	6 mK	1.4 K

We list next the values for the prefactors of $\tau^{-\eta}$ implied by our data. If we write

$$\sigma'(\tau) = \sigma'_\eta(1)/\tau^\eta ,$$

we recall from chapter 1 that

$$\sigma_n'(1) = \sigma_n \Big/ \left(\frac{1}{\pi} T_c R_n \beta_n\right)^n$$

where β_n is defined by

$$D = \beta_n Q^{(n+1)/n} ,$$

Table 3 lists the relevant information.

The numbers, β_n , were obtained by drawing straight lines of appropriate slope through data points. An error analysis shows that β_n is most sensitive to R_n, and that $\frac{\delta\beta_n}{\beta_n} \simeq \frac{\delta R_n}{R_n}$ at the upper portion of the resistive transition. The greatest source of error in $\sigma_n(1)$ is σ_n =normal conductivity, because sample geometry enters here. The estimate of errors shown in table 3 is conservative: 5% for both R_n and T_c.

The prefactors in table 3 can be compared with the models outlined in chapter 1 which predict power law behavior. According to AL we should have

$$\sigma_{\frac{1}{2}}'(1) = e^2/(32\hbar\,\xi(0)) = 22\ /\Omega\,cm \qquad (\pm 1\,\%)$$

$$\sigma_1'(1) = e^2/(16\hbar\, d) = 1\ /\Omega\,cm. \qquad (\pm 3\,\%)$$

The 2D expression agrees with our data, but the 3D prefactor seems to be off by a factor of two. We note that if we were to replace $\xi(0)$ by $2\xi(0)$, the situation would be improved.

In the weak depairing modification of AL due to Maki and

Table 3

Experimental Coefficients, $\sigma_n'(1)$, of τ^{-n} for Power Law Behavior of Fluctuation Conductivity

Data Used to Obtain $\sigma_n'(1)$

Sample	T_c ($^\circ K$)	R_n (Ω)	σ_n $(\Omega\, cm)^{-1}$	$\beta_{1/2}$ $(\Omega\, K)^{-1}$	β_1 $(\Omega\, K)^{-1}$
92D	11.5	432	690	0.57	0.096
92A	10.4	335	730	0.51	0.097
92DX	11.5	343	680	1.4	(0.19)*
error	5%	5%	10%	5%	5%

Prefactors $\sigma_n'(1)$ From the Data

Sample	$\sigma_{1/2}'(1)$ $(\Omega\, cm)^{-1}$	$\sigma_1'(1)$ $(\Omega\, cm)^{-1}$
92D	9	1.5
92A	12	2.2
92DX	7	(0.9)*
error	10%	15%

* Correspond to only two data points, probably not meaningful numbers.

Thompson.

$$\sigma'_{\frac{1}{2}}(1) = 5e^2/(32\hbar\xi(0)) = 110\,/\Omega\,\mathrm{cm} \quad (\pm 1\,\%)$$

$$\sigma'_1(1) = C(\tau)\,e^2/(16\hbar d)\ ;$$

$$C(\tau) = \frac{1}{1+(\tau_c/\tau)} + 2\ln\left(\frac{\tau+\tau_c}{\tau_c}\right) .$$

Referring to the extent of τ^{-1} behavior above, it is clear that there are problems in estimating τ . The inaccuracy associated with our guess at T_c exceeds in size the region over which we see slope 2. If we locate T_c at the low end of the τ^{-1} region, we get $\tau \cong 10^{-3}$. If we associate T_c with the center of the region in which the slope is less than 1, we get $\tau \cong 10^{-2}$. These numbers should be compared with $\tau_c \cong 7 >> \tau$ gotten from T_{co}= 18 K, the transition temperature of bulk NbN. The Maki-Thompson expression is intended for $\tau >> \tau_c$. We are not surprised to find the Maki-Thompson prediction $C(\tau) \cong 10$ for both choices of T_c, in disagreement with our data.

In the strong depairing limit we have only the prediction

$$\sigma'_{1/2}(1) \cong (.385)\,\tau_c\,e^2/(32\hbar\xi(0))$$

for the 3D region. Taking again $\tau_c \cong .7$ we find $\sigma'_{1/2}(1) \cong 6$. If we take $\sigma'_{1/2}(1) \cong 10$ as representative of our data, $T_{co} \cong 24$ K.

If we introduce the strong coupling parameter, α , the above results are reduced by a factor .8 (if α=1.2). In the absence of any correction to AL due to depairing, our 3D data would indicate $\alpha = 2$, but our data, $\alpha = 1$.

With the assumption of <u>strong</u> depairing and strong coupling, our data implies $\tau_c/\alpha = 1.1$. If $T_{co} = 18^oK$, $\alpha < 1$. If $\alpha = 1.2$, $T_{co} = 26^oK$ (<u>intermediate</u> depairing).

All this is summarized in table 4. The theoretical prefactors listed there are all calculated for $\alpha = 1$. $\alpha = 3$ would decrease the preiactors to 1/3 the listed values.

A least squares fitting program was used on a CDC 6600 to extend comparison of data with the models described in chapter 1 beyond the search for power law dependence.* There are only two complete expressions for $\sigma'(\tau)$ which differ from simple τ^{-n} dependence. One is the AL interpolation formula given by Testardi et al.,(34)

$$\sigma'_{AL} = \frac{e^2}{32\hbar d \ln\left(\frac{T}{T_c}\right)}\left(1 + \frac{d}{\xi(T)}\coth\frac{d}{\xi(T)}\right)$$

$$\xi(T) = \xi(0)\frac{T}{T_c} \Big/ \left(\ln\left(\frac{T}{T_c}\right)\right)^{1/2}$$

The other is the weak depairing correction of AL due to Maki and Thompson(43)

$$\sigma'_{MT} = \sigma'_{AL} + \sigma'_{M}$$

$$\sigma'_{M} = \frac{e^2}{8\tau d}\left(\ln\left(\frac{\xi(0)}{d\,\tau_c^{1/2}}\sinh\frac{d\,(\tau+\tau_c)^{1/2}}{\xi(0)}\right) + \frac{1}{2}\ln\frac{\tau+\tau_c}{\tau_c}\right)$$

* As noted on p.21, the Marcelja 2D expression for σ' is inappropriate for our samples. 2D resistances calculated with this expression were in error by more than 100% for any H_{co}.

Table 4

Experimental and Theoretical Prefactors of τ^{-n}

The Prefactor $\sigma_{\frac{1}{2}}'(1)$, in $\sigma_{\frac{1}{2}}'(\tau) = \sigma_{\frac{1}{2}}'(1)/\tau^{1/2}$, $(\Omega cm)^{-1}$

Sample	Experimental	Theoretical (α = 1) AL[(a)]	MT[(b)]	Hoh[(c)]
92D	9 ± 1	22	110	6
92A	12 ± 1	22	110	6
92DX	7 ± 1	22	110	6

The Prefactor $\sigma_1'(1)$, in $\sigma_1'(\tau) = \sigma_1'(1)/\tau$, $(\Omega cm)^{-1}$

Sample	Experimental	Theoretical (α = 1) AL[(a)]	MT[(b)]	Hoh[(c)]
92D	1.5 ± 0.2	1	10	-
92A	2.2 ± 0.3	1	10	-
92DX	0.9 ± 0.1	1	10	-

a) AL = Aslamasov Larkin Formula (no depairing)
b) MT = weak depairing Maki Thompson formula (T_{co} = 18 K in 2D)
c) Hoh = strong depairing Hohenberg expression (T_{co} = 18 K)

We used both of these formulas, even though all evidence indicates that our material is an intermediate or strong depairing superconductor.

The Maki-Thompson expression fared by far the worst of the two interpolation formulas in comparison with the data. Hence extensive use was made only of the AL expression, which we discuss first.

The AL interpolation formula has more trouble accounting for the data which appears as slope 2 on the log-log analysis, than it does with the data that exhibits slope 3. These two sections of data were therefore treated separately in the computer fits.

To attempt to bring the AL formula into coincidence with these two sections of data, $R_n(T)$, T_c and $\xi(0)$ were allowed to assume fit-optimizing values in various combinations. Finally a multiplicative fudge factor was introduced to the AL expression and allowed to vary. The coherence length was determined self consistently with the relationship:

$$\xi(0) = \left(\frac{\phi_0}{2\pi T_c H'}\right)^{1/2}$$

$$H' = \left(\frac{\partial H}{\partial T}\right)_{R = \frac{1}{2} R_{max}}$$

in computer programs where it was held fixed but T_c varied. That is, the slope H' was used as input rather than $\xi(0)$.

The beginning values of the parameters which were varied in the fitting program were:

Sample	$R_n(T)$ (ohms)	T_c(K)	$\xi(0)$ (Å)
92D	437.7 - 0.447T	11.5	34
92A	340.5 - 0.474T	10.4	34
92DX	347.4 - 0.352T	11.5	34

These were the same numbers that were used in the "log-log" analysis. If these are used to calculate the sample resistance, R_{AL}, then this quantity falls off too rapidly approaching T_c. R_{AL} is 10Ω too low in the 3D region, falling to 100Ω below $R_{exp.}$ in the 2D region, for all samples. The results of the computer fits can now be summarized.

1) If $R_n(T)$ alone is allowed to vary, it assumes a value of approximately 1kΩ for the data which showed slope 2 in the "log-log" analysis. $R_n(T)$ likes a value 30Ω to 40Ω above the beginning $R_n(T)$ for the "slope 3 data". For the right functional form of $R_n(T)$, of course, the fit can be made arbitrarily good.

2) The goodness of fit is insensitive to T_c. When T_c alone is varied, it is reduced by about 0.1 K from those valu values listed above.

3) If $\xi(0)$ is left free, the AL interpolation formula accounts for the data to better than 4%. The following optimum values are found.

Sample	slope 3 data optimum	slope 3 data goodness of fit	slope 2 data optimum	slope 2 data goodness of fit
92D	79Å	2%	49Å	4%
92A	62Å	2%	40Å	3%
92DX	97Å	2%	49Å	3%

The numbers labeled "goodness of fit" are RMS averages of $(R_{AL} - R_{exp.})/R_{exp.}$ over all data points (times 100). Goodness of fit should be compared with the corresponding values of

$$\mathcal{R} = (R_h - R)/R \quad ,$$

where $0.03 < \mathcal{R} < 0.15$ for "slope 3 data" and $0.2 < \mathcal{R} < 0.3$ for "slope 2 data".

4) If the fudge factor alone is allowed to vary, agreement with slope 3 data is better than 1%. The situation is rather poor regarding the slope 2 data:

Sample	slope 3 data: optimum fudge factor	slope 3 data: goodness of fit	slope 2 data: optimum fudge factor	slope 2 data: goodness of fit
92D	0.35	0.5%	0.29	5%
92A	0.47	0.7%	0.23	30%
92DX	0.28	0.03%	0.18	15%

The attempts to fit the weak depairing Maki-Thompson formulas to our data were unsuccessful. The "best" value of T_{co} was generally about 20 mK above T_c. With this, and the $R_n(T)$'s used in the "log-log" analysis, calculated values of sample resistance were 0.5 to 0.1 that measured. R_n = 100 kΩ and T_c = 5 K, or $\xi(0) > 105$ Å were necessary to improve the fit to near 10%.

To summarize, we found that the data in the high temperature end of the transition exhibits power law dependence of σ' on τ for the most elementary choice of $R_n(T)$. If we restrict ourselves to the prominent $\tau^{-1/2}$ region of data, quantitative comparison with models predicting power law indicate either effectively weak coupling and T_{co} up to 25 K, or $\alpha = 2$ and no depairing correction. The τ^{-1} data agrees well with the original AL expression in the 2D limit (except for the fact that the temperature range is too large).

The simplest modification of AL which would produce quantitative agreement for all our data in the upper portion of the transition is the ad hoc substitution of $2\xi(0)$ for $\xi(0)$. Computer fits of the AL interpolation formula are consistent with this latter observation.

Zero Magnetic Field Data Below the Mean Field Transition Temperature

Figures 18 to 20 show that as one proceeds to lower temperatures, from the region of the transition where $\tau^{-1/2}$ and τ^{-1} behavior are observed, the slope of the data, α , in the log-log analysis tends to a value less than one. Within the context of this analysis, the assumption of power law dependence of σ' on τ forces us to associate $\alpha > 1$ with $T > T_c$, and $\alpha < 1$ with $T < T_c$ (see page 29). The temperature that corresponds to $\alpha = 1$ is identified with the mean field transition temperature(T_c^{MF}).

If we continue the log-log analysis below T_c^{MF}, however, we find that α begins to increase, rising again to a value greater than 1, which then remains constant for more than a decade of sample resistance. This is illustrated in figures 22 to 24. $\alpha > 1$, here, implies $T > T_c$, yet log-log analysis of the data from the upper portion of the transition(discussed in the last paragraph) indicates these temperatures are below $T_c(T_c^{MF})$. If the fit to power law is not fortuitous, two transition temperatures are necessary to parametrize the complete transition. The lower transition

Figure 22

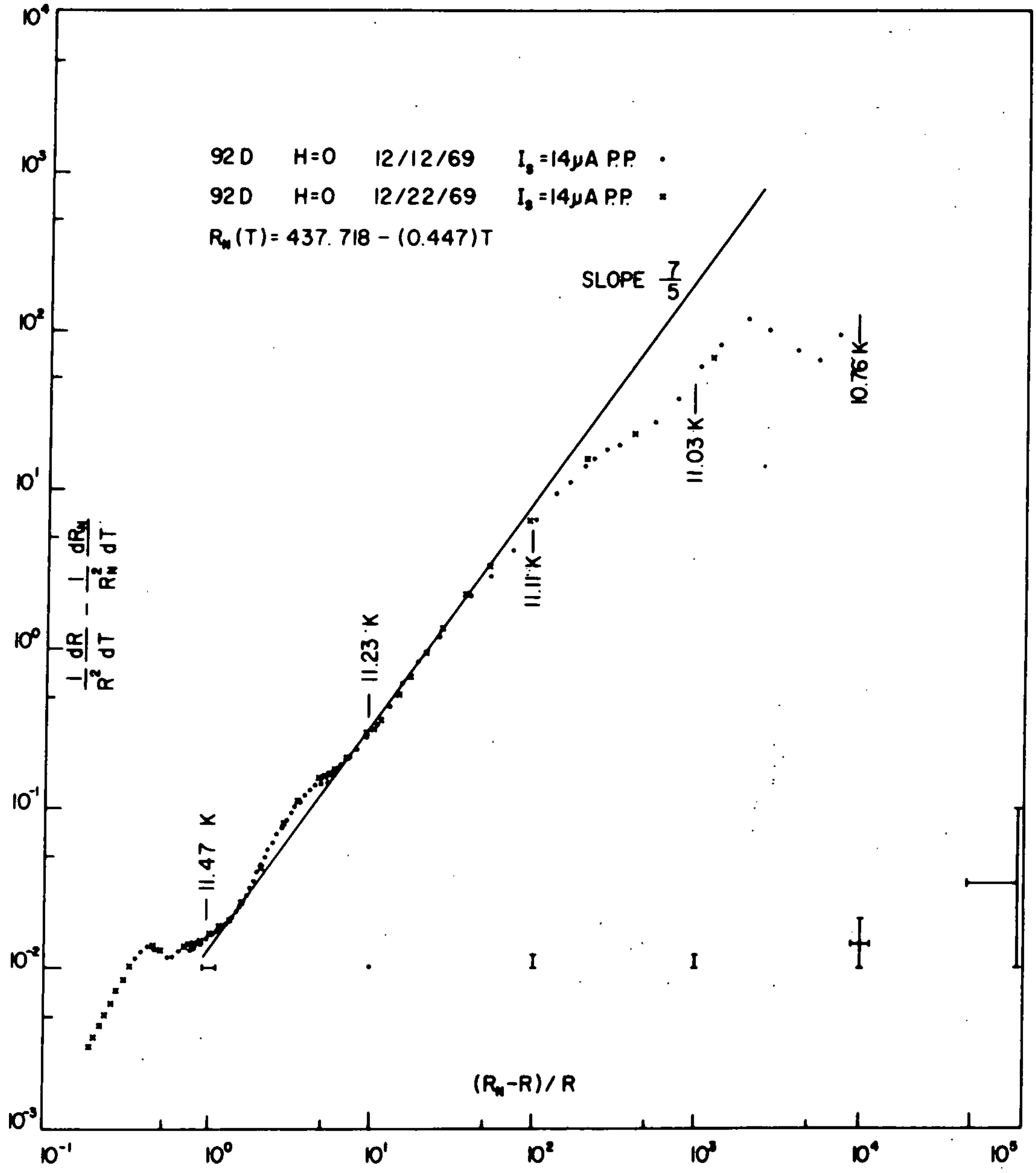

Log-Log Plot of Data for Sample 92D : Lower Portion of Transition

Figure 23

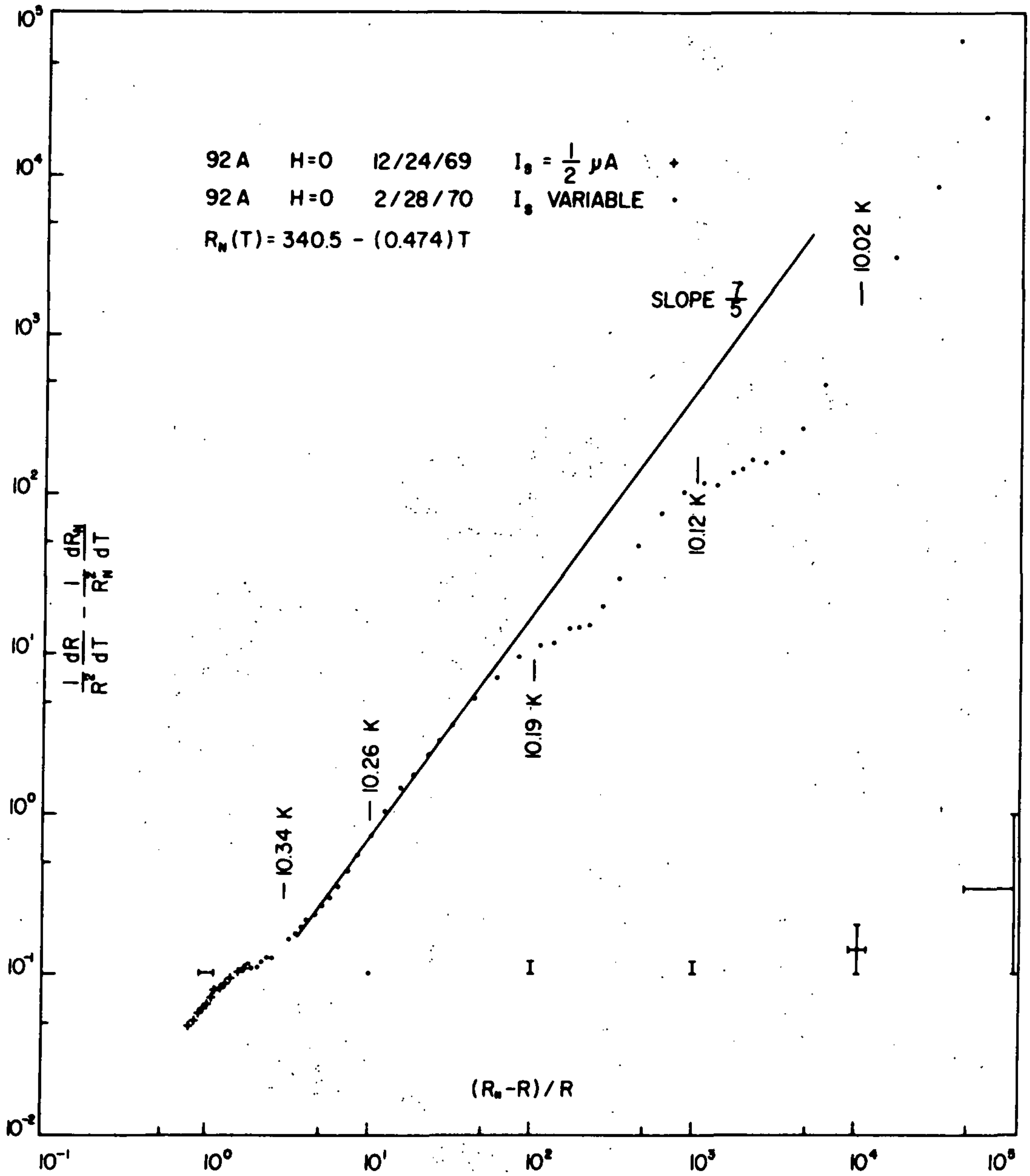

Log-Log Plot of Data for Sample 92A : Lower Portion of Transition

Figure 24

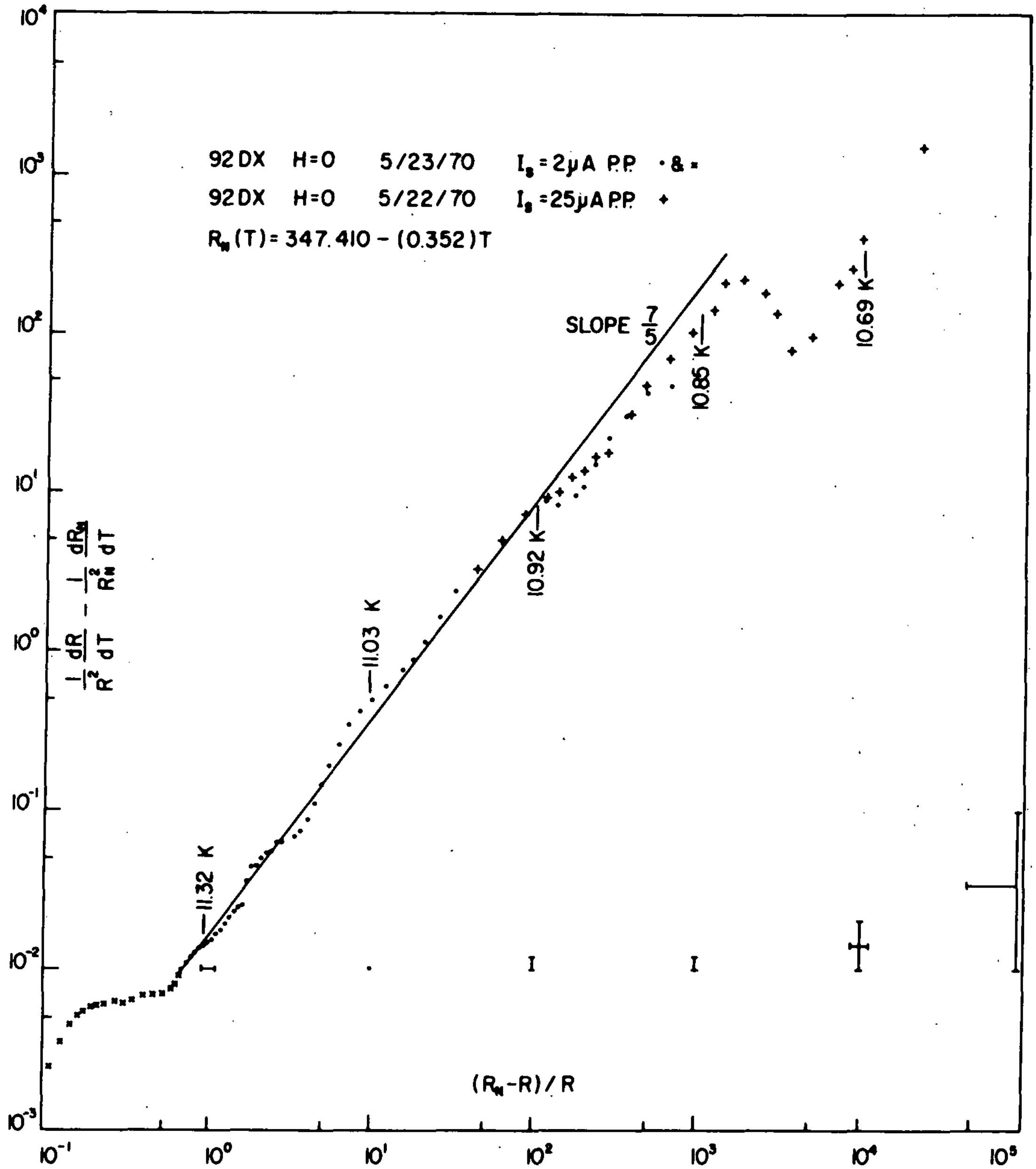

Log-Log Plot of Data for Sample 92DX : Lower Portion of Transition temperature will be called T_c^*.

Below what we interpret to be T_c^{MF}, all three samples exhibit a substantial region of straight line behavior on the plots of $\log(\mathcal{D})$ vs $\log(\mathcal{R})$. In each case, a line of slope 7/5 coincides well with the data. Table 5 describes the extent of this slope 7/5 behavior.

We begin discussion of these observations by noting that the log-log analysis here is less sensitive to our extrapolation of $R_n(T)$ than it was above T_c^{MF}. Using the fact that $\mathcal{R} > 1$ below T_c^{MF}, we find that the largest contribution to error is still $R_n(T)$:

$$\frac{\delta\alpha}{\alpha} \cong \frac{\delta R_n}{R_n} \quad , \quad T < T_c^{MF}$$

Since it is unlikely that $R_n(T)$ is in error by 40% (150Ω) we can say that a power law provides at least a phenomenological fit to the data in this region of the transition.

There is strong evidence that the two T_c's are not artifacts due to sample nonhomogeneities. Presumably the nonhomogeneity is two-fold. If the two components combine electrically in series, R/R_{max} locating the beginning of the transition of lower T_c is not likely to change in a magnetic field. This R/R_{max} in zero field for sample 92D would be 0.6 ± 0.15. There is no evidence of structure in the transition at this R/R_{max} for 92D in 10kOe.* The two components

* The 10kOe data has two power law regions. The slope is always greater than one. The transition between the two power law regions occurs at $R/R_{max} = 0.85 \pm 0.05$. See the next section, on magnetic field behavior.

Table 5

Extent of Regions of Slope 7/5 on Plots of Log(D) vs Log($\mathcal{R}$)

Sample	Illustrated in figure #	Temperature Range	Sample Resistance Range
92D	22	11.42 K to 11.16 K .26 K)	176 Ω to 10 Ω
92A	23	10.30 K to 10.20 K .10 K)	65 Ω to 5 Ω
92DX	24	11.42 K to 10.93 K .49 K)	216 Ω to 3 Ω

Sample	Range in R/R_{max}	Range in $\mathcal{R}$
92D	0.416 to 0.024	1.46 to 42
92A	0.20 to 0.023	4.1 to 43
92DX	0.623 to 0.012	0.63 to 85

cannot be in parallel, either. The portion which causes sample resistance to change the most is the portion with lowest T_c (see table 5). The part with higher T_c should, however, short out the lower T_c portion. So far as graded or distributed nonuniformities are concerned, it seems unlikely that these would produce such an unusual and extensive power law behavior, the same in both samples. We cannot, however, entirely exclude any of these possibilities.

We will assume that $\sigma'(\tau)$ in our samples follows power law in τ, and that one transition temperature, T_c^{MF}, governs the temperature dependence of $\sigma'(T_0)$ for $T > T_c^{MF}$, and that is dominated by T_c^* when $T_c^{MF} > T$.

We list in table 6 the ranges over which data in the log-log analysis has slope $\alpha < 1$. This interpretation is consistent with the ranges of power law behavior expected on the basis of AL. A detailed error analysis shows, however, that in this region of the transition ($R_x \cong 1$)

$$\frac{\delta r}{r} \cong \frac{1}{\ln R_x} \cdot \frac{\delta R_n}{R_n}$$

So in table 6 we will associate T_c^{MF} with the center of the region in which $\alpha < 1$, and use the extent of this region to assign an estimate of error to T_c^{MF}.

T_c^{MF} can also be gotten by fitting portions of the data to the appropriate power laws. This has not yet been done with a computer. Estimates made with representative pairs of data points from both 2D and 3D regions yield the same

T_c^{MF} as is listed in table 6 for each sample.

If we assume that the temperature dependence of our data is governed by T_c^* below T_c^{MF}, then

$$\alpha = 7/5 \quad \text{for} \quad T_c^{MF} > T > T_c^*$$

$$\Rightarrow \sigma'(\tau^*) = \sigma'_{\frac{5}{2}}(1) / \tau^{*5/2} \quad \text{where} \quad \tau^* = \frac{T - T_c^*}{T_c^*}.$$

By using $\sigma'_{\frac{5}{2}}(1) = \sigma_n \left(\frac{5}{2 \beta_{\frac{5}{2}} T_c^* R_n} \right)^{\frac{5}{2}}$ and $\sigma' = \sigma_n \mathcal{R}$

we can estimate T_c^*:

$$T_c^{MF} - T_c^* = \left(\frac{5}{2}\right) / \left(\beta_{\frac{5}{2}} R_n \mathcal{R}^{5/2} (T - T_c^{MF}) \right)$$

The numbers taken from our data which lead to our estimates of T_c^*, and the estimates, are listed in table 7. Listed there also are the coefficients $\sigma'_{\frac{5}{2}}(1)$ that go with the -5/2 power law.

Forcing the data with slope 7/5 to the corresponding power law provides another means of estimating T_c^*. These estimates agree with those listed in table 7.

Marcelja's expression for σ'_{3D} below T_c^{MF} (see pages 22-23) leads to a second transition temperature $T_c^* < T_c^{MF}$, which depends on H_{co}. Although the reasoning leading to the expression for T_c^* rests on an inconsistency, we might still see what it gives for H_{co}. The numbers in table 7 and

Table 6

Extent of Regions on Plots of Log(D) vs Log(θ_x) of Slope Less Than One

Sample	Temperature Range	Range in R/R_{max}	Range in θ_x
92D	11.41 K to 11.58 K	0.42 to 0.74	0.4 to 1.5
92A	10.326 K to 10.365 K	0.28 to 0.45	1.3
92DX	11.42 K to 11.59 K	0.62 to 0.83	0.18 to 0.63

Sample	Estimated T_c^{MF}	Location of T_c^{MF} in R/R_{max}
92D	11.5 ± 0.1K	0.6 ± 0.1
92A	10.35 ± 0.02K	0.35 ± 0.1
92DX	11.5 ± 0.1K	0.7 ± 0.1

Table 7

Estimate of T_c^* From Data Below T_c^{MF} With Coefficients Of -5/2 Power Law Calculated From T_c^*

Sample	$\beta_{5/2}$ $(\Omega K)^{-1}$	T_c^{MF} (K)	$R_x(T_c^{MF})$	$T_c^{MF} - T_c^*$
92D	1.3×10^{-2}	11.5 ± 0.1	0.8 ± 0.5	0.5 ± 0.3
92A	3.1×10^{-2}	10.35 ± 0.02	1.8 ± 0.6	0.19 ± 0.04
92DX	1.5×10^{-2}	11.5 ± 0.1	0.4 ± 0.2	0.7 ± 0.2

Sample	T_c^* (K)	$\sigma_{5/2}(4)$ $(\Omega cm)^{-1}$
92D	11.0 ± 0.4	0.22 ± 0.02
92A	10.16 ± 0.06	0.052 ± 0.004
92DX	10.8 ± 0.3	0.29 ± 0.02

$\xi(0) = 35Å$ lead to $H_{co} = 600$ Oe.

The appearance of a second T_c turns out to be what we would expect in the presence of a magnetic field. It is interesting to conjecture that depairing intrinsic to our samples produces the same effect as a magnetic field in this respect. The temperature dependences are not right, though, as we will see in the next section, where we will discuss magnetic field effects. We will return to this conjecture in the concluding section of this chapter.

<u>Data in Perpendicular Magnetic Fields</u>

The qualitative behavior encountered in large fields when trying to quench superconductivity has been discussed in chapter 1 (pages 61-62), chapter 2 (page 52) and in this chapter (page 128). We will discuss here data taken in smaller fields.

The theoretical expressions chosen for comparison with the data were those of Stevens and Abraham, Prange, and Stevens (hereafter APS; see pages 30-31). These expressions give $\sigma'(H,T)$ in terms of $\sigma'(0,T)$. Thus the data at constant temperature, where a measurement of R(H=0) is taken with every set of R(H) data, is most appropriate for general comparison with theory. The data at constant field is used in a search for power law behavior predicted by APS in certain limits. We will discuss the search for power law behavior first.

Log-log plots of the magnetic field data taken in constant fields are shown in figures 25 and 26. Data of this sort was only taken on sample 92D. The normal resistance

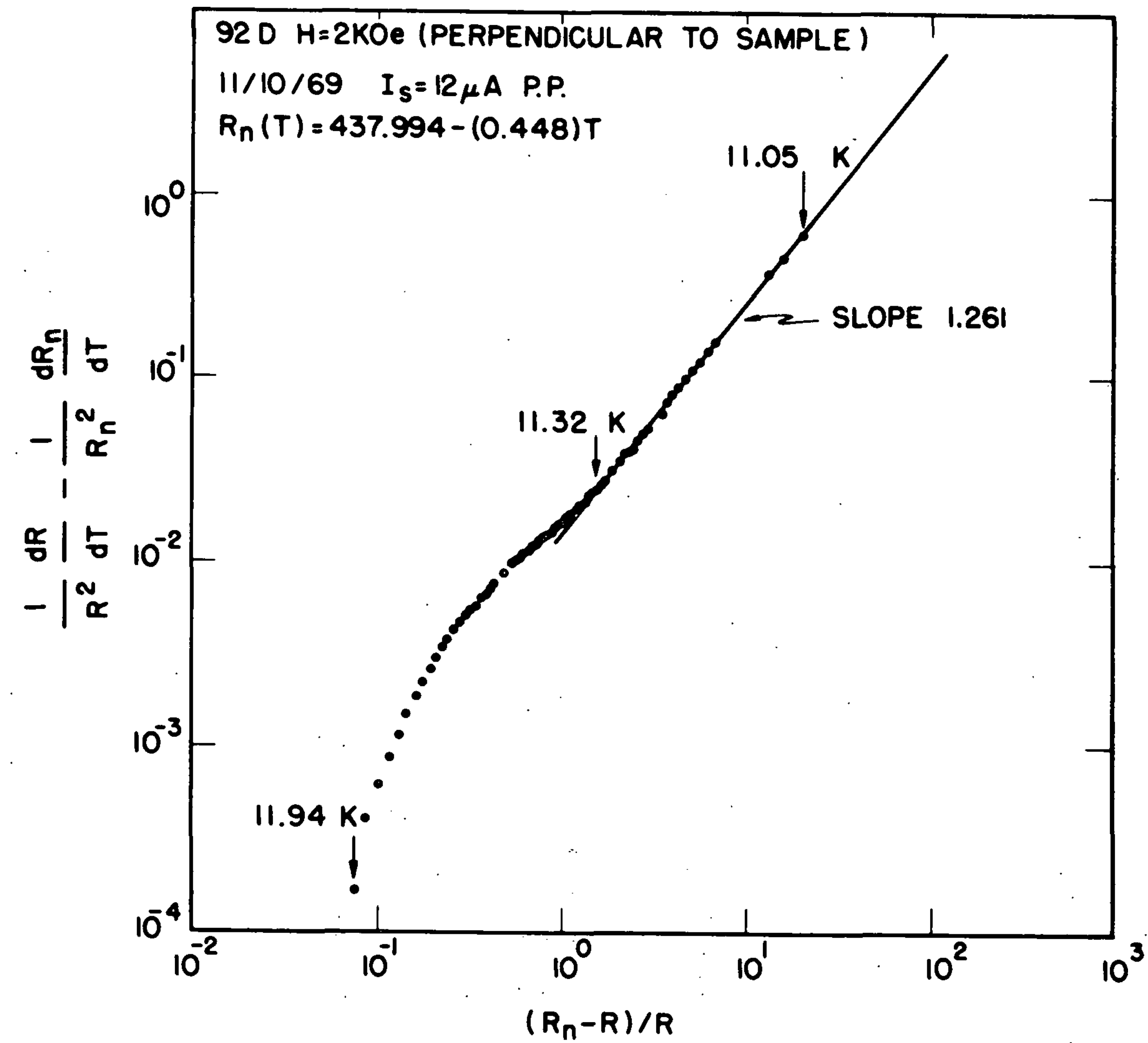

Figure 25: Log-Log Plot of Data Taken In A 2kOe Perpendicular Magnetic Field.

Figure 26: Log-Log Plot Of Data Taken In A 10kOe Perpendicular Magnetic Field.

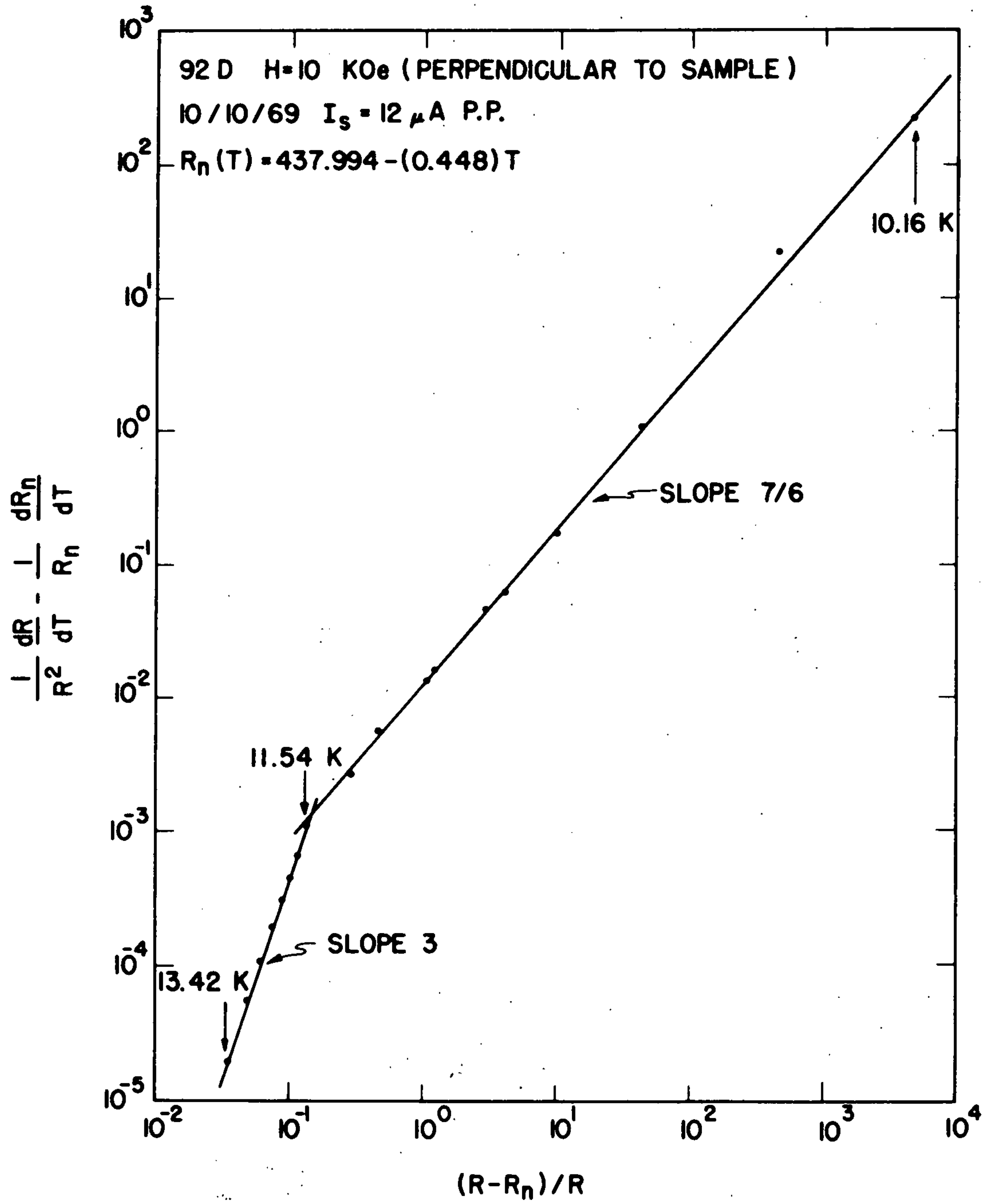

used in this analysis was the same linear extrapolation from high temperatures used in the zero field analysis.

Looking first at the 2k Oe data, we see that the slope of the log-log plot is not monotonic, reminiscent of the twofold behavior in zero field. However the slope is nowhere less than one. There is a suggestion of power law dependence with a peculiar exponent, in the low resistance end of the transition. The data looks otherwise uninteresting.

The 10k Oe data looks entirely different. There is no evidence of the twofold behavior seen in smaller fields. In fact, the entire transition seems to follow some power law or another. Most interestingly, there is a region of slope 3 within the same region of sample resistance that showed this behavior in zero field. The lower portion of the transition follows a different power law (one corresponding to τ^{-6}), and does so for nearly four decades of sample resistance. This, together with the zero field behavior, strongly suggests sample uniformity.

Table 8 shows the extents of the constant slope portions of the data. The corresponding power laws are indicated there also.

The limiting forms of the APS expressions which are applicable here, for

$$x = \left(\frac{T - T_c(0)}{T_c(0)}\right) \Big/ \left(\frac{2H\xi^2(0)}{\phi_0}\right)$$

where $T_c(0)$ is the transition temperature in zero field, are:

Table 8

Extent of Regions of Power Law Behavior in Perpendicular Magnetic Fields For Sample 92D

$H = 2\,kOe$

Temperature Interval Over Which There Is Approximate τ^{-4} Behavior	Sample Resistance Interval Over Which There Is Approximate τ^{-4} Behavior	Interval In R/R_{max} Over Which There Is Approximate τ^{-4} Behavior
11.324 K to 11.031 K	170.92 Ω to 20.11 Ω	0.404 to 0.048

Interval In $\mathcal{R}_x$ Over Which There Is Approximate τ^{-4} Behavior
1.5 to 21

$H = 10\,kOe$

	Temperature Interval Over Which There Is:		Sample Resistance Interval Over Which There Is:	
	$\tau^{-1/2}$ Behavior	τ^{-6} Behavior	$\tau^{-1/2}$ Behavior	τ^{-6} Behavior
	13.42 K to 11.538 K	11.538 K to 10.16 K	417.26 to 382.07	382.07 to 0.1

	Interval in R/R_{max} Over Which There Is:		Interval in $\mathcal{R}_x$ Over Which There Is:	
	$\tau^{-1/2}$ Behavior	τ^{-6} Behavior	$\tau^{-1/2}$ Behavior	τ^{-6} Behavior
	0.987 to	0.904 to 0.0002	0.035 to	0.13 to 4310

$$\sigma'_{3D}(H,T) \simeq \left(\frac{T - T_c(0)}{T_c(0)}\right)^{-1/2}$$ above $T_c(0)$, $(x >> 1)$,

$$\sigma'(H,T) \simeq \sigma'(0,0)\left(1 - O(x)\right)$$ near $T_c(0)$,

(for $|x| << 1$, both 2D and 3D)

and $$\sigma'_{2D}(H,T) \simeq \left(\frac{T - T_c(H)}{T_c(H)}\right)^{-1}$$ near $T_c(H)$, $(x \cong -1/2)$.

The power laws we do see are not entirely consistent with these predictions. We do see the -½ power, but it should be easier to see in the smaller field, where it is absent. In the 10kOe data, where there two power laws, there is not the clear evidence that they are referred to different transition temperatures that there was in zero field. Estimates of T_c obtained by forcing representative pairs of points to appropriate power laws show, however, that the two power laws go with different transition temperatures separated more than before. The transition temperatures, together with power law coeffecients calculated from them, are listed in table 9.

The prefactor to the $\tau^{-1/2}$ extra conductivity should be the same as that obtained in zero field according to APS. Referring to page 139, we see that it is, but it again $\sigma'_{\frac{1}{2}}(H)$

Table 9

Transition Temperatures And Coefficients Of τ^{-r} Determined From Power Law Portions Of Data Taken In Magnetic Fields (Sample 92D)

Magnetic Field (Oe)	Power Law Exponent (-r)	β_r $(\Omega\ K)^{-1}$	T_c (^oK)
2	3.83	1.43×10^{-2}	10.78
10	0.5	5.1×10^{-1}	11.40
10	6	1.35×10^{-2}	10.66
Error		5%	5%

Power Law Exponent (-r)	Prefactors $\sigma_r'(1)$ $(\Omega\ cm)^{-1}$	Error
3.83	1.22×10^{-2}	20%
0.5	9.7	10%
6	5.6×10^{-4}	20%

does not agree with any of the zero field predictions.

Attempts to fit the APS expressions to the data at constant field were in general unsuccessful. Giving the available parameters (R_n, T_c and $\xi(0)$) the values listed on page 141, APS overestimates the increase in sample resistance due to magnetic field by about 20%. Varying R_n doesn't improve the fit; instead, R_n seeks an "optimum" value less than the measured $R(H_{max})$ at each fixed temperature. The fit is improved only by nonphysical T_c's and $\xi(0)$'s , different for each fixed temperature.

To summarize the behavior we found in magnetic fields, we note that the -½ power law we found in zero field disappears in 2kOe , then returns in 10 kOe. It returns to the same portion of the transition, with the same power law prefactor. Again this prefactor would agree with mean field theory predictions only if $\xi(0) \rightarrow 2\xi(0)$. In the 10 kOe data we find different portions of the transition referred to different transition temperatures, as suggested by APS. We observed this in zero field data too, but in 10kOe the "ΔT_c" is 0.7K compared with 0.5K in zero field. If we calculate $\Delta H/\Delta T$ for the two portions of the transition, the $\xi(0)$ that we obtain from the upper part is half $\xi(0)\big|_{100\ kOe}$; from the lower part, roughly twice $\xi(0)\big|_{100\ kOe}$. (See discussion in middle of page 61.)

In the lower portion of the transition, where we found $\tau^{-5/2}$ in zero field, we find τ^{-4} in 2 kOe and τ^{-6} in 10 kOe.

This reflects a broadening transition in increasing field where $\tau < 1$. None of these power laws are predicted (at least in an obvious way) by any of the mean field theories.

<u>Voltage Dependence of Sample Resistance</u>

The data on the nonohmic behavior of our samples is complicated and incomplete. We note immediately that the voltage dependence of resistance is not generally monotonic, not the same for both samples and also persists up to room temperature. The effect is, at least, small, except for the lowest resistances.

Checks performed with the sample replaced by various resistors confirmed that the effect is not instrumental. Heating due to measuring current could not produce what we see, since it does not change when the slope of sample R(T) changes.

In general, the response in our samples to increasing voltage is first a decrease, then, with sufficient voltage, an increase in resistance. The voltage at which this change occurs decreases when temperature decreases.

The decreasing contribution to R(V) is probably unrelated to superconductivity, since it exists even at room temperature. For this reason, and since all three models for nonohmic behavior discussed in chapter 1 predict increasing R(V), we will disregard data dominated by the decreasing contribution to R(V).

Except at the lowest resistances, $\sigma'(V)$ changes so slowly that a comparison with theory requires a computer. This has not yet been done. We outline below a few rough comparisons that have been made where the effect is most pronounced.

The models discussed in chapter 1 (pages 32-34) can be written, for our purposes,

$$\frac{\sigma'(V)}{\sigma'(0)} \underset{V \ll V_c}{\sim} 1 - a_m \frac{V^2}{V_c^2} \quad ; \quad a_m \gtrsim \begin{cases} 2 \text{ for } 3D \\ 6 \text{ for } 2D \end{cases}$$

$$\frac{\sigma'(V)}{\sigma'(0)} \underset{V \gg V_c}{\sim} \left(\frac{V_c}{V}\right)^{\frac{4-n}{3}} \qquad n = \text{dimensionality}$$

$$V_c \cong \left(7. \times 10^3 \text{ volts}\right) \times T^{3/2}$$

Since our sample voltages are almost certainly less than V_c, we try the first expression. According to this expression,

$\dfrac{R(V) - R(0)}{R(V)}$ ought to be linear in V^2 for small resistances.

A plot of our data would show this is not the case. This expression underestimates R(V), yielding a V_c(exp.) at least an order of magnitude too low.

Gor'kov's formula (page 34) predicts log(R(0)/R(V)) approximately linear in 1/V for small R. Here again the data is not like this, the model under estimates R(V) by the same amount as above.

The formula appropriate for $V >> V_c$ predicts log(R(V)) linear in log(V) for small R. This is not so either. R(V) in this case is overestimated. The data does approach the appropriate slope for 3D behavior, at the highest voltages, in this analysis, but that part of the data is fit with $V_c \cong .2mV$.

Attempts to fit the models for nonohmic behavior to our data have been entirely unsuccessful.

Conclusion

The resistive transition in these samples seems to divide itself naturally into two portions. In the upper part, we find agreement only with Aslamasov and Larkin, and then only if our measured $\xi(0)$ is replaced by $2\cdot\xi(0)$. This rests on an assumed normal resistance suggested by high tmeperaure and high magnetic field data. The lower part of the transition, insensitive to $R_n(T)$, can be fit to a power law, but one referred to a lower T_c than that encountered above this region.

Perhaps the most striking outcome of this analysis is the suggestion of fluctuation conductivity above 20K. In fact, resistance increases in very high fields could be detected at 20 K.

In the upper portion of the transition, the theoretical picture is far from complete. A weak depairing expression cannot account for our data there. The only strong depairing expression (one for 3D) indicates $\tau_c/\alpha \cong 1$ (i.e., intermediate depairing, for which there is no model).

The behavior observed in the lower part of the transition is inconsistent with anything except the most exotic sort of graded nonuniformity. There are clear evidences of nonuniformities at the very lowest resistances. There, in each sample, one sees several shifts to lower and lower T_c's, each preserving the same power law (-5/2) (figures 22-24). The bulk of the evidence seems to weigh, though not conclusively, against sample nonuniformity causing the other behavior we see.

The appearance of the whole transition in zero field is reminiscent of what mean field theory predicts in a magnetic field. The exponents of the power laws are not right , but the reference to two transition temperatures and probable intrinsic depairing in our samples make this an interesting conjecture. There are some difficulties with this conjecture: 1) An extensive region of power law behavior seen in zero and 10 kOe is absent in a 2 kOe field. 2) $T_c^{MF}-T_c^*$ in zero field indicates an effective field of 13 kOe; this is inconsistent with the observed changes in T_c's with magnetic field. 3) $T_c^{MF}-T_c^*$ corresponds to weak depairing, while there has been no success in attempts to fit the Maki-Thompson expressions to our data.

These reservations are less serious in the light of the fact that expressions for the extra conductivity have not yet been worked out in the case of strong coupling and intermediate or strong depairing. The model by which we sought to determine the strong coupling nature of our material is not even on firm ground. A more complete and perhaps satisfactory analysis of this data awaits these theoretical results.

APPENDIX I

The subroutine for computer calculation of temperatures from thermometer resistances is reproduced here. This illustrates the use of the interpolation formula for thermometer calibration in sections covering different thermometer resistances (RT).

SUBROUTINE FOR CALCULATION OF TEMPERATURES*

FROM CRYOCAL THERMOMETER RESISTANCES (FOR H = 0)

RT = CRYOCAL RESISTANCE

STATEMENT 40 IS THE EXIT FROM THE ROUTINE

```
      I=1
      B(1,1)=103.8918409 $ B(1,2)=-85.14880859
      B(1,3)=30.51294989 $ B(1,4)=-4.07446789
      B(2,1)=179.5363792 $ B(2,2)=-193.31902103
      B(2,3)=     82.07306915  $B(2,4)=-12.26693539
      B(3,1)=79.15 36481   $B(3,2) =-12.1941895
      B(3,3) =-26.99587197  $B(3,4)=9.6509259
      B(4,1)=-1026.13182278  $B(4,2)=4512.15502088
      B(4,3)=-7401.18524543 $B(4,4) =5991.85715781
      B(4,5)=-2415.64062559  $B(4,6)=388.48244071
      B(5,1)=411.36762526  $B(5,2)=-1244.98370864
      B(5,3)=1709.16144959   $B(5,4)=-1089.08985451
      B(5,5)=263.27854694
    5 READ 20,RRT,RRS,RTBRG,RSBRG
   20 FORMAT (2X,4F10.0)
      RT=RRT*RTBRG
      RS=RRS*RSBRG
      T(I)=0.
      IF(RT.LE.0.) GO TO 40
      IF(RT.LE.12.5) GO TO 21
      IF(RT.LE.26.) GO TO 19
      IF(RT.LE.49.) GO TO 17
      IF(RT.LE.112.) GO TO 15
      K=1
      L=4
      GO TO 25
   15 K=2
      L=4
      GO TO 25
   17 K=3
      L=4
      GO TO 25
   19 K=4
      L=5
      GO TO 25
   21 K=5
      L=5
   25 DO 26 M=1,L
   26 T(I)=T(I)+B(K,M)*((ALOG10(RT))**(M-2))
```

* See chapter three for discussion.

APPENDIX II

Calibration of National Carbon Co., Inc. thermistor (designated by manufacturer as unit #4) in zero magnetic field. See chapter 3 for further discussion.

THERMISTOR CALIBRATION DATA

THERMISTOR UNIT #4 THERMISTOR POWER = 1 Watt at 1.5 KHz

PRECISION: RESISTANCE: ±3 in last digit or better
TEMPERATURE: See section on CryoCal calibration in chapter three.

TEMPERATURE (K)	THERMISTOR RESISTANCE (ohms)	TEMPERATURE (K)	THERMISTOR RESISTANCE (ohms)
4.5	43055	17.0	23.160
4.75	28530	18.0	18.892
5.00	19435	19.0	15.732
5.5	10580	20.0	13.357
6.0	5743.2	22.0	10.080
6.5	3324.1	24.0	8.0154
7.0	2038.2	26.0	6.6720
7.5	1301.0	28.0	5.7900
8.0	872.69	30.0	5.2538
8.5	612.86	32.0	4.7744
9.0	438.34	34.0	4.2248
9.5	328.23	36.0	3.7378
10.0	247.70	38.0	3.3270
11.0	151.75	40.0	2.9807
12.0	99.31	45.0	2.3282
13.0	68.725	55.0	1.5826
14.0	49.750		
15.0	37.392		
16.0	29.044		

REFERENCES

1. J. S. Langer and M. E. Fisher, Phys. Rev. Letters 19, 560(1967).

2. W. A. Little, Phys. Rev. 156, 396(1967).

3. R. D. Parks and R. P. Groff, Phys. Rev. Letters 18, 342 (1967).

4. T. K. Hunt and J. E. Mercereau, Phys. Rev. Letters 18, 551(1967).

5. R. P. Groff, S. Marcelja, W. E. Masker and R. D. Parks, Phys. Rev. Letters 19, 1328(1967).

6. R. J. Warburton and W. W. Webb, Proceedings of the International Conference on the Science of Superconductivity-Stanford(1969): to be published in Physica.
W. W. Webb and R. J. Warburton, Phys. Rev. Letters 20, 461(1968).

7. J. S. Langer and V. Ambegaokar, Phys. Rev. 164, 498(1967).

8. D. E. McCumber and B. I. Halperin, Phys. Rev. B1, 1054 (1970).

9. V. Ambegaokar, Proc. of the 11th Int. Conf. on Low Temperature Physics, p.781, St. Andrews(1968).

10. L. D. Landau and E. M. Lifshitz, Statistical Physics, translated by E. Peierls and R. F. Peierls, Addison-Wesley, Reading, Mass., 1958, Ch.15, 149.
T. M. Rice, Phys. Rev. 140, A1889(1965).
N. D. Mermin and H Wagner, Phys. Rev. Letters 17, 1133 (1966).
P. C. Hohenberg, Phys. Rev. 158, 383(1967).
N. D. Mermin, Phys. Rev. 176, 250(1968).

11. W. A. Little, Phys. Rev. A134, 1416(1964).

12. R. A. Ferrell, Phys. Rev. Letters 13, 330(1964).

13. L. D. Landau Phys. Z. Sowiet Un. 11, 26(1937).

14. P. Weiss, J. de physique (4)6, 661(1907).

15. L. D. Landau and V. L. Ginzburg, Zh. Eksper. i. Teor. Fiz. 20, 1064(1950).

16. A. B. Pippard, Proc. Roy. Soc. (London) A203, 210(1950).

17. V. L. Ginzburg, Fiz. Tverd. Tela 2, 2031(1960). (English translation Sov. Phys. -S. S. 2, 1824(1960).

18. J. E. Neighbor, J. F. Cochran and C. A. Shiffman, Proc. of the 9th Int. Conf. on Low Temperature Physics, Part A, Columbus, Ohio (1964).

19. P. W. Anderson, Proc. of the Conf. on Critical Phenomena, eds. M. S. Green and J. V. Sengers (Washington, 1965), p.102.

20. J. S. Shier and D. M. Ginsberg, Phys. Rev. 147, 147(1966).

21. R. A. Ferrell and H. Schmidt, Phys. Letters 25A, 544 (1967).

22. R. E. Glover III, Phys. Letters 25A, 542(1967).

23. L. G. Aslamazov and A. I. Larkin, Fiz. Tverd. Tela 10, 1104(1968) & Sov. Phys.-Solid State 10, 875(1968). L. G. Aslamasov and A. I. Larkin, Phys. Letters 26A, 238 (1968).

24. R. E. Glover III and M. Tinkham, Phys. Rev. 108, 243 (1957). R. E. Glover III, 11th Int. Conf. on Low Temperature Physics, St. Andrews, Scotland(1968).

25. O. C. Naugle and R. E. Glover, Phys. Letters 28A, 110 (1968).

26. R. O. Smith, B. Serin and E. Abrahams, Phys. Letters 28A, 224(1968).

27. M. Strongin, O. F. Kammerer, J. Crow, R. S. Thompson and H. L. Fine, Phys. Rev. Letters 20, 922(1968).

28. G. Bergmann, Z. Physik 225, 430(1969).

29. J. I. Gittleman, R. W. Cohen and J. J. Hanak, Phys. Letters 29A, 56(1969).

30. M. A. Klenin, J. E. Crow and A. K. Bhatnagar, Int. Conf. Science of Superconductivity, Stanford, Calif., (August, 1969).

31. M. A. Klenin and M. A. Jensen, Int. Conf Science of Superconductivity, Stanford, Calif., (August, 1969).

32. S. Marcelja, W. E. Masker and R. D. Parks, Phys. Rev. Letters 22, 124(1969).
S. Marcelja, W. E. Masker and R. D. Parks, Phys. Rev. 188, 745(1969).

33. B. Serin, R. O. Smith, T. Mizusaki, Int. Conf. of Superconductivity, Stanford, Calif. (August, 1969).

34. L. R. Testardi, W. A. Read, P. C. Hohenberg, W. H. Haemmerle and G. F. Brennert, Phys. Rev. 181, 800 (1969).

35. A. K. Bhatnagar, P. Kahn and T. J. Zammit, Solid State Communications 8, 79(1970).

36. J. E. Crow, R. S. Thompson, M. A. Klenin and A. K. Bhatnagar, Phys. Rev. Letters 24, 371(1970).

37. S. Marcelja, Phys. Letters 28A, 180(1968).

38. A. Schmid, Phys. Kondensierten Materie 5, 302(1966).
E. Abrahams and T. Tsuneto, Phys. Rev. 152, 416(1966).
C. Caroli and K Maki, Phys. Rev. 159, 306(1967).

39. L. P. Gor'kov and G. M. Eliashberg, Zh. Eksp. Teor. Fiz. 54, 612(1968).
(English translation: Sov. Phys.-JETP 27, 328(1968).)
I. O. Kulik, Zh. Eksp. Teor. Fiz. 57, 600(1969).
(English translation: Sov. Phys.-JETP 30/2 (1970)

40. A. A. Abrikosov, L. P. Gor'kov and I. E. Dzhaloshinski, Methods of Quantum Field Theory in Statistical Physics, Prentice Hall, Inc. (1964) p.325.

41. K. Maki, Prog. Theoret. Phys. (Kyoto) 39, 897(1968).
K. Maki, Prog. Theoret. Phys. (Kyoto) 40, 193(1968).

42. A. A. Abrikosov and L. P. Gor'kov, Zh. Eksperim. i Teor. Fiz. 39, 1781(1960).
(English translation: Soviet Phys.-JETP 12, 1243(1961)

43. R. S. Thompson, Phys. Rev. B1, 327(1970).

44. E. Abrahams and J. W. F. Woo, Phys. Letters 27A, 117 (1968).

45. H. Schmidt, Z. Physik 216, 336(1968).

46. A. Schmid, Z. Physik 215, 210(1968).

47. G. M. Eliashberg, Zh. Eksperim. i Theor. Foz. 38, 966 (1960); 39, 1437(1960).
(English translation: Soviet Phys.-JETP 11, 696(1960); 12, 1000(1961).)
Y. Nambu, Phys. Rev. 117, 648(1960).

48. P. Fulde and K. Maki, Phys. D. Kond. Mat. 8, 371(1969).

49. K. Maki and P. Fulde, Phys. Rev. 140, A1586(1965).
H. Schmidt, Phys. Letters 27A, 65B(1968).

50. P. C. Hohenberg, Proc. of the 12th Int. Conf. on Low Temperature Physics, Tokyo (1970), to be published.

51. G. Eilenberger, (to be published; referred to in Hohenberg's LT 12 paper).

52. J. Bardeen, L. N. Cooper and J. R. Schreiffer, Phys. Rev. 108, 1175(1957).

53. G. Eilenberger and V. Ambegoakar, Phys. Rev. 158, 332 (1967).

54. T. Tsuzuki and K Kawasaki, Phys. Letters 28A, 40(1968).

55. T. Tsuzuki, Prog. Theor. Physics (Kyoto) 41, 296(1969).

56. J. P. Hurault and K. Maki, Phys. Rev. B2, 2560(1970).

57. A. Schmid, Z. Physik 229, 81(1969).

58. H. Schmidt, Z. Physik 232, 443(1970).

59. A. M. Goldman, Private communication.

60. H-J. Mikeska and H. Schmidt, Journal of Low Temperature Physics 2, 371(1970).

61. K. Maki Journal of Low Temperature Physics 1, 513(1969).

62. E. Abrahams, R. E. Prange and M. J. Stephen, Preprint.

63. M. J. Stephen, Private communication to A. M. Goldman.

64. Klaus-Dieter Usadel, E. Physik 227, 260(1969).

65. R. S. Thompson, Proc. of the Int. Conf. on the Science of Superconductivity, Stanford, Calif., Aug.,1969 (to be published in Physica).

66. J. P. Hurault, Phys. Rev. 179, 494(1969).

67. T. Tsuzuki, Phys. Letters(Netherlands) 30A, 285(1969).

68. T. Tsuzuki, Progr. Theor. Phys.(Japan) 42, 1020(1969); 42, 1030(1969).

69. L. P. Gor'kov, ZhETF Pis. Red. 11, 52(1970).

70. J. Zbasnik, L. E. Tom, Y. M. Shy and E. Maxwell, J. Appl. Phys. 40, 2147(1969)

71. P. M. Tedrow, R. Meservey and B. B. Schwartz, Phys. Rev. Letters 24, 1004(1970).

72. B. Abeles, R. W. Cohen and R. W. Stowell, Phys. Rev. Letters 18, 902(1967).

73. Y. M. Shy, Ph.D. Thesis, University of Minnesota, Unpublished (1970).

74. H. Bell, Y. M. Shy, D. E. Anderson and L. E. Toth, J. Appl. Phys. 39, 2797(1968).

75. G. K. Wehner and D. Rosenberg, J. Appl. Phys. 31, 177 (1960).

76. Neugebauer and R. H. Wilson, Basic Problems in Thin Film Physics, edited by R. Niedermayer and H. Mayer (Vandenhoeck and Ruprecht, Gottingen, 1966) p.579.
L. F. Drummeter, Jr. and G. Haas, Physics of Thin Films, edited by G. Haas and R. E. Thun (Academic Press, Inc., N. Y., 1964) p.305

77. Douglas Finnemore, private communication.

78. N. Pessall, R. E. Gold and H. A. Johansen, J. Phys. Chem. Solids 29, 19(1968).

79. R. B. Laibowitz, V. Sadagopan and P. E. Saiden, Phys. L Letters 31A, 133(1970)

80. K. Komenou, T. Yamashita and Y. Onodera, Phys. Letters 28A, 335(1968).

81. T. H. Geballe, B. T. Mattias, J. P. Remeiko, A. M. Clogston, V. B. Compton, J. P. Maita and H. J. Williams, Physica 2, 293(1966).

82. Westinghouse superconductivity group, private communication.

83. R. R. Haake, Appl. Phys. Letters 10, 189(1967)

84. H. A. Kierstead, Phys. Rev. 153, 258(1967).

85. W. F. Schlosser and R. H. Munnings, Rev. Sci. Instrum. 40, 1359(1969).

86. A. M. Goldman, F. M. Schaer, L. E. Toth and J. Zbasnik, Physica (in press).